

A Study on Gas Quench Steel Hardenability

by

Yuan Lu

A Thesis

Submitted to the Faculty

of the

WORCESTER POLYTECHNIC INSTITUTE

in partial fulfillment of the requirements for the

Degree of Master of Science

in

Materials Science & Engineering

Jan. 2015

APPROVED:

Yiming (Kevin) Rong

Richard D. Sisson, Jr.

ABSTRACT

Gas quench technology has been rapidly developed recently with the intent to replace water and oil quench for medium and high hardenability steel. One of the significant advantages is to reduce the distortion and stress, compared to water and oil quench. However, not like liquid quench, no gas quench steel hardenability test standard exists.

The fundamental difference between liquid quench and gas quench is heat transfer coefficient. The workpiece with the same hardness after liquid and gas quench process may have different microstructure due to different cooling curves. The concept of equivalent gas quench heat transfer coefficient (HTC) is proposed to have the same cooling curve, microstructure and hardness when compared with liquid quench.

Several influencing factors on steel hardenability have been discussed, such as austenizing temperature, heating rate, holding time, composition variation and grain size difference. The phase quantification by X-ray Diffraction and Rietveld Refinement method is developed to measure phase percentage for steel microstructure, including martensite, ferrite and carbides.

The limitations and improvements of modified Jominy gas quench test are discussed. The fundamental limitation of Jominy gas quench test is that one gas quench condition cannot be used for both low hardenability steel and high hardenability steel at the same time. The same steel grade would have different hardenability curves under different gas quench conditions, which made it difficult to compare the hardenability among different steels.

The critical HTC test based on Grossmann test is proposed to overcome the limitations. In the test, different gas quench HTC conditions are applied to the sample with the same geometry. After sectioning each bar at mid-length, the bar that has 50% martensite at its center is selected, and the applied gas quench HTC of this bar is designated as the critical

HTC. This test has many advantages to take the place of modified Jominy gas quench test.

Since one of the advantages of gas quench is greater process flexibility to vary cooling rates, gas marquenching technology is proposed to obtain martensite with less severe cooling rate and reduce the distortion and stress.

ACKNOWLEDGEMENTS

I am grateful to my advisor, Prof. Yiming (Kevin) Rong, for his valuable guidance and advice throughout the research project.

I am appreciated that my co-advisor, Prof. Richard Sisson, for his guidance on heat treatment.

I am also grateful to Jeffrey C Mocsari from Praxair, Libo Wang, Boquan Li, Lei Zhang, Anbo Wang, Xiaoqing Cai, Haixuan Yu from Worcester Polytechnic Institute and Center for Heat Treating Excellence members for their suggestions and support.

I would like to thank CHTE at WPI for providing me with financial support.

Last, but not the least, I simply could not have come this far without the support from my parents Zhanhui Lu and Xipai Liu.

Contents

1	Introduction.....	1
1.1	Quenching of steel	1
1.2	Gas quench technology	3
1.3	Steel hardenability test.....	6
1.4	Gas quench hardenability test	9
1.4.1	Current gas quench steel hardenability test	9
1.4.2	Limitation and possible improvement of current gas quench steel hardenability test.....	13
1.5	Objectives	19
1.6	Thesis Organization	21
2	Comparison between liquid and gas quench.....	22
2.1	Grossmann quench model.....	22
2.2	HTC measurement and model verification	23
2.3	Equivalent gas quench HTC prediction based on Grossmann quench model	26
2.4	Microstructure and hardness comparison based on Jominy test.....	33
2.5	Summary and Conclusion	35
3	Steel hardenability analysis.....	36
3.1	Influencing factors on steel hardenability.....	36
3.2	Water quench steel hardenability test and simulation.....	43
3.3	Determination of 50% martensite microstructure and hardness	55
3.4	Quantitative analysis of steel microstructure by XRD measurement	58
3.4.1	Introduction.....	58
3.4.2	Sample preparation	61
3.4.3	Steel microstructure analysis based on Rietveld refinement	63
3.5	Summary and Conclusion	70
4	Critical HTC test for gas quench steel hardenability	71
4.1	Critical HTC test and critical HTC	71
4.2	Praxair gas quench system and sample design	73
4.3	4140 Gas quench hardenability test and analysis	77
4.4	52100 gas quench hardenability test.....	82
4.5	Pyrowear53 gas quench hardenability test and gas quench steel hardenability simulation.....	87
4.6	Gas pressure and velocity influence on gas quench hardenability test.....	89
4.7	Sample diameter influence on gas quench hardenability test	93
4.8	Summary and Conclusion	95
5	Controllable gas quench process.....	96
6	Summary and Conclusion	101

Figures

Figure 1.1 Process of heat treatment cycle	1
Figure 1.2 Crystal structures of steel microstructure	2
Figure 1.3 ALD gas quench system ⁴	3
Figure 1.4 Solar Atmosphere gas quench system ⁴	3
Figure 1.5. HTC of different quench media (experiment)	5
Figure 1.6 Grossmann hardenability ⁴	7
Figure 1.7 Jominy end quench test setup ²	8
Figure 1.8 Hardness measurement	8
Figure 1.9 Jominy hardenability ⁴	8
Figure 1.10 Solar Atmosphere Jominy gas quench test (room pressure)	9
Figure 1.11 Solar Atmosphere Jominy quench test (high pressure) 12	10
Figure 1.12 IWT Jominy quench test.....	10
Figure 1.13 Achievable hardenability curves for steel grades 90MnCrV8 after gas end quenching (with different cooling parameters) and standard Jominy testing ¹³	11
Figure 1.14 CHTE gas quench test device.....	12
Figure 1.15 The sketch of CHTE gas quench test device.....	12
Figure 1.16 CHTE Jominy gas quench test result.....	13
Figure 1.17 Water Jominy quench sketch.....	14
Figure 1.18 Gas Jominy quench sketch	14
Figure 1.19 Gas Jominy quench sketch with insulation	14
Figure 1.20 Comparison between air cooling and insulation influence under gas quench condition	15
Figure 1.21 Hardenability test modification for high hardenability steel.....	16
Figure 1.22 Gas quench Jominy test under low HTC (500 W/m ² C) gas quench	17
Figure 1.23 Gas quench Jominy test under high HTC (2000 W/m ² C) gas quench	17
Figure 2.1. Grossmann quench model sketch	23
Figure 2.2 Heat transfer coefficient calculation.....	24
Figure 2.3. 4140 cooling profile comparison between experiment and simulation.....	25
Figure 2.4. 4140 cooling profile comparison (simulation)	26
Figure 2.5. 4140: equivalent gas quench HTC compared to oil quench (simulation)	28
Figure 2.6. 4140 cooling profile comparison (simulation)	28
Figure 2.7. Jominy quench model sketch.....	29
Figure 2.8. 4140 Jominy test: cooling profile comparison (simulation).....	30
Figure 2.9. 4140 Jominy test comparison (simulation).....	30
Figure 2.10. 52100 Jominy test: cooling profile comparison (simulation).....	32
Figure 2.11. 52100 Jominy test comparison (simulation).....	32
Figure 2.12. 4140 cooling curve comparison between water and gas quench (simulation)	33
Figure 2.13. Microstructure comparison between water quench and gas quench (simulation).....	34
Figure 3.1 4140 TTA diagram generated by JMatPro	37
Figure 3.2 Holding time effect on grain size generated by JMatPro	38

Figure 3.3 The chemical composition of AISI 4140 ¹⁹	39
Figure 3.4 Variation of chemical elements impact on 4140 TTT diagram generated by Jmatpro.....	40
Figure 3.5 4140 TTT diagram based on different grain size generated by JMatPro	41
Figure 3.6 4140 CCT diagram based on different grain size	41
Figure 3.7 Grain size effect on martensite formation generated by JMatPro	42
Figure 3.8 Furnace and thermocouple	44
Figure 3.9 Jominy end quench test	44
Figure 3.10 4140 Jominy end quench test in the lab.....	45
Figure 3.11 8620 Jominy end quench test in the lab.....	46
Figure 3.12 Cooling rate comparison between experiment (Timken) and simulation for Jominy water quench	47
Figure 3.13 HTC curves of different quench media	48
Figure 3.14 Cooling rate of different quench media in Jominy test	49
Figure 3.15 Cooling rate of Jominy test.....	50
Figure 3.16 4140 phase simulation for Jominy test	50
Figure 3.17 4140 TTT diagram.....	51
Figure 3.18 4140 phase percentages simulation in water and gas for Jominy test	51
Figure 3.19 4140 Jominy hardenability comparison.....	53
Figure 3.20 4340 Jominy hardenability comparison.....	53
Figure 3.21 1020 Jominy hardenability comparison.....	54
Figure 3.22 5120 Jominy hardenability comparison.....	54
Figure 3.23 Photomicrograph and corresponding chart showing abrupt transition from predominantly martensitic to predominantly pearlite microstructure ²⁰	56
Figure 3.24 Hardnesses at the centers of quenched round bars in progressively larger sizes, one series quenched in oil, one series quenched in water ²⁰	56
Figure 3.25 Hardness of quenched structures containing 50% Martensite, for different carbon contents ²⁰	57
Figure 3.26 Austenite theoretical XRD pattern	59
Figure 3.27 As quenched Martensite theoretical XRD pattern.....	59
Figure 3.28 Ferrite theoretical XRD pattern	60
Figure 3.29 XRD comparison between hot mounted and cold mounted samples	61
Figure 3.30 52100 Test6 XRD pattern for cold mounted sample after different grit	62
Figure 3.31 The full range XRD pattern of Test6: 52100 steel austenizing 1050C for 40min – water quench – cut - cold mounted– ground and polished – etched with 4% nital	65
Figure 3.32 64-72 degree XRD pattern of Test6: 52100 steel austenizing 1050C for 40min – water quench – cut - cold mounted– ground and polished – etched with 4% nital	66
Figure 3.33 100-110 degree XRD pattern of Test6: 52100 steel austenizing 1050C for 40min – water quench – cut - cold mounted– ground and polished – etched with 4% nital	67
Figure 3.34 Part2-1 microstructure: 52100 steel austenizing 850C for 40min – 810 W/m ² C gas quench – cut - cold mounted– ground and polished – etched with 4% nital	68

Figure 3.35 1045 XRD pattern when different tempering temperature is applied --peak (011).....	69
Figure 3.36 Lattice parameter and line profile parameter of 1045 steel tempering.....	69
Figure 4.1 The sketch of critical HTC test.....	72
Figure 4.2 Praxair gas quench system sketch	73
Figure 4.3 Praxair gas quench system ³⁰	74
Figure 4.4 Praxair gas quench system assembly ³⁰	75
Figure 4.5 Praxair gas quench sample sketch ³⁰	76
Figure 4.6 4140 gas quench HTC	77
Figure 4.7 4140 gas quench critical HTC test result.....	78
Figure 4.8 4140 cooling profile comparison between test and simulation	79
Figure 4.9 4140 critical HTC comparison between test and simulation.....	80
Figure 4.10 4140 CCT diagram	81
Figure 4.11 52100 gas quench critical HTC test result.....	82
Figure 4.12 Gas quench HTC for 52100 tests.....	82
Figure 4.13 52100 CCT diagram	83
Figure 4.14 Hardness result for tests.....	83
Figure 4.15 T10 Microstructure: 52100 steel austenizing 850C for 40min – 579 W/m ² C gas quench – cut - hot mounted – ground and polished – etched with 4% nital.....	84
Figure 4.16 T11 microstructure: 52100 steel austenizing 850C for 40min – 788 W/m ² C gas quench – cut - hot mounted– ground and polished – etched with 4% nital.....	85
Figure 4.17 T12 microstructure: 52100 steel austenizing 850C for 40min – 983 W/m ² C gas quench – cut - hot mounted– ground and polished – etched with 4% nital.....	86
Figure 4.18 Critical HTC for steels.....	87
Figure 4.19 Simulated critical HTC for different steels	87
Figure 4.20 HTC and hardness result for gas quench.....	89
Figure 4.21 4140 cooling curves for gas quench under the same HTC.....	90
Figure 4.22 4140 Part2-3 microstructure: 4140 steel austenizing 850C for 40min – 502 W/m ² C gas quench – cut - cold mounted– ground and polished – etched with 4% nital	91
Figure 4.23 4140 part2-4 microstructure: 4140 steel austenizing 850C for 40min – 502 W/m ² C gas quench – cut - cold mounted– ground and polished – etched with 4% nital	92
Figure 4.24 4140: Bar diameter influence on critical HTC	93
Figure 4.25 Critical HTC for different sample geometry	94
Figure 5.1 Marquenching technology ²	96
Figure 5.2 HTC comparison among different quench technology	98
Figure 5.3 Cooling profile comparison between different quench technology	98
Figure 5.4 Gas marquenching distortion.....	99
Figure 5.5 Gas marquenching stress.....	99
Figure 5.6 Oil quench distortion	100
Figure 5.7 Oil quench stress.....	100

1 Introduction

1.1 Quenching of steel

Quenching is the rapid cooling of a workpiece to obtain certain material properties¹. In metallurgy, it is most commonly used to harden steel by introducing martensite². Figure 1.1 is the typical process of heat treatment cycle.

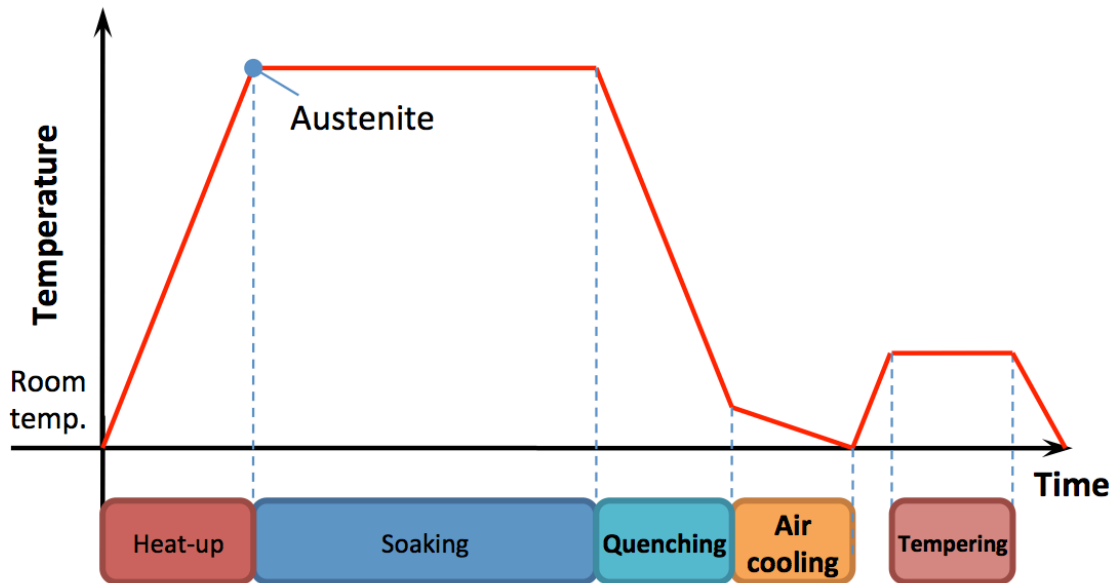


Figure 1.1 Process of heat treatment cycle

During the cooling process, the Austenite with Face Center Cubic (FCC) crystal structure will transform to Martensite with either Body Center Cubic (BCC) or Body Center Tetragonal (BCT) crystal structure. The transformation occurs rapidly and carbon does not have enough time to diffuse from the BCC or BCT crystal structure. This

phenomenon causes the highly distortion of BCC or BCT crystal structures, which is the main reason that the steel is hardened after rapid cooling.

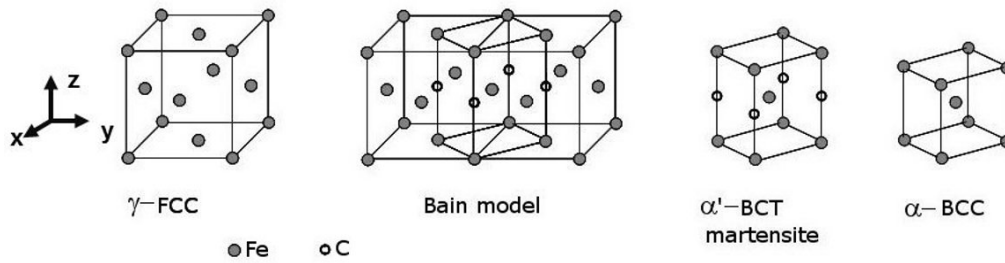


Figure 1.2 Crystal structures of steel microstructure³

The selection of a quenching medium depends on the hardenability of the steel, the shape and thickness, and the cooling rates needed to obtain the desired microstructure¹. The most common quenching media are water, oil, polymer solutions and gases.

1.2 Gas quench technology

The oldest, most common, and least expensive quenching medium is air⁴. Compared to the water and oil quench, the heat transfer coefficient of air is not large enough to quench steels to make 100% Martensite. With the development of the modern steel quench technology, high pressure and high velocity gas quench has been widely used. The heat transfer coefficient of gas quench could be as high as $2000 \text{ W/m}^2\text{k}$ and is large enough to quench high hardenability steels (such as 4340) and some medium hardenability steels (such as 4140 and 52100).

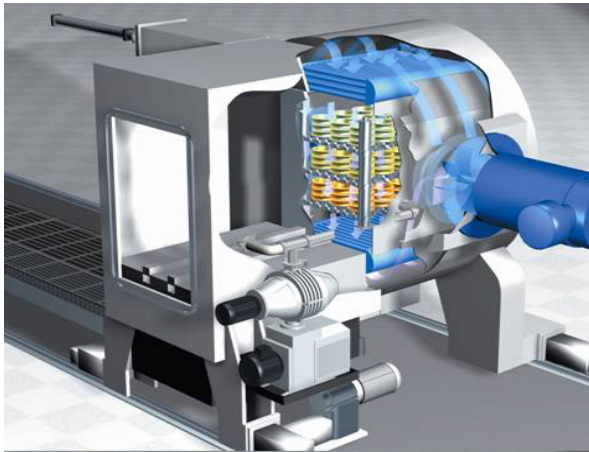


Figure 1.3 ALD gas quench system⁴



Figure 1.4 Solar Atmosphere gas quench system⁴

Figure 1.3 and Figure 1.4 present two different gas quench system. ALD system uses fans to generate high pressure and velocity gas flow, while the Solar Atmosphere system utilizes nozzles to generate high pressure and velocity gas flow.

One of the significant advantages of gas quench is to get the similar mechanical properties compared to water or oil quench, and reduce the distortion and stress at the same time⁵. Gas quench process usually has lower cooling rates compared to water or oil quench. The more uniform cooling process reduces the distortion caused by the cooling rate difference between the surface and the core of the metal parts. Since the gas pressure, velocity and temperature are more flexible to control compared with water or oil; gas quench process has greater process flexibility to vary cooling rates rapidly based on different necessities. Currently nitrogen is used for gas quench in industry. Compared to oil quench, the gas quench leaves dry and clean parts after quenching process. It is not only more environmental friendly, but also increases the efficiency applying the gas quench process.

Gas quench has various disadvantages. It requires to use high-pressure vessel resulting in high equipment investment⁴. Based on the relatively low heat transfer coefficient of gas quench, low hardenability steels (carbon steels) cannot be used for gas quench. The high pressure and velocity gas also cause high noise levels⁴. Currently, the gas quench technology is only applied for medium and high hardenability steels.

The comparison between liquid and gas quench process has been studied. Current studies are focused on the gas flow in the furnace. Based on the work of previous work⁶⁷⁸⁹, the gas pressure and velocity changes dramatically in the furnace. The uniformity of gas quench process is an issue compared with liquid quench.

Considering the complicated flow pattern of gas pressure and velocity, the gas quench heat transfer coefficient (HTC) is noted, since the HTC has direct influence on cooling curves⁴.

HTC is the only difference between liquid quench and gas quench. The chemical reaction of gas with the steel surface is ignored in the thesis.

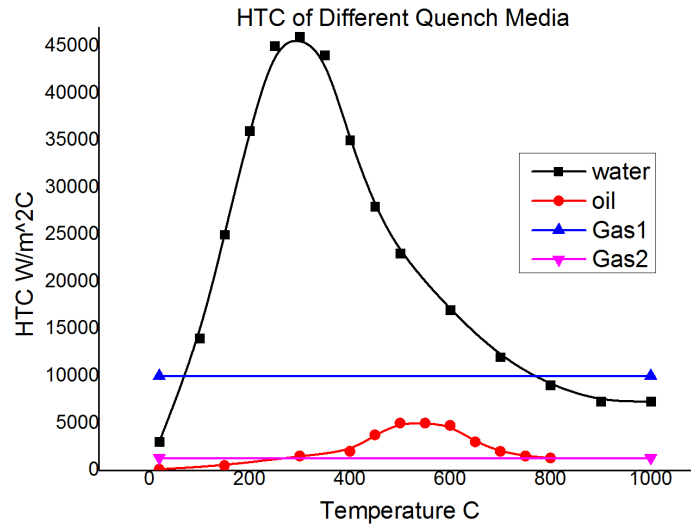


Figure 1.5. HTC of different quench media (experiment)

Figure 1.5 is the HTC of different quench media. Liquid quench exhibits three characteristic quenching processes, film boiling, bubble boiling and convection¹⁰. For gas quench, the single-phase heat transfer process means that the cooling rate is more uniform⁴. The concept of the equivalent HTC will be proposed and discussed in the thesis.

1.3 Steel hardenability test

Hardenability is the ability of the Fe-C alloy to be hardened by forming martensite. It is qualitative measure of the rate at which hardness decreases with distance from the surface because of decreased martensite content ⁴.

Steel hardenability test is used to select proper steel for different purpose. For example, for large workpiece, high hardenability steel is often selected to ensure the core can be hardened.

Based on the previous discussion, not all the steel can be used for gas quench, such as low hardenability steel. In order to select proper steel for gas quench, the gas quench steel hardenability needs to be defined and measured, however, no standard gas quench steel hardenability test is widely accepted by industry.

Many methods exist to measure hardenability, which including Grossmann's method, Jominy bar end-quench test, SAC rating, P-F test and etc. The most familiar and commonly used procedures are Jominy test and Grossmann's method.

Grossmann's method of measuring hardenability uses a number of cylindrical steel bars of different diameters hardened in a given quenching medium. After sectioning each bar at mid-length and examining it metallography, the bar that has 50% martensite at its center is selected, and the diameter of this bar is designated as the critical diameter ⁴.

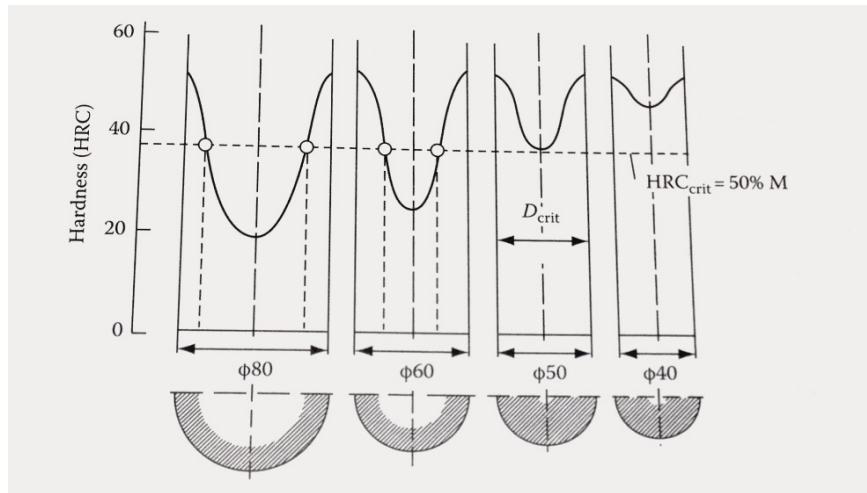
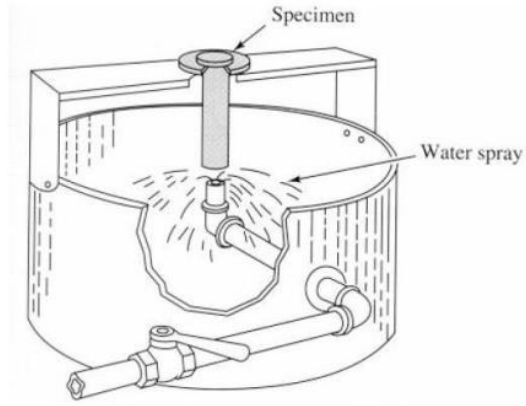


Figure 1.6 Grossmann hardenability ⁴

The Jominy bar end-quench test is the most familiar and commonly used procedure for measuring steel hardenability. This test has been standardized and is described in ASTM A 255, SAE J406, DIN 50191, and ISO 642.

For this test, a 100mm long by 25mm diameter round bar is austenitized to the proper temperature, dropped into a fixture, and one end rapidly quenched with 20-25°C water from a 12.5mm orifice under specified conditions. The austenizing temperature is selected according to the specific steel alloy. Cooling velocity of the test bar decreases with increasing distance from the quenched end. After quenching, parallel flats are ground on opposite sides of the bar and hardness measurements made along the bar as illustrated below ⁴.



Jominy End Quench Test Setup

Figure 1.7 Jominy end quench test setup²

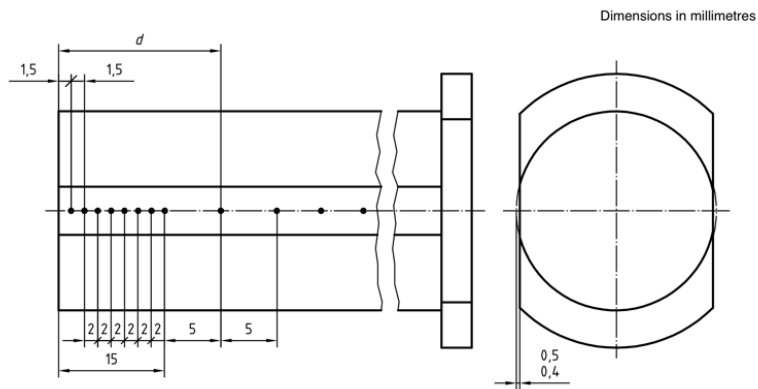
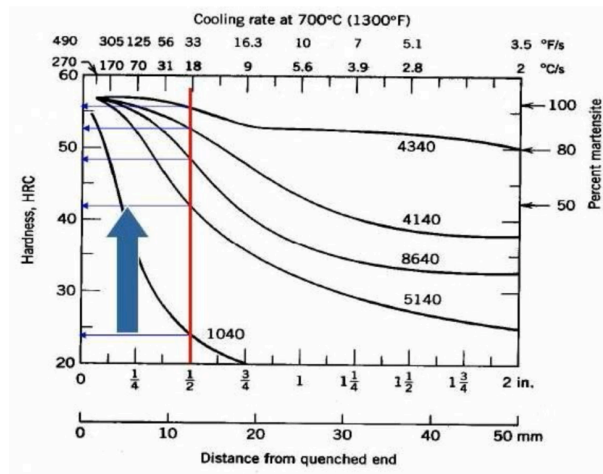


Figure 1.8 Hardness measurement¹¹



Hardenability curves for different grade of steels

Figure 1.9 Jominy hardenability⁴

1.4 Gas quench hardenability test

1.4.1 Current gas quench steel hardenability test

Since water quench Jominy test is widely used in industry, the current gas quench steel hardenability tests are based on the prototype of Jominy test. Figure 1.10, Figure 1.11 and Figure 1.12 are all current Jominy gas quench steel test.

Figure 1.10 test is designed by Solar Atmosphere¹². The device can generate high velocity gas with room pressure. In Figure 1.11 test, also designed by Solar Atmosphere¹², high pressure and high velocity gas can be generated for gas quench, however the gas velocity cannot be controlled and the gas flow is not steady¹². The Figure 1.12 test, designed by IWT¹³, uses insulation brick around the Jominy bar during gas quench process, in order to prevent the side-flow gas cools the sample. Figure 1.13 presents the gas quench hardenability test result from IWT system¹³.



Figure 1.10 Solar Atmosphere Jominy gas quench test (room pressure)¹²

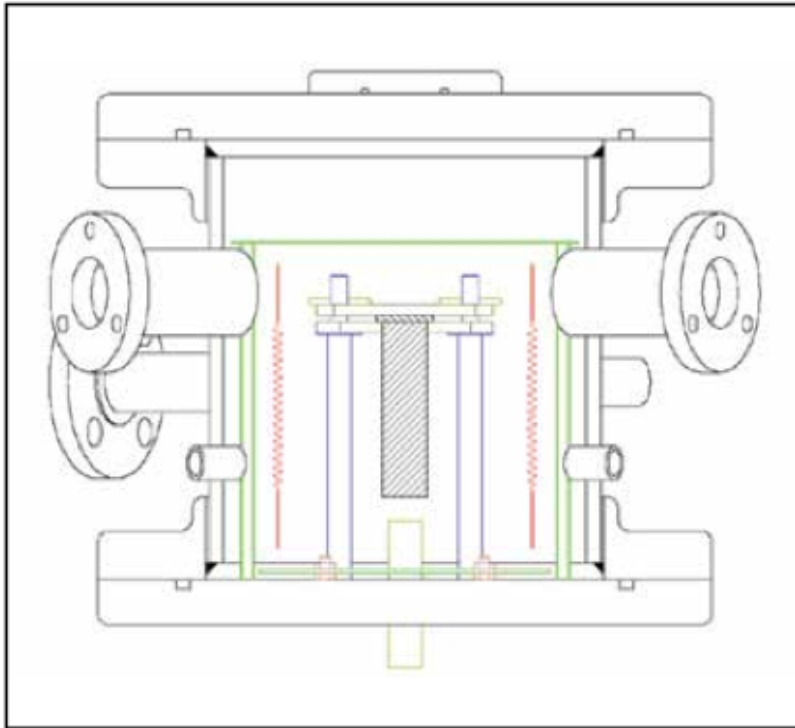


Figure 1.11 Solar Atmosphere Jominy quench test (high pressure) 12

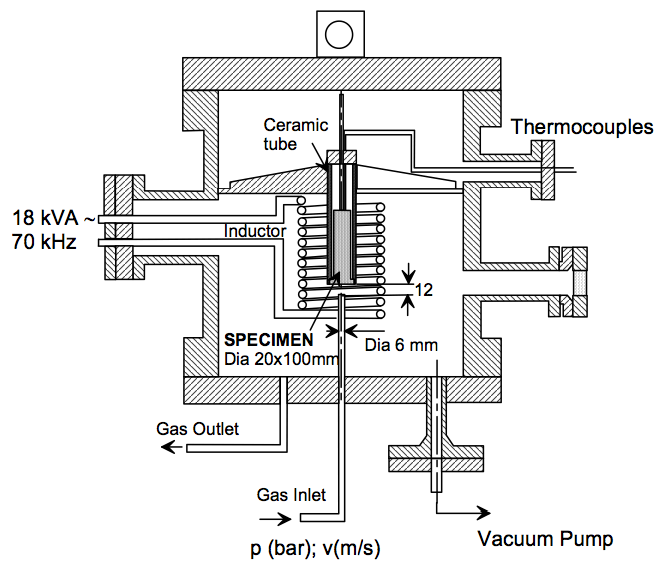


Figure 1.12 IWT Jominy quench test¹³

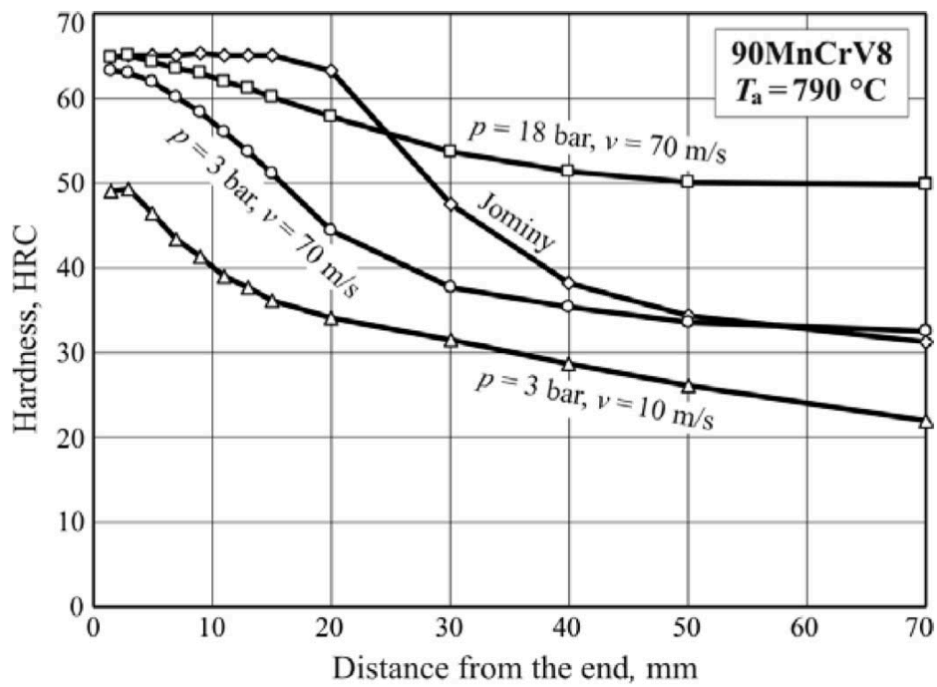


Figure 1.13 Achievable hardenability curves for steel grades 90MnCrV8 after gas end quenching (with different cooling parameters) and standard Jominy testing¹³

The CHTE gas quench device, which is similar to Solar Atmosphere, is built in Worcester Polytechnic Institute. The gas is compressed air.



Figure 1.14 CHTE gas quench test device

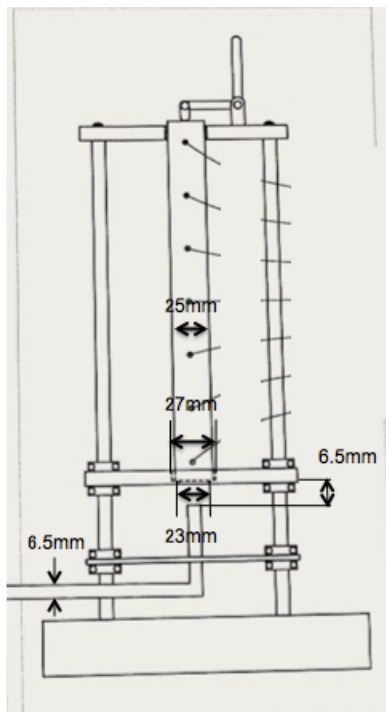


Figure 1.15 The sketch of CHTE gas quench test device

The fixture could be adjusted and changed for the sample with different length and diameter. The bolt on the top of the fixture is to fix the sample in position when the high-pressure air is applied. The experiments were conducted at room pressure. Figure 1.16 is the test result of high velocity gas quench process.

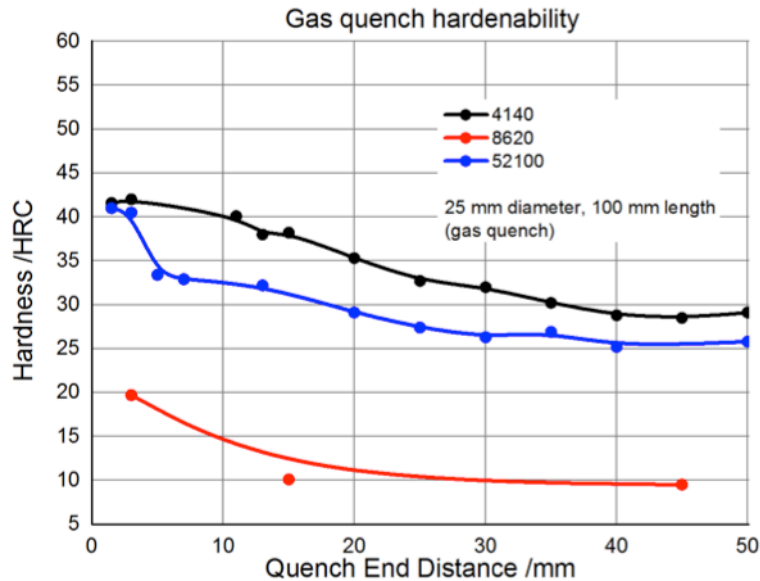


Figure 1.16 CHTE Jominy gas quench test result

1.4.2 Limitation and possible improvement of current gas quench steel hardenability test

In water quench test, the HTC of water spray is much higher than air cooling at the side of the Jominy bar. The heat transfer is assumed one-dimensional. In gas quench test, the HTC is relatively low, so the air cooling at the side of the sample will also have effect on the cooling profile. In Figure 1.20, the cooling rate of side insulation sample is much lower than side air cooling sample. The hardenability curves changes when insulation is considered. Solar Atmosphere test (room pressure) and Solar Atmosphere test (high pressure) can add insulation to prevent the gas side flow effect, just like IWT system.

Figure 1.17 is the water Jominy quench sketch. The water flow does not quench the sample side, since its dead weight. Figure 1.18 is the gas Jominy quench sketch. The gas flow does not only quench the end of the bar, but also the side of the bar. In order to reduce the side flow effect, the insulation around the bar should be added. Figure 1.20 presents the hardenability curve comparison between sample without insulation and with insulation during the same gas quench condition. It should be noted that insulation layer couldn't perfect insulate all the heat flux from the sample side. When low gas quench HTC condition is applied, the heat flux from the sample side would still break the ideal 1D heat transfer assumption.

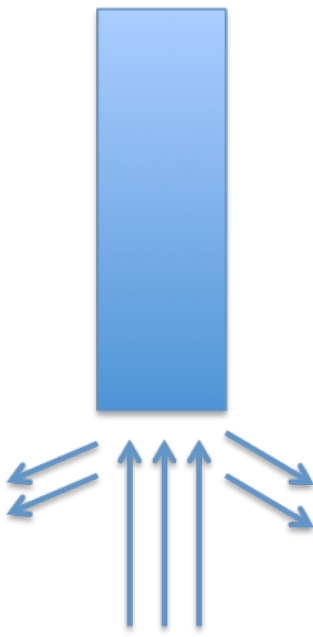


Figure 1.17 Water Jominy quench sketch

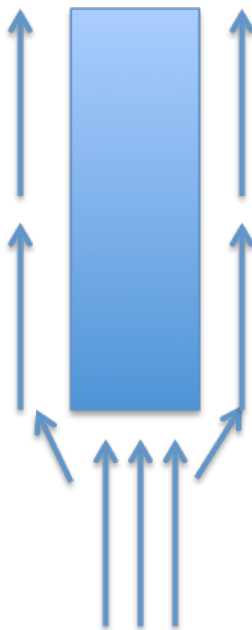


Figure 1.18 Gas Jominy quench sketch

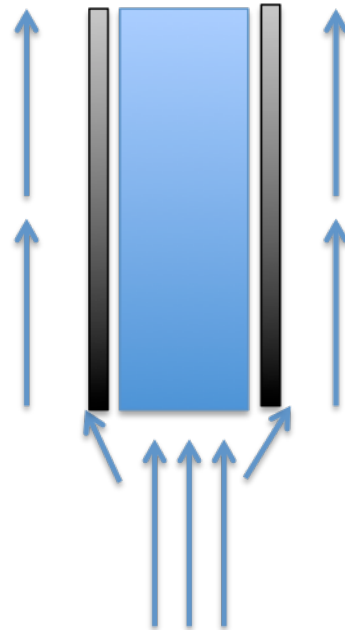


Figure 1.19 Gas Jominy quench sketch with insulation

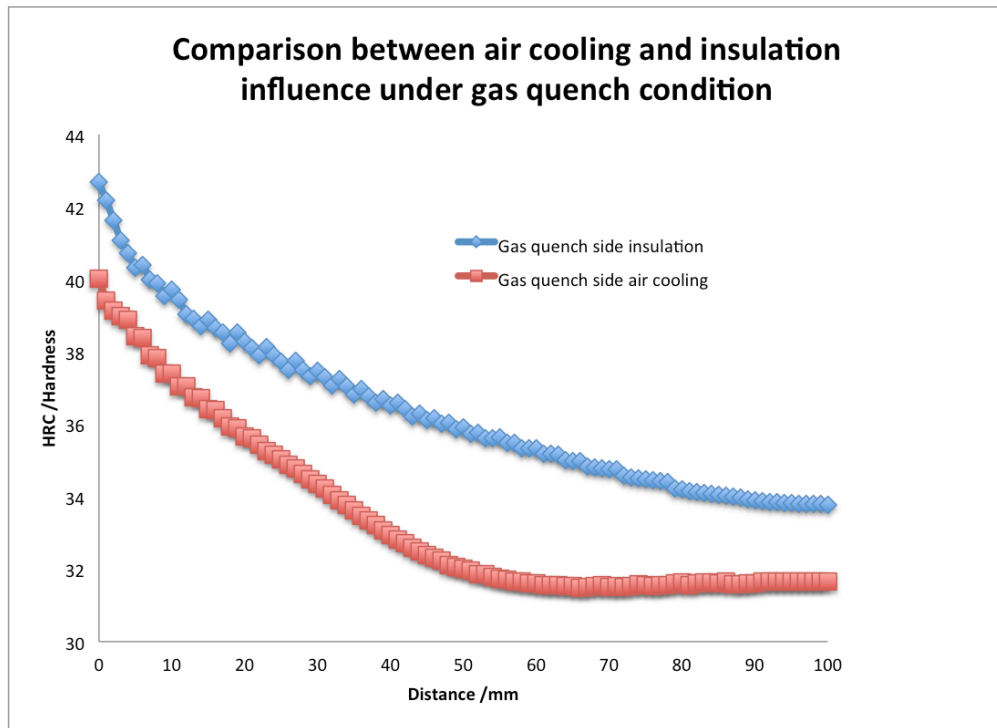


Figure 1.20 Comparison between air cooling and insulation influence under gas quench condition

Based on Solar Atmosphere’s work¹², Figure 1.11 device was built. After multiple tests, they discovered that they could not successfully control the velocity of gas impinging upon the end of the test bar within the furnace¹². Additionally, the gas flow could not be maintained due to the restrictions of the gas inherent to the small chamber¹². In IWT’s test, the gas also directly impinges the quenched end. Under this condition, the gas pressure and velocity along the quenched surface is not uniform. Non-uniform gas pressure and velocity means unsteady heat transfer coefficient (HTC) during gas quench steel hardenability test. The gas quench steel hardenability under this condition cannot be well defined, analyzed and repeated. Applying 45° or other inclination angle may increase the uniformity of gas pressure and velocity.

Another limitation is that very low cooling rate cannot be achieved using standard Jominy bar. For steels such as 4340 and Pyrowear53 (high hardenability steel), very low

cooling rate is needed to test its high hardenability limitation. From the simulation, even after insulation at the sample side is added, very low cooling rate such as 1C/s cannot be reached in standard Jominy bar. At this condition, the far end of Jominy bar is still fully hardened. Figure 1.21 presents the method to decrease the cooling rate by adding mass at the opposite end of the sample. However, for different steels, the geometry of the “cap” should be different.

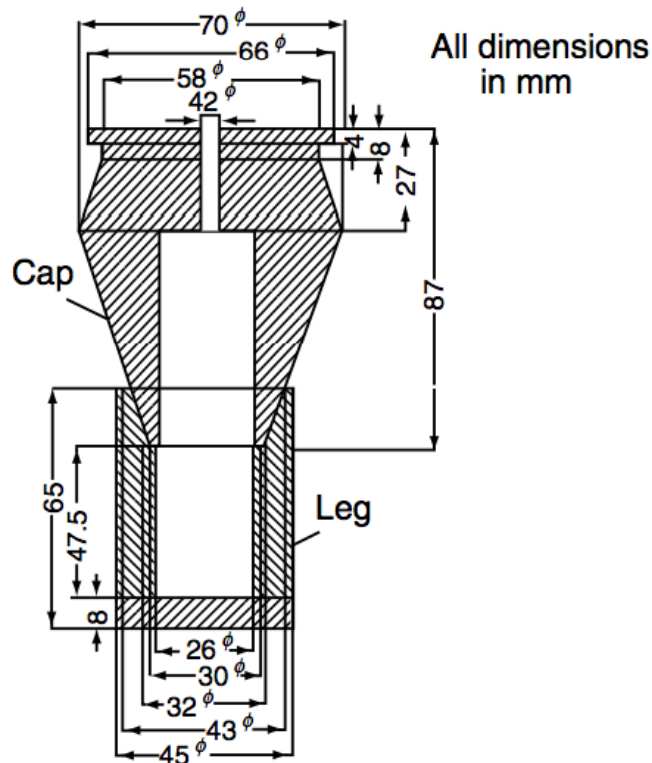
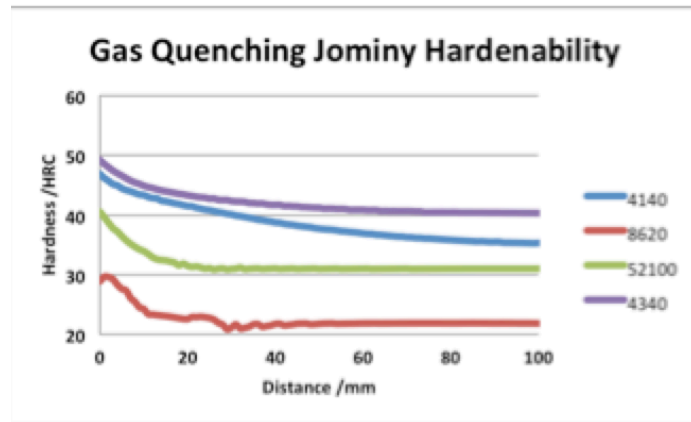


Figure 1.21 Hardenability test modification for high hardenability steel¹⁴

Although many improvements were made to modify Jominy gas quench test, the fundamental limitations of this method still exist.

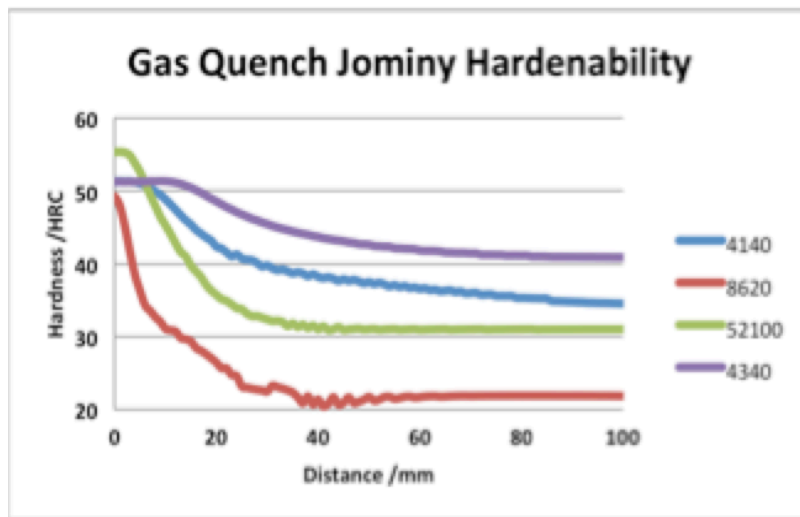
Low hardenability steel (8620), medium hardenability steel (4140) and high hardenability steel (4340) can be tested by the Jominy water quench test, applying the same water spray

(same HTC) quench condition. However, in Jominy gas quench test, one gas quench condition cannot be used for both low hardenability steel and high hardenability steel at the same time.



*Low pressure and velocity gas quench
(Low HTC)*

Figure 1.22 Gas quench Jominy test under low HTC ($500 \text{ W/m}^2\text{C}$) gas quench



*High pressure and velocity gas quench
(High HTC)*

Figure 1.23 Gas quench Jominy test under high HTC ($2000 \text{ W/m}^2\text{C}$) gas quench

The simulation results based on Abaqus and Dante are shown in Figure 1.22 and Figure 1.23. From the results, the hardenability of 8620 (low hardenability steel) cannot be revealed when low HTC gas quench condition is applied, since even the quenched end cannot form martensite at low cooling rate. Although the hardenability of 4340 (high hardenability steel) can be measured under high HTC gas quench condition, 4340 still shows high hardenability under low HTC gas quench conditions.

For low hardenability steels such as 8620, high HTC gas quench condition should be used to ensure martensite could be formed at the quenched end. For high hardenability steels such as 4340, low HTC gas quench condition should be used to reveal its complete ability to be hardened at low cooling rate.

Figure 1.13 also reveals the limitations of modified Jominy gas quench hardenability test. The same steel grades, 90MnCrV8, has different hardenability curves under different gas quench conditions. If different steel grades need to be compared, the same gas quench condition should be used to obtain the same quenched end HTC. It is pointed out that for different steel grades, different gas quench condition (different HTC) should be used. As a conclusion, the modified Jominy gas quench steel hardenability test cannot be used to identify the gas quench steel hardenability

1.5 Objectives

This work is dedicated to have the fundamental understanding of gas quench process and gas quench hardenability. Specifically, the objectives of this work are:

1) Comparison between liquid quench and gas quench

The liquid quench (water and oil) quench has been thoroughly discussed ⁴. The fundamental difference between liquid quench and gas quench is the HTC. For liquid quench HTC, the scale is large and shape varies due to different liquid phase transformation during quench process. For gas quench HTC, the scale is relatively small and the shape is a horizontal line due to single phase during the whole quench process. The equivalent HTC for gas and liquid quench is proposed in the thesis.

2) The steel hardenability test for gas quench

Hardenability is the key property of steel to access whether the specific steel is suitable for quench process. The Jominy and Grossmann water quench steel hardenability tests have been successfully used by industry to define what steel is suitable for liquid quench process. When gas quench is applied, the steel hardenability test needs to be redefined. Based on the previous discussion, the current modified Jominy gas quench steel hardenability test cannot be utilized. A new gas quench steel hardenability is proposed in the thesis and used to classify proper gas quench steel.

3) The possibility to apply controllable quench process using gas quench.

Since gas quench has greater process flexibility to vary cooling rates, the controllable quench process is proposed based on the gas quench. The process is to control the gas quench HTC and achieve the desired cooling rates and cooling curves. The controllable quench process will generate the desired microstructure for specific purposes, such as 100% martensite with lowest cooling rates and lowest distortion.

1.6 Thesis Organization

In chapter 2, the comparison between liquid quench and gas quench is discussed. A concept of equivalent HTC is proposed to compare liquid and gas quench.

In chapter 3, the influence factors on steel hardenability are discussed. 50% martensite hardness is an important concept for steel hardenability. A new method to determine 50% martensite microstructure based on X-ray diffraction and Rietveld Refinement method is proposed.

In chapter 4, the critical HTC test for gas quench steel hardenability, based on Grossmann's test is proposed. The test result proves this method has many advantages compared to the modified Jominy gas quench test and can be used as gas quench steel hardenability standard.

In chapter 5, the possibility to apply controllable quench process using gas quench is discussed.

2 Comparison between liquid and gas quench

The fundamental difference between liquid and gas quench is heat transfer coefficient of quench media. In this chapter, the HTC and cooling curve comparison between liquid and gas quench is conducted. The concept of equivalent HTC is proposed to compare liquid and gas quench. In industry, same hardness is often used to indicate same microstructure and mechanical properties. It is pointed that after gas quench, the workpiece, which has the same hardness compared with liquid quench, may have different microstructure.

2.1 Grossmann quench model

In order to compare the liquid and gas quench, the Grossmann quench model based on Dante and Abaqus is build, presented in Figure 2.1. The cylinder sample with 25mm diameter and 100mm length is used. The gas flow is assumed to be the same at the free end of the sample and the sample sides, since the slenderness ratio is large. Gas flow is assumed as laminar flow. In this condition, the gas pressure and velocity are steady during gas quench process.

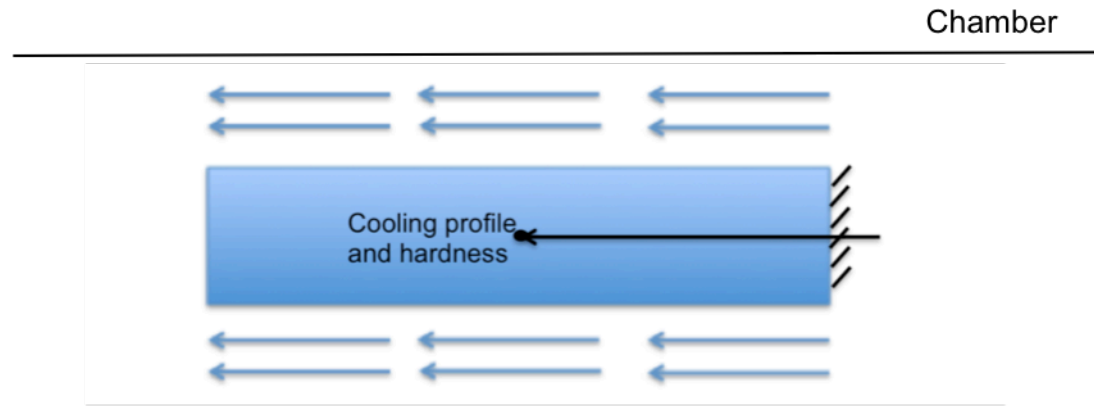


Figure 2.1. Grossmann quench model sketch

The experiments are done with the help of Praxair and the liquid and gas quench simulation model (based on Abaqus and Dante) is developed with the help of Dante. The steel is 4140 in the experiment.

2.2 HTC measurement and model verification

In the experiment, the high pressure and high velocity nitrogen gas is used. Chamber pressure and gas temperature inside chamber is measured. The gas velocity is calculated based on the gas flow rate, since the chamber geometry is fixed. In the simulation, the HTC is the input of the simulation model.

Step		Parameters
1)	Specify gas type, chamber pressure, and gas temperature inside chamber	Gas MW P_{gas} (Pa) T_{gas} (K)
2)	Determine gas compressibility and density @ (T_{gas} , P_{gas})	$Z = F(T_{\text{gas}}, P_{\text{gas}})$ $\rho = P/ZRT$ (kg/m ³)
3)	Determine gas properties @ (T_{gas} , P_{gas}) (Based on gas tables or empirical curves for properties: F(T,P))	Dynamic viscosity, μ (kg/m-s) Thermal Conductivity, k (W/m-K) Gas Specific Heat, C_p (J/kg-K)
4)	Calculate Prandtl Number (Pr)	$Pr = (\mu \cdot C_p / k)$
5)	Specify characteristic length (part diameter) circulating gas velocity (fan power)	L (m) V (m/s)
6)	Calculate Reynolds Number (Re_L)	$Re_L = (\rho V L / \mu)$

Step		Parameters
7)	Calculate Nusselt Number (Nu_L) = $0.0296(Re_L)^{(4/5)} * (Pr)^{(1/3)}$ (turbulent flow, $0.6 < Pr$)	$(Nu_L) = hL/k_{\text{gas}}$
8)	Calculate convective heat transfer coefficient from (Nu_L) calculated in Step (7). (T_{gas} is held constant as first approximation; therefore, h is NOT a function of T_{load}). T_{gas} is a weak function of T_{load} since T_{gas} increases during initial quench period, but is cooled by chamber heat exchangers through the quench process and as T_{load} drops during quenching)	$h = Nu_L k_{\text{gas}} / L = (W/m^2-K)$
9)	Calculate load surface heat flux, q'' at decreasing T_{load} points. (q'' is a function of heat transfer coefficient, T_{load} and T_{gas})	$q'' = h(T_{\text{load}} - T_{\text{gas}}) = (W/m^2)$
10)	Compare q'' for different gases, P_{gas} , T_{gas} , and V	

Figure 2.2 Heat transfer coefficient calculation¹⁵

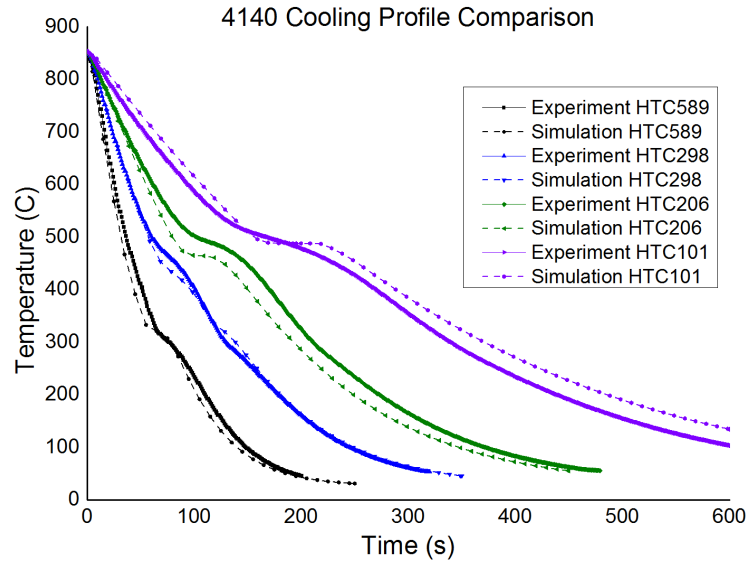


Figure 2.3. 4140 cooling profile comparison between experiment and simulation

The cooling curves under different gas quench condition are measured by thermocouple and simulated by liquid and gas quench model. The simulation results match the experimental result and it demonstrates the accuracy of the model.

In the simulation, the ambient temperature, transfer time from the heating furnace to the quenching chamber and the time required to reach the desired pressure and gas flow speed are considered.

2.3 Equivalent gas quench HTC prediction based on Grossmann quench model

The verified Grossmann quench model is used to simulate the liquid and gas quench process and predict the equivalent HTC.

The equivalent HTC between liquid and gas quench is defined as the HTC, which has the same cooling curves at the core of the sample. After two different quench processes, if the cooling curves of the core are the same, these two quench HTCs are considered as the equivalent HTC.

Oil quench and gas quench are compared in the thesis. The HTCs of oil quench and gas quench are from Figure 1.5.

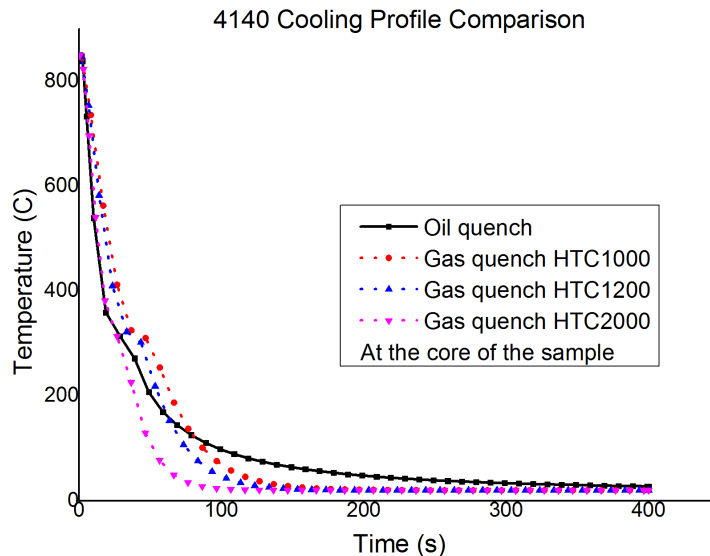


Figure 2.4. 4140 cooling profile comparison (simulation)

Figure 2.4 (simulation) is the cooling profile comparison between oil quench and gas quench. The cooling profiles of different gas quench HTCs are simulated to match the cooling profile of oil quench. For gas quench HTC 1000 W/m²C (constant from 20C to 1000C) and HTC 1200 W/m²C (constant from 20C to 1000C), the cooling rates from 850C to 200C is lower than oil quench. In order to increase the cooling rates from 850C to 200C, the gas quench HTC 2000 W/m²C is used. The cooling curves for HTC 2000 W/m²C (constant from 20C to 1000C) matches the oil quench from 850C to 300C. From 300C to 20C, the cooling rates for gas quench 2000 W/m²C is higher than oil quench. No gas quench with constant HTC can become the equivalent HTC compared to oil quench. It should be pointed out that the steel would only have the same microstructure with the same cooling history (cooling curve).

One of the advantages of gas quench is great process flexibility that allows to vary cooling rates by adjusting gas pressure and velocity. Gas quench with varying HTCs are considered to find the equivalent HTC compared to oil quench.

The HTC shown in Figure 2.5 (simulation) is the equivalent HTC for oil quench. From 1000C to 300C, the HTC is 2000 W/m²C. From 300C to 180C, the HTC is 1200 W/m²C. From 180C to 100C, the HTC is 500 W/m²C. From 100C to 20C, the HTC is 100W/m²C. At each stage, the gas quench HTC is the constant. Figure 2.6 (simulation) are the cooling profiles of oil quench and equivalent gas quench at the core of the sample. Gas quench with varying HTCs is the equivalent HTC compared to liquid quench.

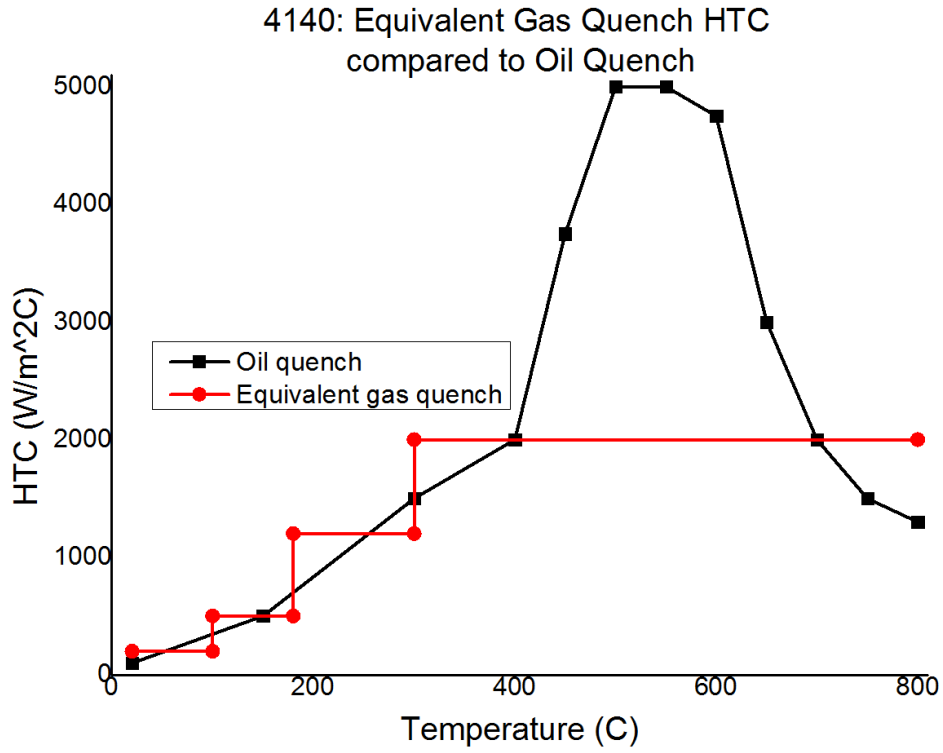


Figure 2.5. 4140: equivalent gas quench HTC compared to oil quench (simulation)

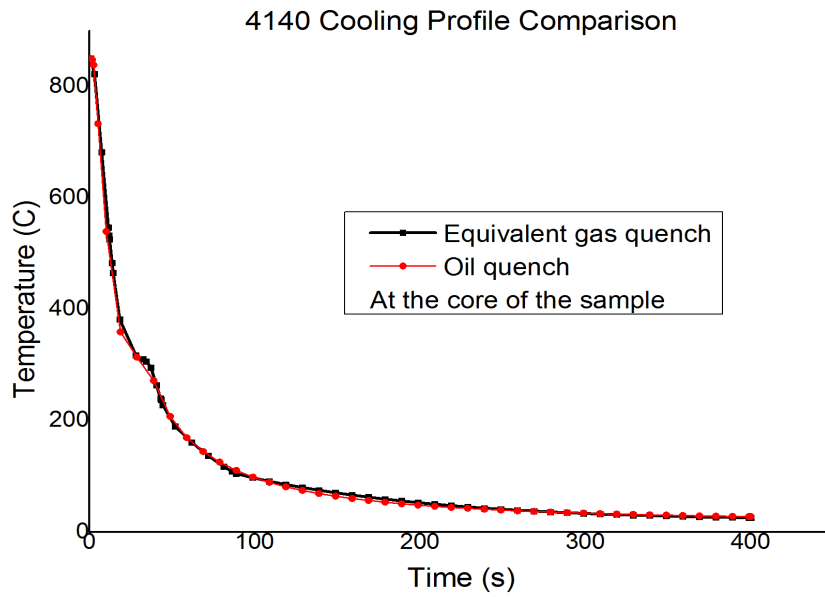


Figure 2.6. 4140 cooling profile comparison (simulation)

Simulation based on Jominy test is finished to extent the concept of the equivalent HTC. The sketch is shown in Figure 2.7. The Jominy bar is 25mm diameter and 100mm length. Boundary conditions 2,3 and 4 are air-cooling and boundary condition 1 is oil quench or equivalent gas quench in Figure 2.5. The temperature profile and the Jominy hardenability (along the black line in Figure 2.7) are compared to verify the equivalency of oil quench and gas quench.

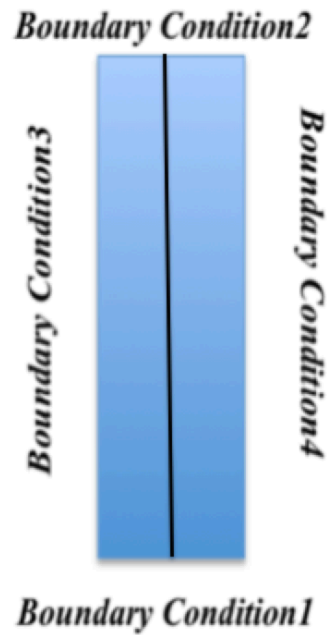


Figure 2.7. Jominy quench model sketch

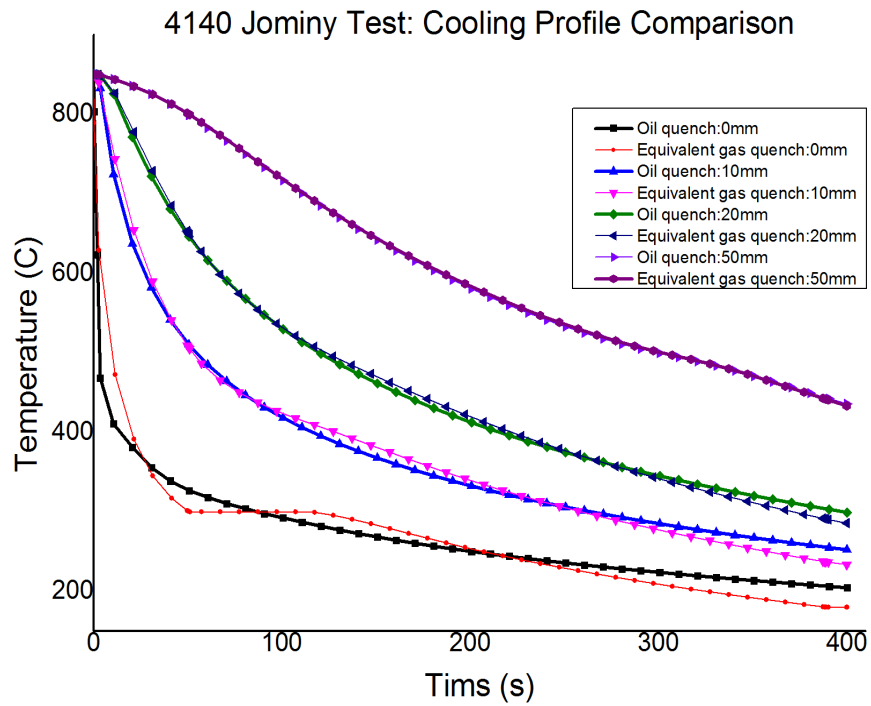


Figure 2.8. 4140 Jominy test: cooling profile comparison (simulation)

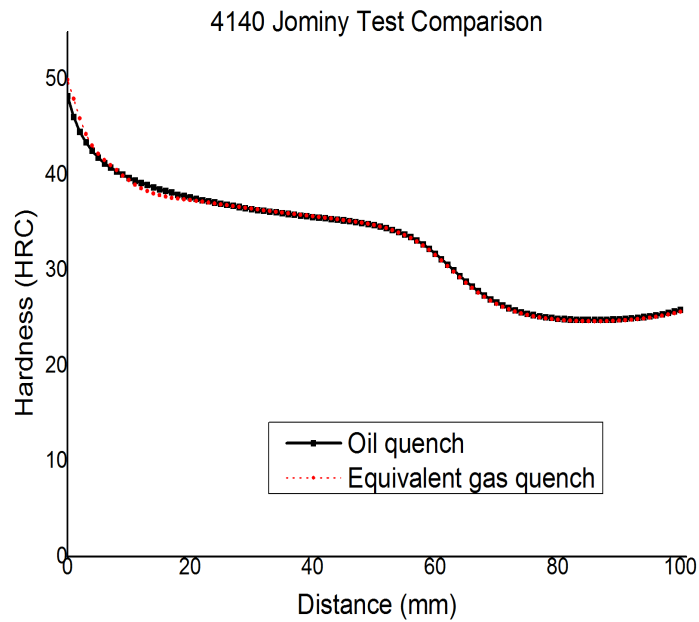


Figure 2.9. 4140 Jominy test comparison (simulation)

In Figure 2.8 (simulation), the cooling profiles along the Jominy bar for oil quench and the equivalent gas quench are compared. At 0mm, 10mm, 20mm and 50mm position from the quenched end, the cooling profiles are considered to be the same for oil quench and the equivalent gas quench. In Figure 2.9 (simulation), the hardenability of 4140 under oil quench and the equivalent gas quench is simulated. Two hardenability curves match perfectly, which demonstrates that the two quench processes generate the same microstructures and properties.

The concept of equivalent HTC should be redefined. After two different quench processes, if the cooling curves, microstructures and properties of all the workpiece are the same, these two quench HTCs are considered as the equivalent HTC.

52100 equivalent gas quench process is simulated as well. The equivalent gas quench HTC is the same as 4140's (in Figure 2.5). The cooling profile comparison and Jominy hardenability for 52100 are in Figure 2.10 (simulation) and Figure 2.11 (simulation).

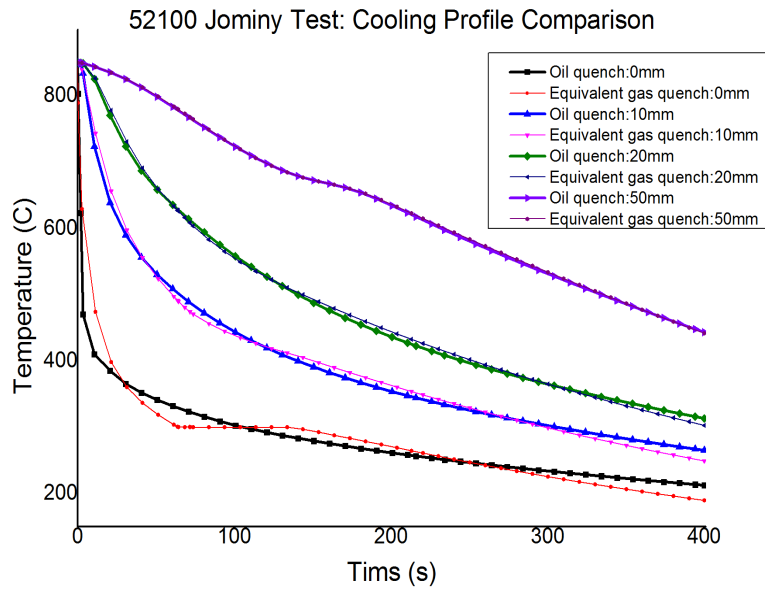


Figure 2.10. 52100 Jominy test: cooling profile comparison (simulation)

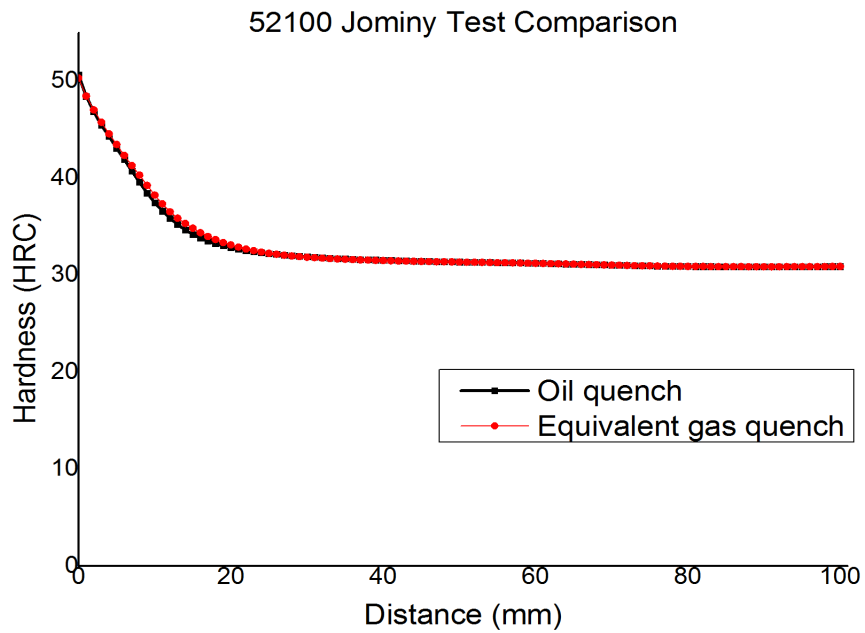


Figure 2.11. 52100 Jominy test comparison (simulation)

2.4 Microstructure and hardness comparison based on Jominy test

In industry, same hardness is often used to indicate same microstructure and mechanical properties. After gas quench, the workpiece may have the same hardness compared with liquid quench. However, the cooling curves are not the same and it leads to different microstructure.

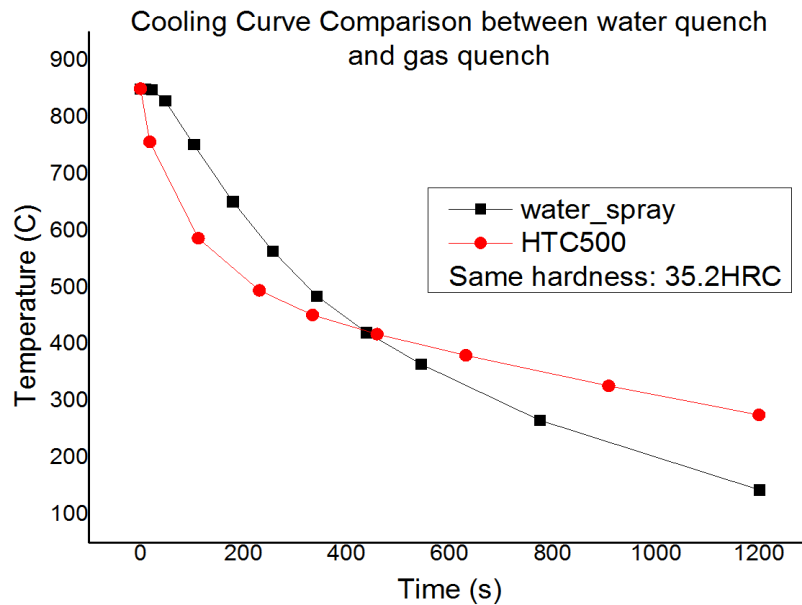


Figure 2.12. 4140 cooling curve comparison between water and gas quench (simulation)

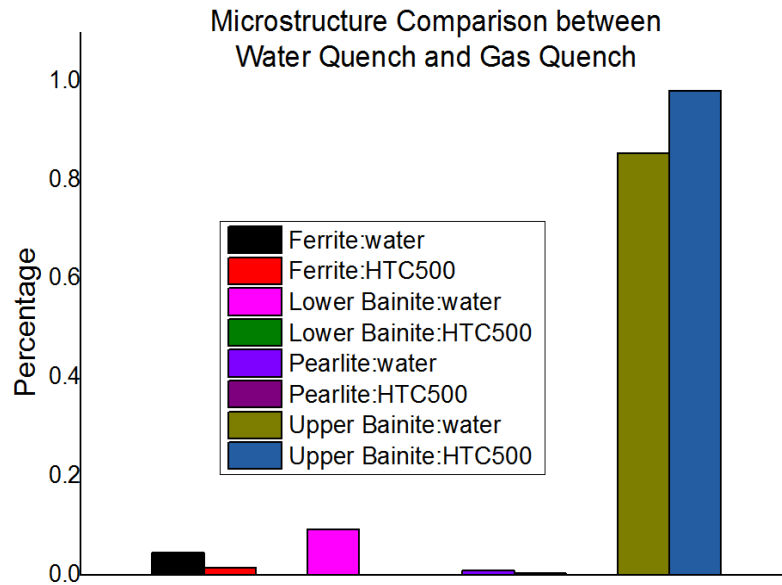


Figure 2.13. Microstructure comparison between water quench and gas quench
(simulation)

In Figure 2.12 (simulation), the black line is from 50mm distance from the quenched end under water quench condition. The red line is from 5mm distance from the quenched end under HTC500 W/m^2C gas quench condition. These two positions have the same hardness, 35.2 HRC with different cooling curves. The microstructure analysis is shown in Figure 2.13 (simulation). The percentage of lower bainite of water quench is higher than gas quench, while the percentage of upper bainite of water quench is lower than gas quench. Generally, the mechanical properties of lower bainite are better than upper bainite, such as strength, toughness and ductility [16].

After liquid quench and gas quench process, the steel with the same hardness may have different microstructure and different mechanical properties.

2.5 Summary and Conclusion

The concept of equivalent HTC, which is the fundamental difference between liquid and gas quench, is established. After two different quench processes, if the cooling curves of the sample core are the same, these two quench HTCs are considered as the equivalent HTC. The equivalent HTC prediction is made based on the Grossmann quench simulation model. It was proved that when compared between oil quench and gas quench, no gas quench with constant HTC can be the equivalent HTC, since the cooling curve cannot be the same as in water quench process. With the great process flexibility to vary cooling rates, gas quench with varying HTCs is proved to be the equivalent HTC.

After determining the equivalent gas quench HTC, Jominy test is simulated to compare the cooling curves and hardness for the entire workpiece. The concept of equivalent HTC is redefined. After two different quench processes, if the cooling curves, microstructures and properties of all the workpiece are the same, these two quench HTCs are considered as the equivalent HTC.

In industry, same hardness is often used to indicate same microstructure and mechanical properties. After gas quench, the workpiece may have the same hardness compared with liquid quench. However, the cooling curves are not the same and it leads to different microstructure and properties.

The cooling process, microstructures and properties such as hardness and toughness should be examined when designing the new gas quench process to replace the traditional liquid quench process.

3 Steel hardenability analysis

In this chapter, after analysis of the influencing factors on steel hardenability, a gas quench model, including cooling process model, phase transformation model and hardness model is developed. This model can be used to simulate gas quench process. In steel hardenability test, 50% martensite microstructure concept is often used. A new method to determine 50% martensite microstructure by X-ray diffraction is proposed.

3.1 Influencing factors on steel hardenability

Heat treating process has influence on the hardenability. Usually the heat treating process could be divided into austenizing process and quenching process. The purpose of austenizing process is to get homogeneous austenite at defined grain size.

During austenizing process, there are two important metallurgical phenomena occurring in the Austenite. First, the ferrite and pearlite transform to Austenite and the carbide can dissolve into the Austenite. Contemporarily, the Austenite grains are growing. Both the Austenite composition and the grain size affect the hardenability of the steel.

To get fully understand of austenizing process, austenizing temperature, heating rate and holding time should be considered.

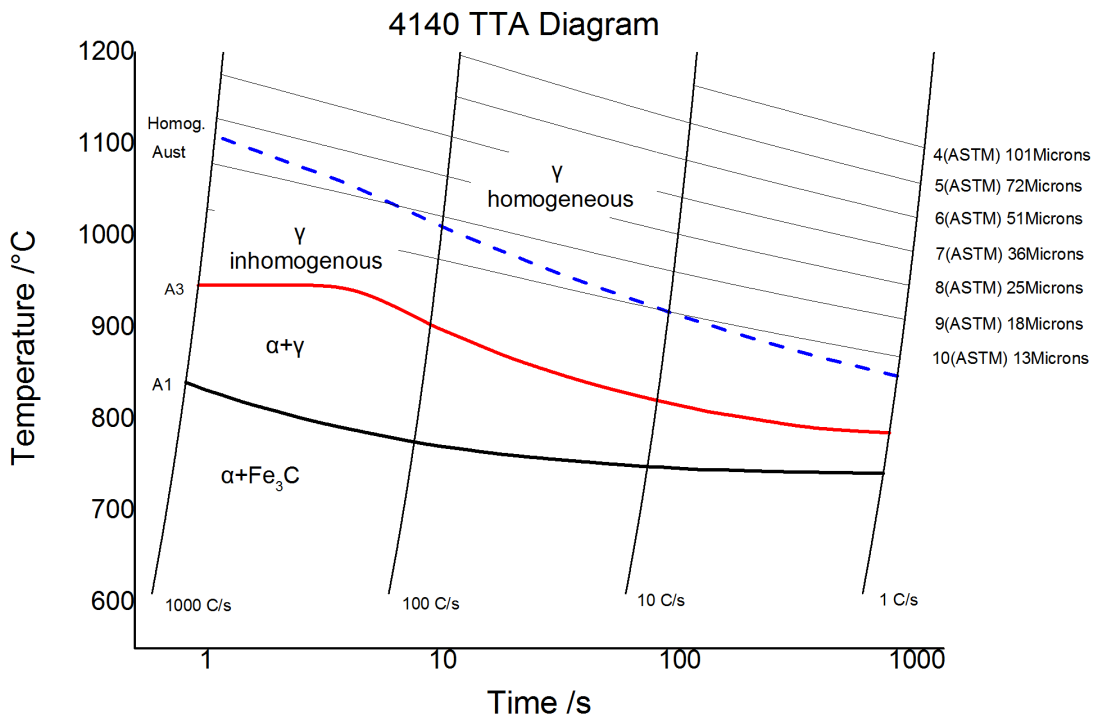


Figure 3.1 4140 TTA diagram generated by JMatPro

The Figure 3.1 is 4140 TTA Diagram. TTA diagram is time-temperature-austenizing diagram. From the figure, the homogeneous austenite is formed at 1100 C within 10s, compared to at 900 C within 100s. The homogenous austenite is formed more quickly at higher austenizing temperature. The austenite is not homogeneous at 1000 C with 100 C/s heating rate. When 10C/s heating rate is applied, the homogeneous austenite is formed at 1000 C. When austenizing temperature is defined, homogeneous austenite is more easily formed with low heating rate.

Grain size increases with higher austenizing temperature and lower heating rate. ASTM grain size equation $G=[3.322*\text{Log}(N_a)]-2.95$ was utilized¹⁷. N_a is the number of the grains per square millimeter.

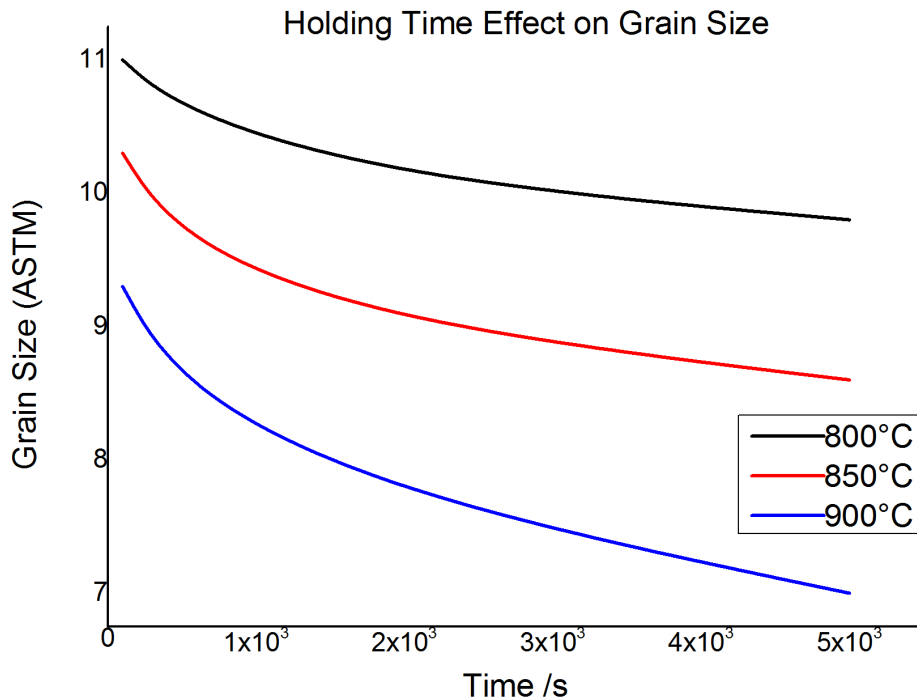


Figure 3.2 Holding time effect on grain size generated by JMatPro

Holding time also has impact on the grain size. From Figure 3.2, at 850 C, the grain size increases with the time. From Erik Khzouz's work on grain growth kinetics in steels ¹⁷, holding time's influence on the grain size is small compared to the austenizing temperature. For AISI 4140 steel, the grain size is ASTM10 after heat treating at 850 C within 9 hours. At 1050 C within 9 hours, the grain size increases to ASTM6.5 ¹⁷.

As a conclusion, the austenizing temperature, heating rate and holding time should be defined as the standard condition. For Jominy end quench standard, it says that the test piece shall be heated uniformly to the temperature specified in the relevant product standard or fixed by special agreement for at least 20 min and then maintained for 30 min at the agreed-upon temperature ¹¹. The JMatPro simulation result indicates that above 850 C austenizing temperature, nearly all the steels have formed homogeneous austenite after 20 min heating process and 30 min holding process.

The variations of chemical elements and grain size have influence on TTT and CCT diagrams. The chemical composition is varied within a small range for specific steel. And this small variation has impact on the TTT and CCT diagrams which determines the hardenability of steel. The chemical composition of AISI 4140 alloy steel and the variation of chemical elements impact on TTT diagram are listed as Figure 3.3 and Figure 3.4. Usually, the TTT diagram will move to right with the increase of the alloy, such as Cr, Mn, Si, Mo. In this report, the chemical elements of steel are not varied since the sample is from the same batch of steel.

Element	Content (%)
Iron, Fe	96.785 - 97.77
Chromium, Cr	0.80 - 1.10
Manganese, Mn	0.75 - 1.0
Carbon, C	0.380 - 0.430
Silicon, Si	0.15 - 0.30
Molybdenum, Mo	0.15 - 0.25
Sulfur, S	0.040
Phosphorous, P	0.035

Figure 3.3 The chemical composition of AISI 4140 ¹⁹

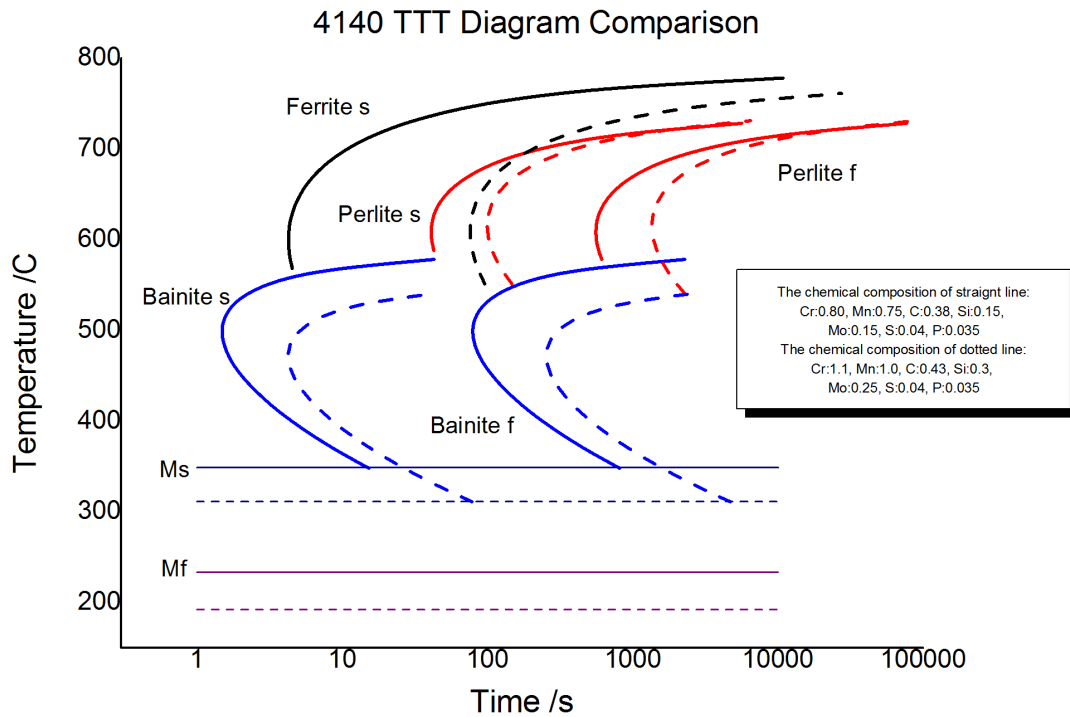


Figure 3.4 Variation of chemical elements impact on 4140 TTT diagram generated by Jmatpro

Austenizing temperature, heating rate and holding time have impact on the grain size. If the heating process is changed, the TTT and CCT diagram is changed at the same time with different grain size. That is the reason why the heating process should be defined in the standard hardenability test. Figure 3.5 is how grain size impact TTT diagram. Figure 3.6 is how grain size impact CCT diagram. Usually the TTT and CCT diagram move right with the increase of grain size, while the temperature of martensite start forming is not changed. Figure 3.7 is another example to demonstrate how different grain size has impact on martensite formation. The cooling rate is calculated when the temperature decreases from 860 C to 20 C. The grain size of the sample should be highlighted in hardenability test.

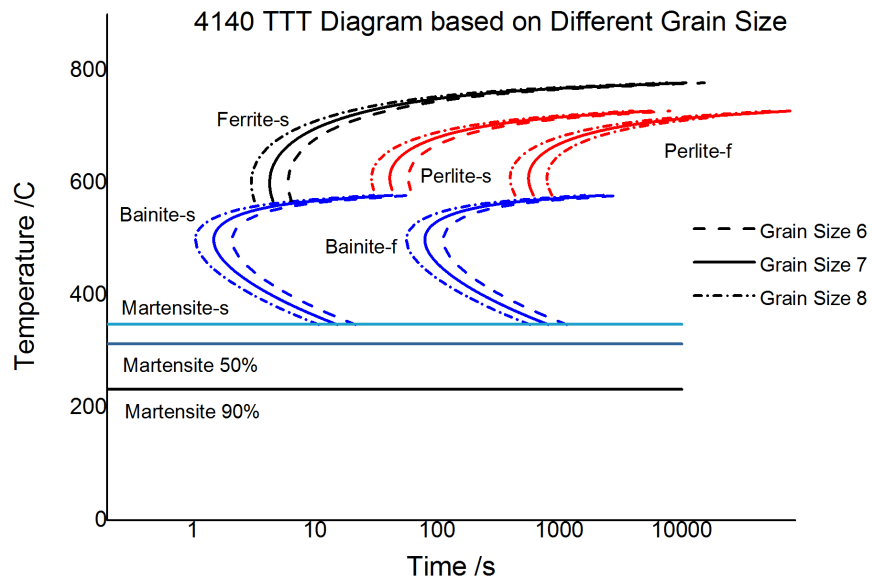


Figure 3.5 4140 TTT diagram based on different grain size generated by JMatPro

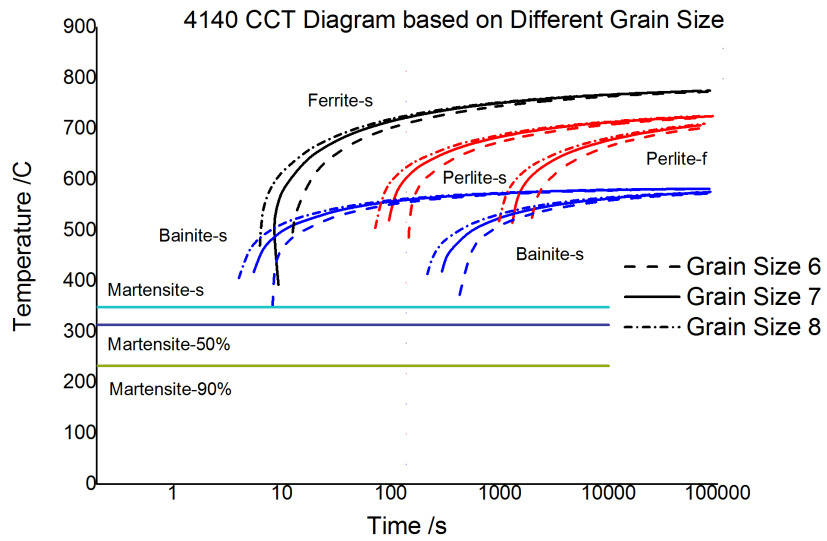


Figure 3.6 4140 CCT diagram based on different grain size

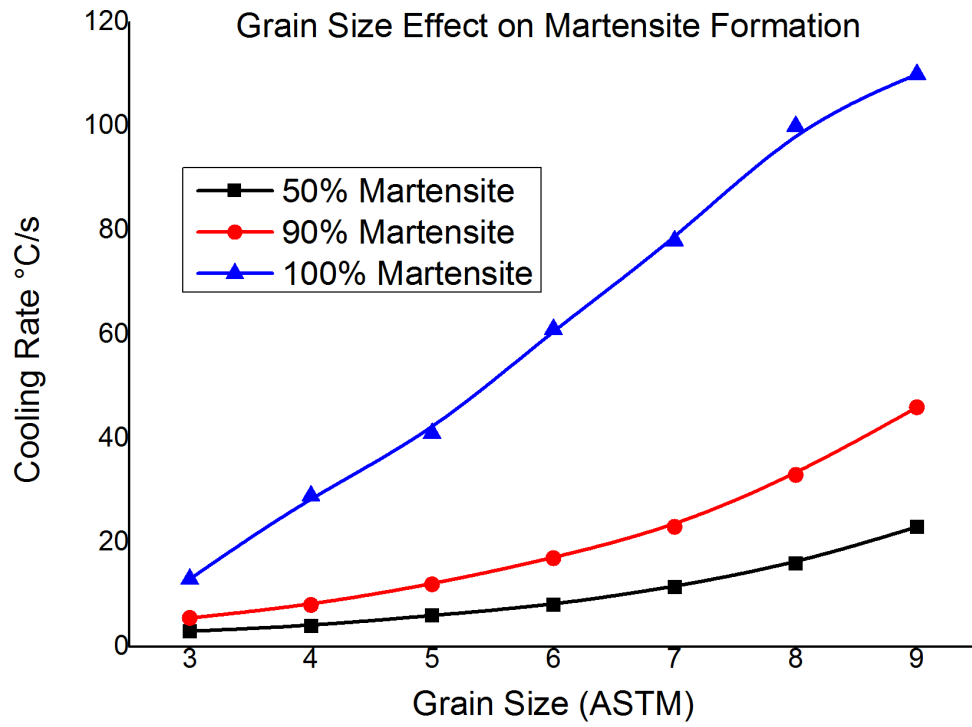


Figure 3.7 Grain size effect on martensite formation generated by JMatPro

3.2 Water quench steel hardenability test and simulation

Based on previous discussion, the only difference between liquid and gas quench is HTC. After determining the cooling curves, the phase transformation, microstructure and mechanical properties should be determined. In order to build a gas quench simulation model, the cooling process model, phase transformation model and hardness model should be established. The phase transformation model and hardness model are the same for gas quench compared to the liquid quench.

4140 and 8620 were selected to repeat the Jominy test. For 4140, the austenized temperature is 843°C (following reference data from isothermal transformation diagrams of United States Steel), maintained for 30min at the austenized temperature. All the procedures are strictly followed the *ISO 642-1999 Steel – Hardenability test by end quenching (Jominy test)*.



Figure 3.8 Furnace and thermocouple

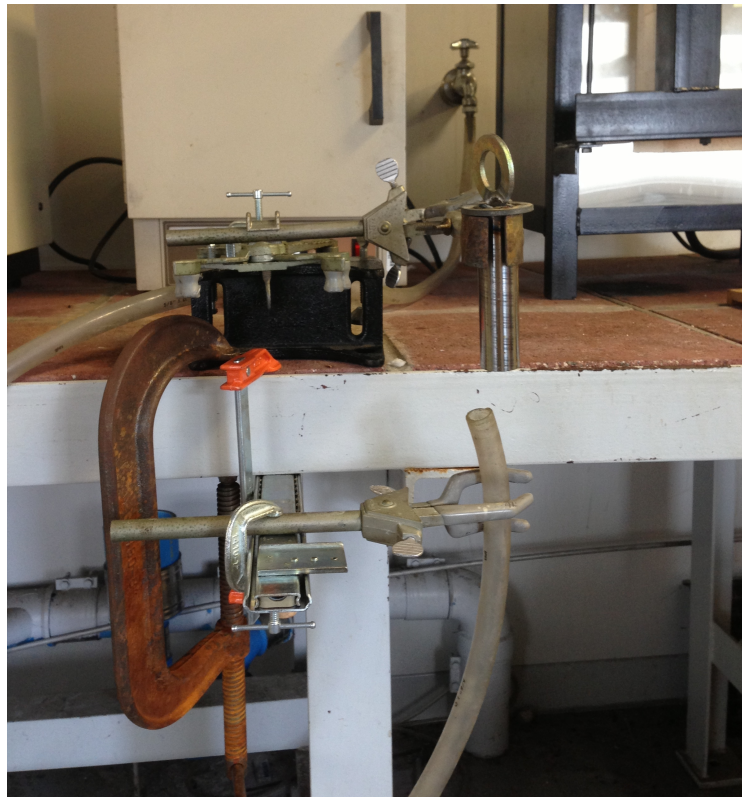


Figure 3.9 Jominy end quench test

The test results fit the USS reference and it indicates that the Jominy test has been repeated successfully. During hardness test, *ISO 6508, Metallic materials – Rockwell hardness test* is followed. The result is shown below. The alloy elements of experiment result is from OES measurement.

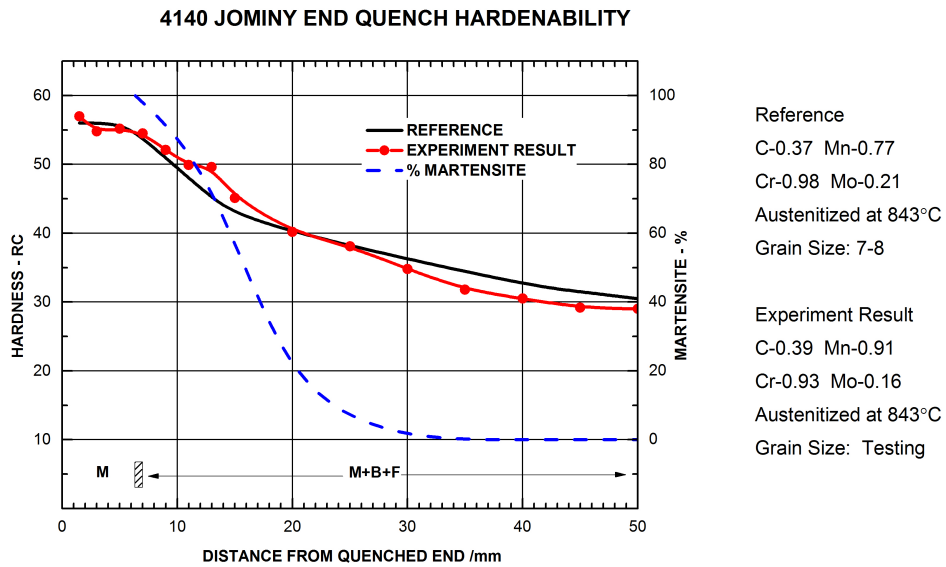


Figure 3.10 4140 Jominy end quench test in the lab

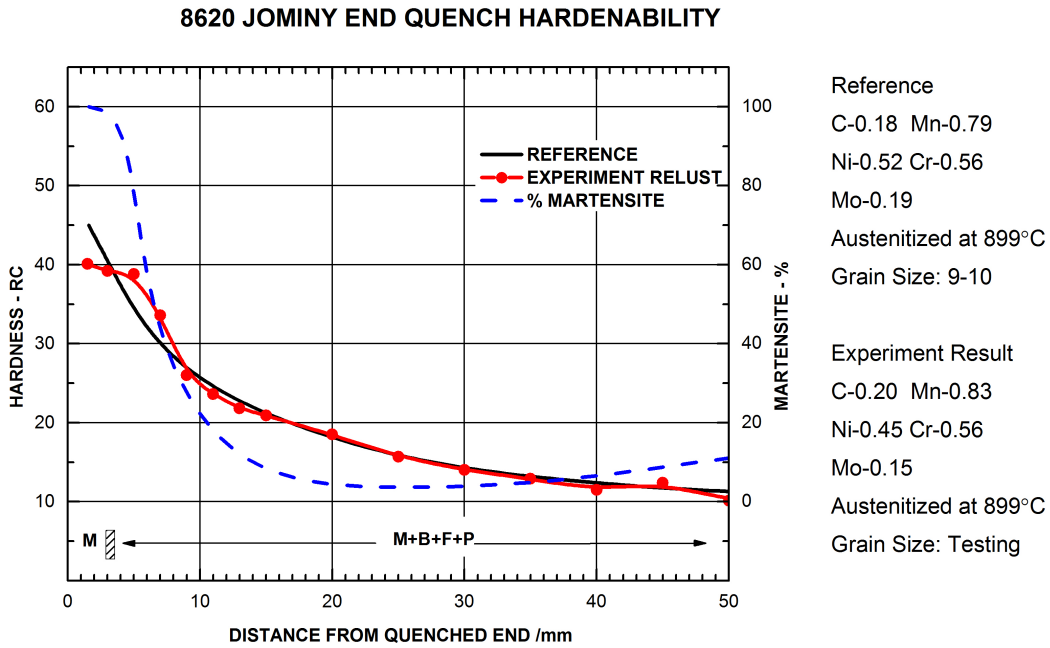


Figure 3.11 8620 Jominy end quench test in the lab

In the quench process, the temperature field, phase and properties of the material will change dramatically. In order to fully understand and analyze the gas quench of steel, the steel quench simulation model should be established and verified.

In the previous chapter, the temperature field simulation of Grossmann model is verified to be accurate. In this chapter, the Jominy end quench model is established based on water quench process and verified based on the Jominy hardenability test results.

Phase transformation model and hardness model will be verified. If the simulated results fit the Jominy end quench test, the phase transformation model and hardness model of the specific steel can be used for gas quench, since these models are the internal properties of the steel.

The accuracy of the temperature field model is important, since it has direct influence on the phase transformations. The temperature can be measured by thermocouples and

simulated by Abaqus. The temperature field model is based on Abaqus and heat transfer coefficients database of Dante. In order to verify the accuracy of the model, the comparison between the experiment and the simulation for the standard Jominy water quench process has been made. The simulation result fits the experiment result, which demonstrates the accuracy of the model. The experiment data are from Timken¹⁸.

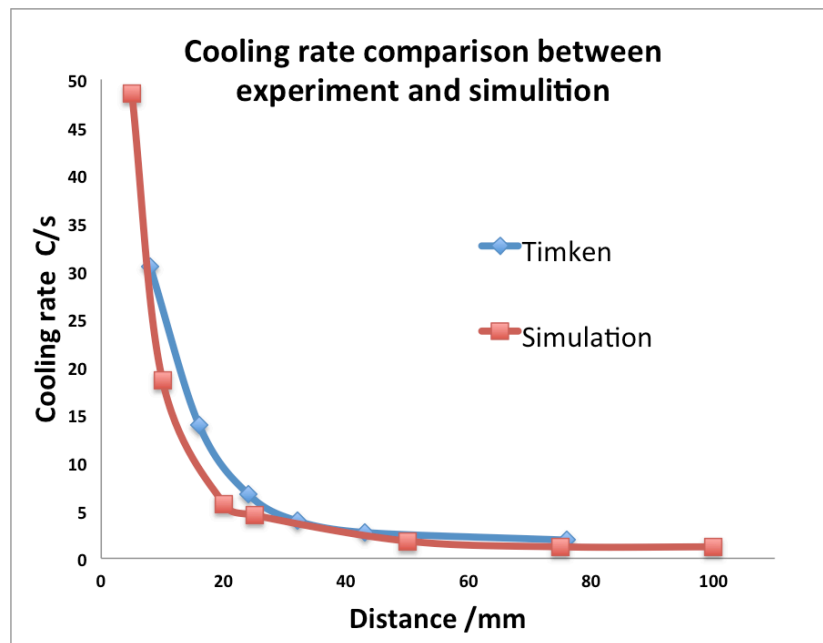


Figure 3.12 Cooling rate comparison between experiment (Timken) and simulation for Jominy water quench

After successfully simulated the temperature field for water quench process, temperature field for gas quench process has been analyzed based on the model. In the quench process, the HTC has direct influence on the temperature field. The different quench media have various HTC curves with the temperature variation, as shown in Figure 3.13. Based on the different HTC curves, the temperature field comparison between liquid quench and gas quench has been made in Jominy test as shown in Figure 3.14. Gas HTC2000 means the heat transfer coefficient of the gas is 2000 W/m²C and Gas HTC

1000 means the HTC of the gas is 1000 W/m²C. The HTC shapes of gas are all considered as horizontal lines as shown in Figure 3.13.

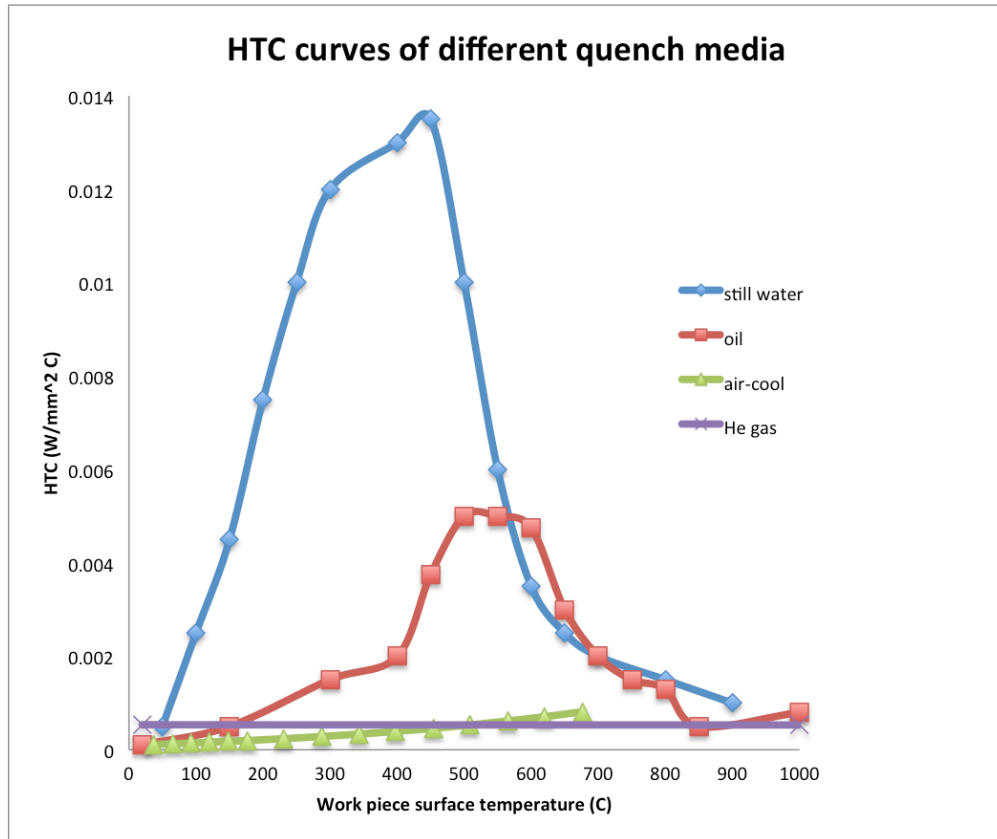


Figure 3.13 HTC curves of different quench media

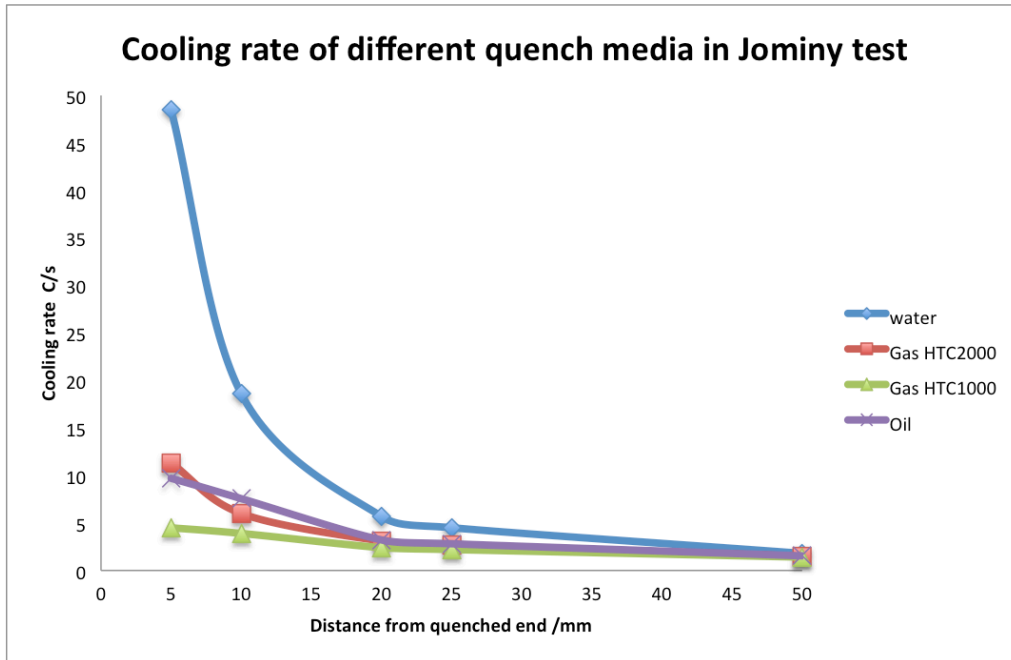


Figure 3.14 Cooling rate of different quench media in Jominy test

The cooling rate in Figure 3.14 shows that the different HTC of quench media will have different cooling rate. Although the cooling rate of water is relatively high near the quenched end, the cooling rate difference far from the quenched end is not severe when compared with other quench media such as oil and high pressure and velocity gas.

The cooling rate of oil and gas HTC2000 are similar, although the shape of these two quench media are totally different.

The phase transformations model has direct impact on properties such as hardness. Figure 3.15 is the cooling rate of Jominy bar. Based on different cooling rate, different microstructures are formed, as shown in Figure 3.16. The phase transformation model based on Dante is considered as accurate after verifying the result with the Figure 3.17, 4140 TTT diagram¹⁹. The simulation shows that the percent of upper bainite is increasing when the cooling rate is decreasing.

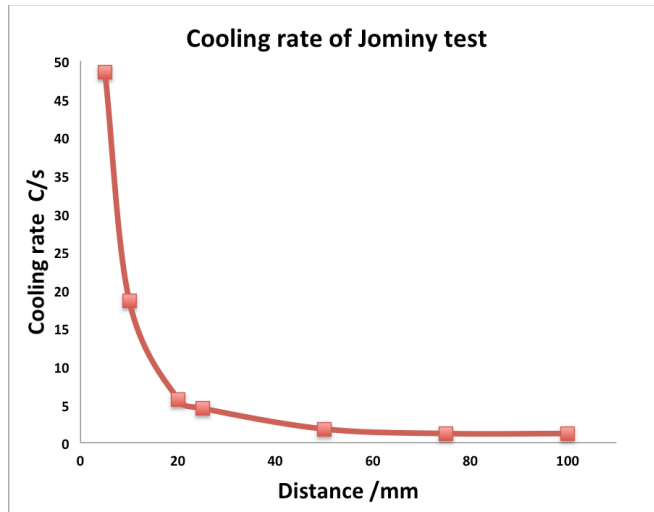


Figure 3.15 Cooling rate of Jominy test

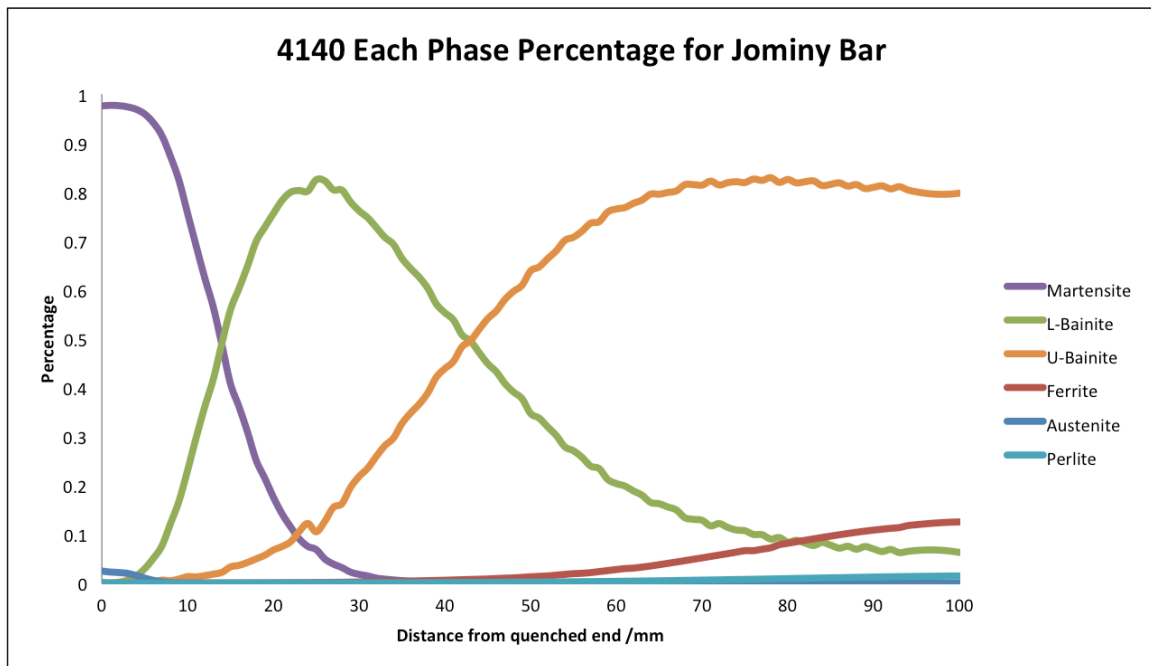


Figure 3.16 4140 phase simulation for Jominy test

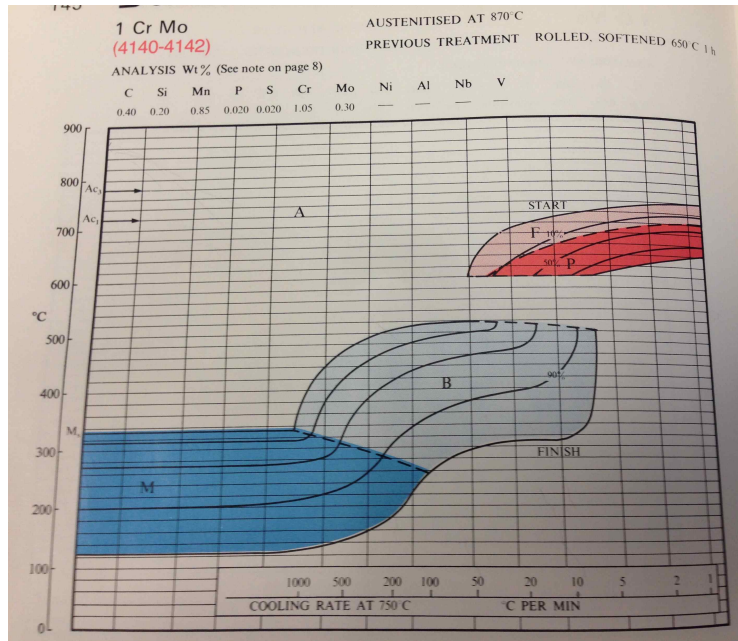


Figure 3.17 4140 TTT diagram

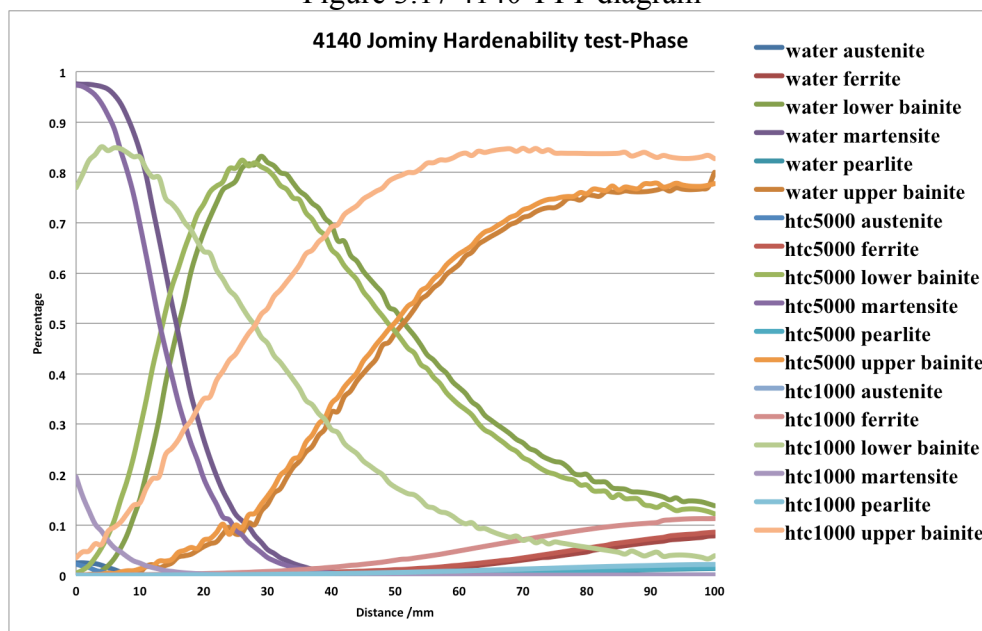


Figure 3.18 4140 phase percentages simulation in water and gas for Jominy test

Figure 3.18 shows the phase transformation differences when different quench media are applied. HTC5000 stands for gas with HTC 5000 W/m²C and HTC1000 stands for gas with HTC 1000 W/m²C. From the simulation, when the cooling rate decreases, the percent of martensite decreases and the percent of upper bainite increase. With different

quench media, the phases of the same sample are different after quench process. It is the reason that gas quench hardenability test has different phases compared to water quench hardenability test.

Rockwell hardness testers can be used to measure the hardness. HTC is usually used for steel hardenability test.

$$Hardness = \sum_{n=1}^n P_n \times H_{n,carbon}$$

The hardness model is listed above. P_n stands for the amount of phase n . Carbon stands for the carbon composition of the steel. $H_{n,carbon}$ stands for the hardness of each phase based on carbon composition of the steel.

The hardness database (based on Dante) about the relationship between microstructure and hardness has been used for hardness simulation. The blue line and the red line indicate the hardenability band for each steel. The green line is the simulation result. The comparison between Jominy hardenability reference¹⁹ and simulation result shows that the hardness model is accurate. This hardness model can also be used in gas quench process.

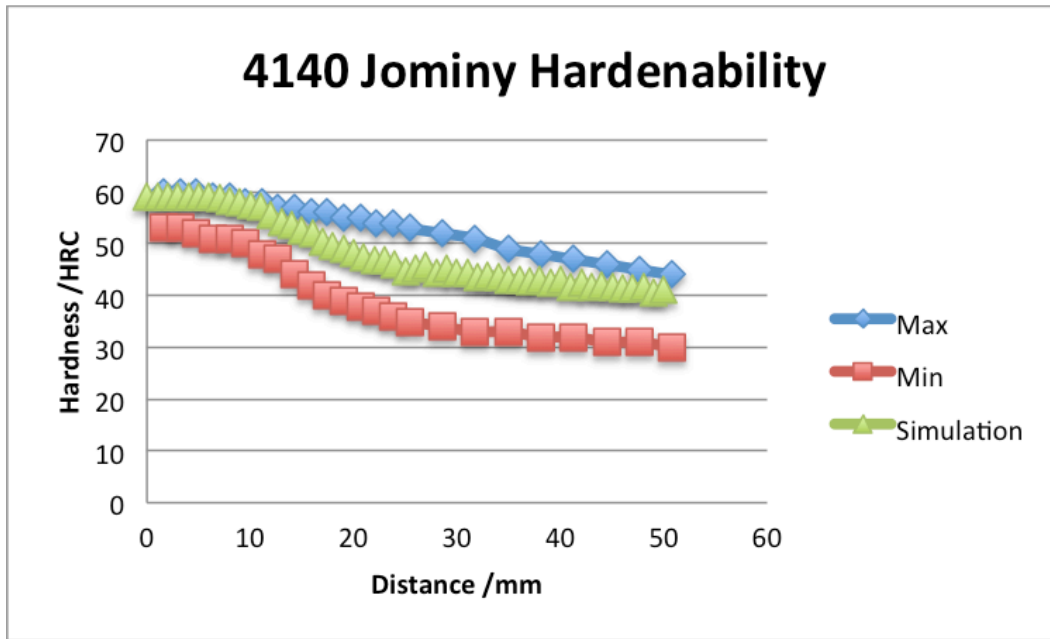


Figure 3.19 4140 Jominy hardenability comparison

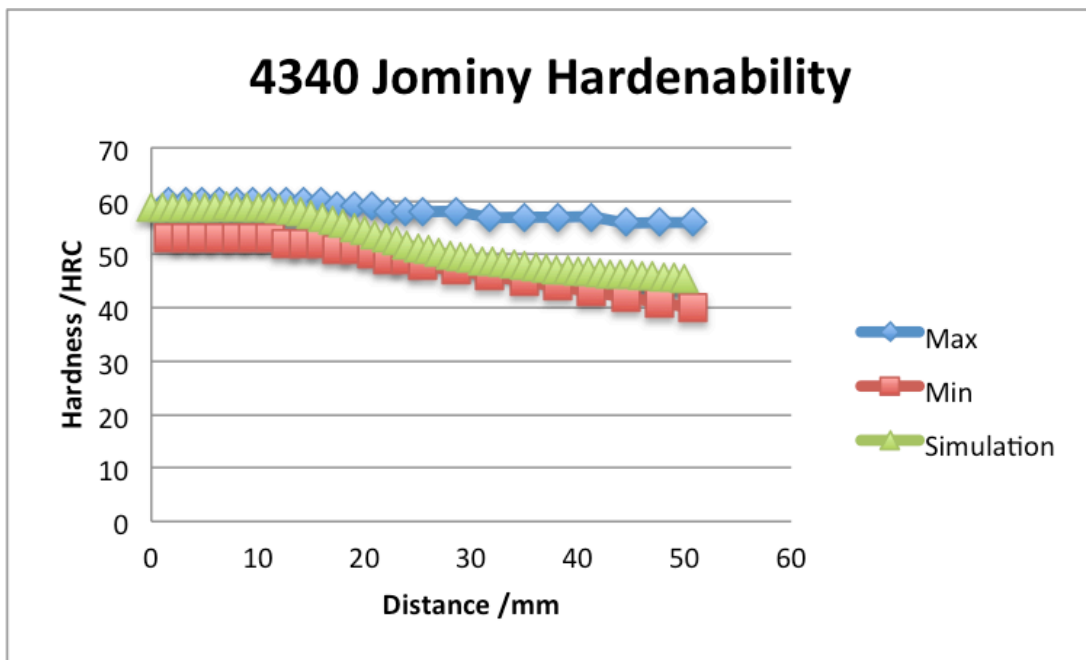


Figure 3.20 4340 Jominy hardenability comparison

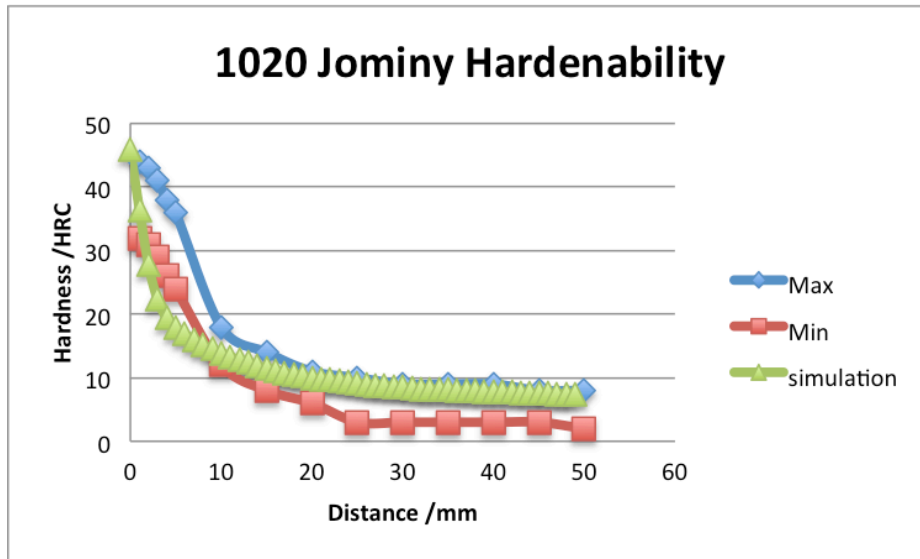


Figure 3.21 1020 Jominy hardenability comparison

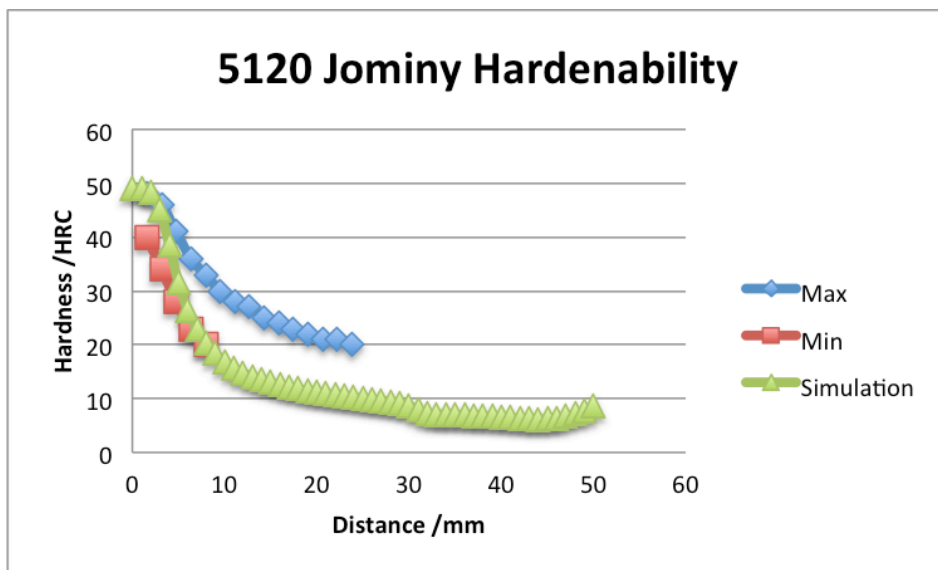


Figure 3.22 5120 Jominy hardenability comparison

3.3 Determination of 50% martensite microstructure and hardness

50% Martensite hardness is designated as the critical hardness in steel hardenability test²⁰. Figure 3.23 shows drop in hardness. It has been demonstrated that the main reason is the proportion of Martensite decreases²⁰. Based on the theory, the position, which has the largest gradient in Jominy hardenability curve, contains 50% Martensite. Figure 3.24 reveals the process to determine 50% Martensite hardness. The test was carried out simply by hardening a bar by quenching it, breaking the bar and observing the microstructure. The scale of the photomicrograph does not include in the reference.

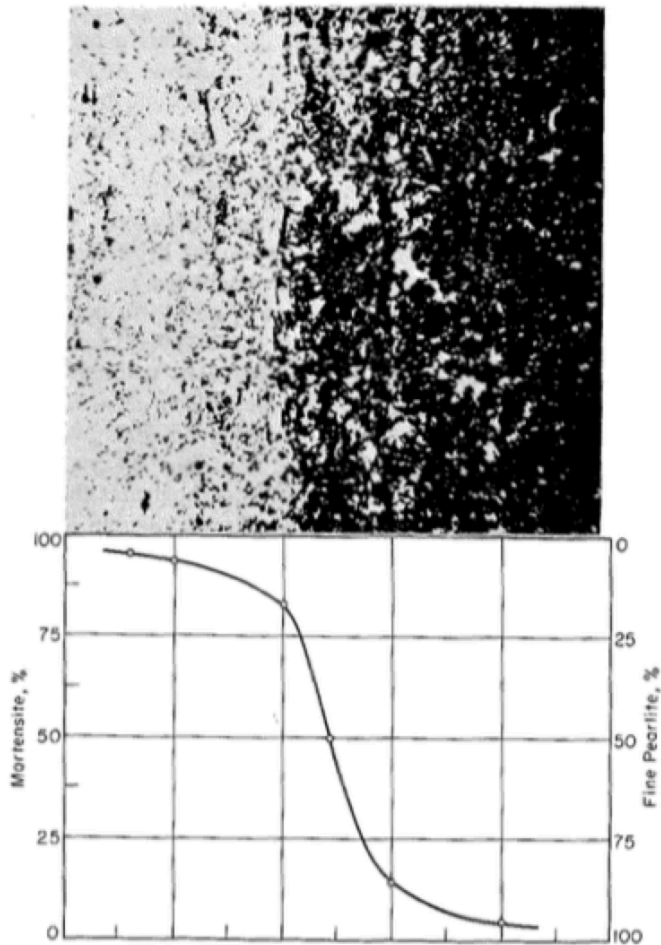


Figure 3.23 Photomicrograph and corresponding chart showing abrupt transition from predominantly martensitic to predominantly pearlite microstructure²⁰

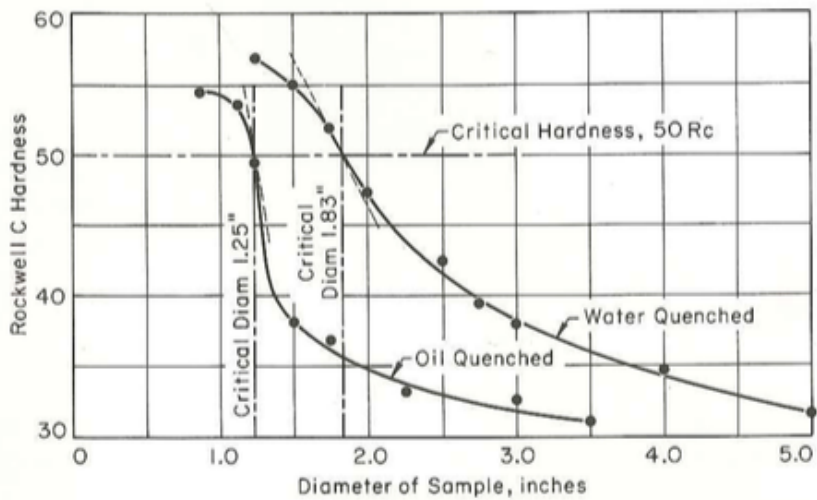


Figure 3.24 Hardnesses at the centers of quenched round bars in progressively larger sizes, one series quenched in oil, one series quenched in water²⁰

However, it is not always easy to find 50% Martensite for all the steels, since not all hardenability curves represent abrupt change. It is believed that the 50% Martensite hardness are mainly related to the carbon content, though the hardnesses are likely to be very slightly higher in alloy steels²⁰. Figure 3.25 shows a probable band of values, assembled from available data. These points were all determined on plain carbon steels, and are therefore shown at the lower limit of the band. In this report, the 50% Martensite hardness is chosen based on this theory.

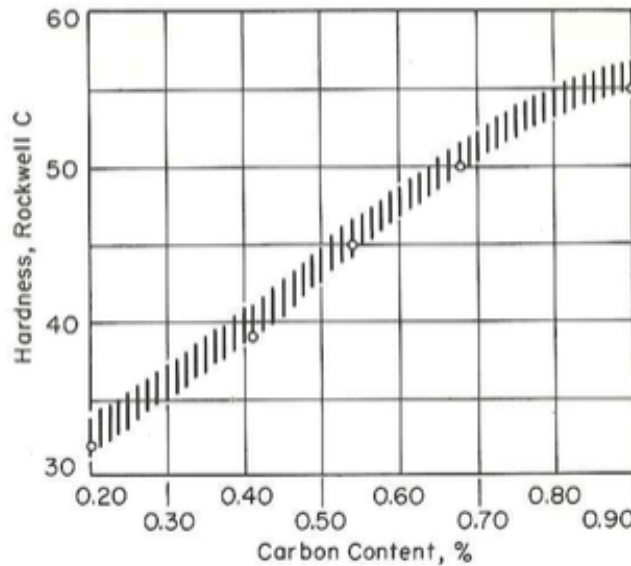


Figure 3.25 Hardness of quenched structures containing 50% Martensite, for different carbon contents²⁰

3.4 Quantitative analysis of steel microstructure by XRD measurement

3.4.1 Introduction

Microstructure analysis in steel is important to get understanding of heat treatment process and properties. Usually, the microstructure in steel contains as-quenched Martensite, tempered Martensite, upper Bainite, lower Bainite, ferrite, and/or retained Austenite and carbides.

Although metallograph, SEM and TEM can detect each phases, the identification and quantification for each phases are difficult, especially between upper and lower Bainite, lower Bainite and Martensite. For the steel, which has 10% or lower retained Austenite, it is not easy to be observed.

Based on the previous discussion, the 50% martensite microstructure is determined based on hardness variation, not directly observation. In this chapter, a new method is developed to measure 50% martensite, which demonstrates whether the Grossmann's method to get 50% martensite hardness is right or not.

Since X-Ray Diffraction (XRD) is a powerful tool to determine crystal structure²¹, it is used to identify and quantify each phases.

Based on literature, The Martensite, of which carbon content is higher than 0.6 wt. %, is BCT structure²². The Martensite, of which carbon content is lower than 0.6 wt. %, is BCC structure²². The retained Austenite has FCC structure and the ferrite is BCC structure²². The carbides have complex structures²². The Bainite is the mixture of ferrite and carbides²². Although the ferrite and low carbon Martensite have both BCC structure, the lattice parameter for Martensite is larger.

For 52100 steel under water quench condition, Martensite and retained Austenite will form. Because the crystal structure of Martensite is BCT and the crystal structure of Austenite is FCC, the different XRD patterns between Martensite and Austenite can be utilized for phase identification and quantitative analysis.

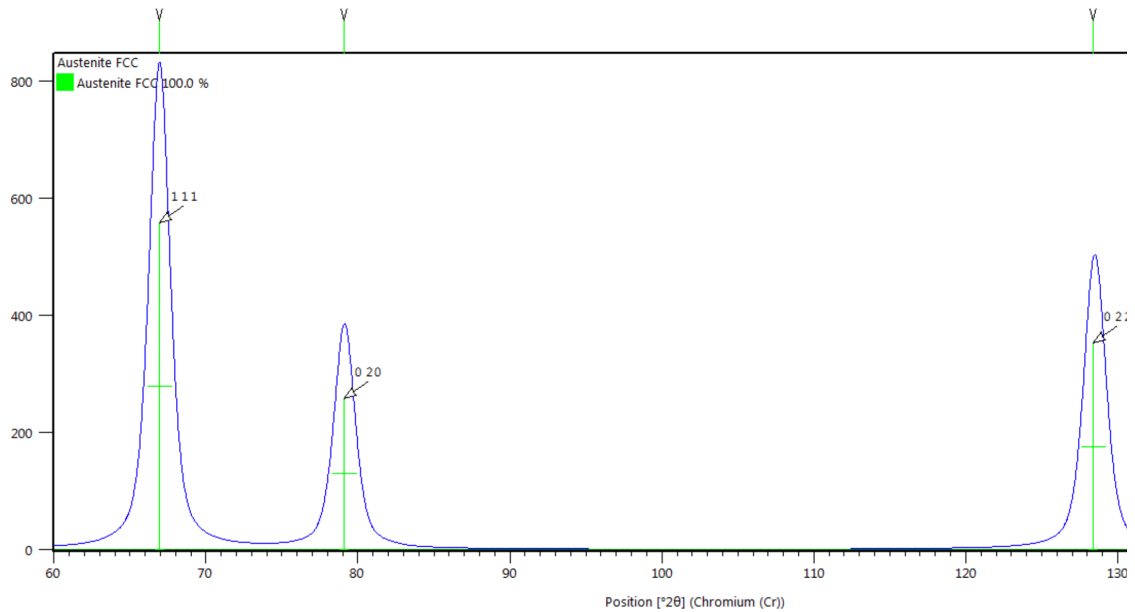


Figure 3.26 Austenite theoretical XRD pattern

Figure 3.26 is the Austenite theoretical XRD pattern. The peaks will drift due to the amount of dissolved carbon in Austenite.

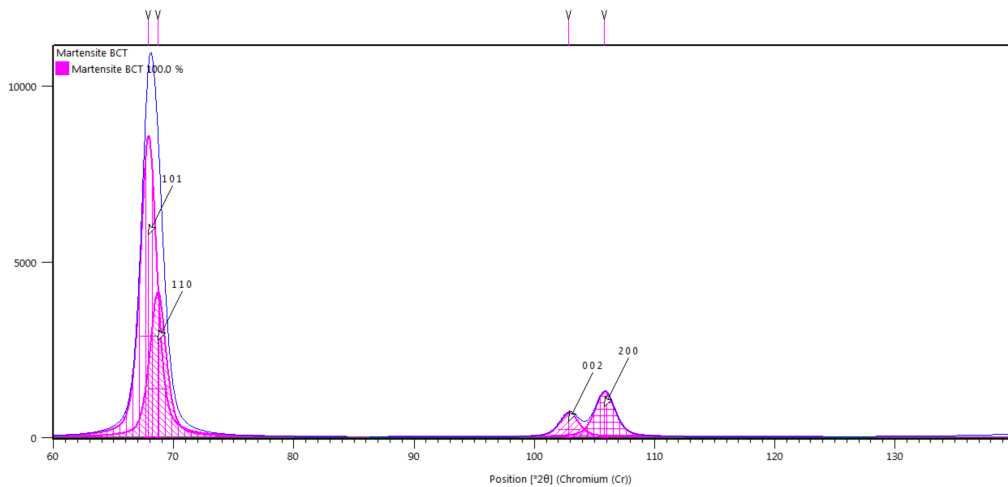


Figure 3.27 As quenched Martensite theoretical XRD pattern

Figure 3.27 is the as quenched Martensite theoretical XRD pattern. The peaks will drift due to the amount of dissolved carbon in Martensite.

When 52100 steel is cooling in oil, it may form Bainite. The Bainite is the mechanic mixture of Ferrite and cementite. When the quenched Martensite is tempered, it will form tempered Martensite. The crystal structure of Ferrite and tempered Martensite is both BCC and the XRD pattern is very similar. The only difference is that the amount of carbon in Martensite is higher than Ferrite. Compared to Ferrite peak, the Martensite peak will drift towards left and be broadened.

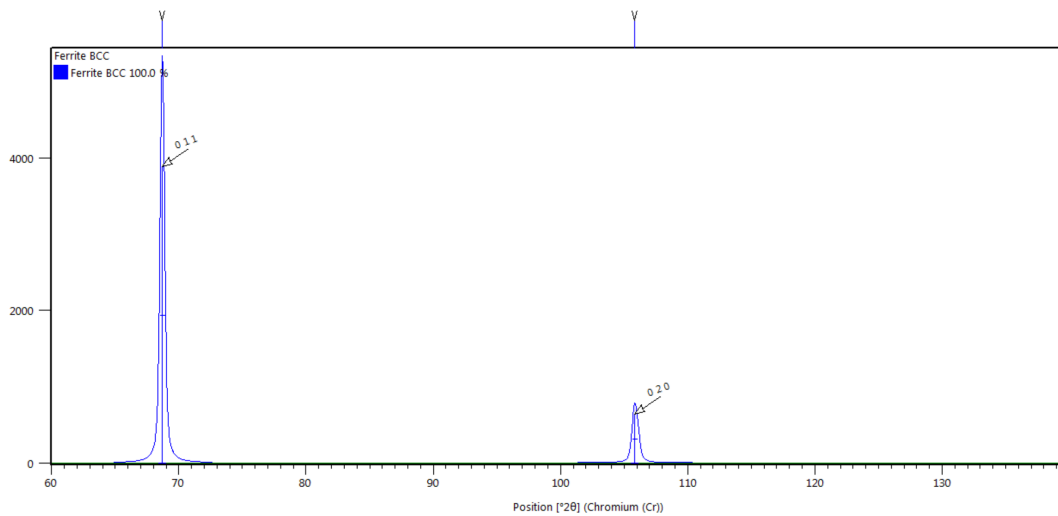


Figure 3.28 Ferrite theoretical XRD pattern

3.4.2 Sample preparation

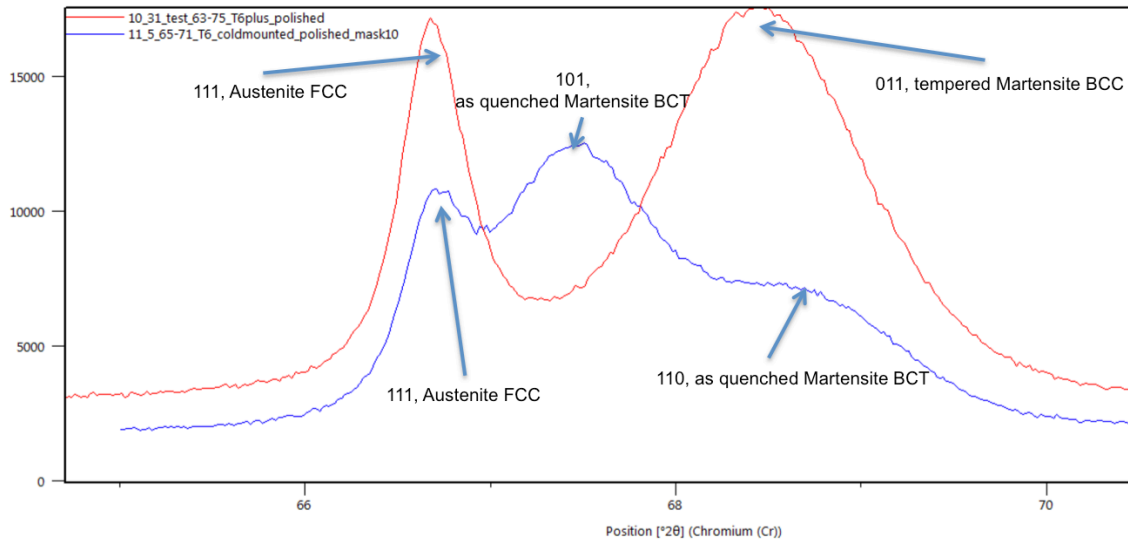


Figure 3.29 XRD comparison between hot mounted and cold mounted samples

Usually, the steel sample is cut and then hot mounted. After grinding, polishing and etching, the microstructure can be examined. The etched 52100 sample is measured by XRD in Figure 3.29. The red line is XRD pattern of hot mounted sample. The heat treatment process for 52100 Test6 (short for T6) sample is austenized to 1050C for 40mins and then water quenched. Compared to the previous theoretical XRD pattern for different phases, Austenite (111) is observed. Considering the hardness of this sample is higher than 63HRC, the other peak (011) should represent Martensite. However, the Martensite XRD pattern for 52100 is not like the pattern in Figure 3.27.

In Figure 3.28, it shows the XRD pattern of Ferrite or tempered Martensite. Compared with Figure 3.29, the (011) peak of hot mounted sample is the tempered Martensite. Although no tempering process is applied to the sample, the Martensite seems to become tempered after quench. It is because hot mount method is used. After checking the process of hot mount, the heating time is around 150C for 1min. In order to see whether

the hot mount process tempers the quenched Martensite, the water-quenched Martensite is also cold mounted. The blue line is XRD pattern for cold mounted sample. The heat treatment process is the same expect this sample is cold mounted. Compared to Figure 3.27, the quenched Martensite pattern (101 and 110) in cold mounted sample is the same to the theoretical as quenched martensite XRD pattern.

From the discussion above, we can conclude that the original BCT as quenched Martensite transform to BCC tempered Martensite in hot mount process. In order to determine the original crystal structure of the quenched steel, cold mount process has to be used.

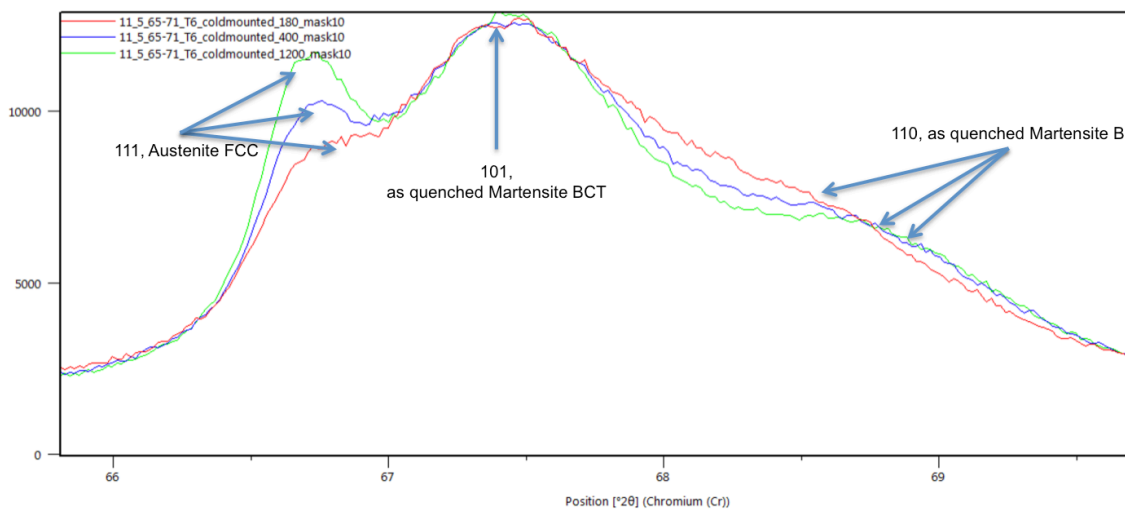


Figure 3.30 52100 Test6 XRD pattern for cold mounted sample after different grit

The cold mounted sample will be ground for the XRD measurement. In order to determine the grind effect on the XRD pattern²³, the same sample is measured by XRD after different grit. The result is shown in Figure 3.30. The bottom red line represents 180grit and the top green line represents 1200grit. The Austenite peak intensity increases,

which indicates the percentage of Austenite increases, when higher number of grit (smoother surface) is used.

One possible explanation for this phenomenon is that the grinding will generate a deformation layer on the surface of the sample^{24 2526}. The thickness of deformation layer is dependent on the number of grit. The Austenite in deformation layer will transform to Martensite. The stress-induced Martensite is well known. With lower number of grit (say 60grit), the deformation layer is deeper. With higher number of grit (say 1200grit), the deformation layer is shallower. After the same XRD measurement condition, the penetration depth for XRD is the same. However, for lower number of grit, the XRD intensity is mainly the contribution of deformation layer, which has less Austenite and more Martensite, not of sample matrix.

As a conclusion, in order to accurately measure the microstructure of steel by XRD, the sample should be cold mounted, ground with the highest number of grit and electropolished in order to minimize the depth of deformation layer.

3.4.3 Steel microstructure analysis based on Rietveld refinement

Rietveld refinement is a technique devised by Hugo Rietveld for use in the characterization of crystalline materials^{27 28}. The neutron and x-ray diffraction of powder samples results in a pattern characterized by reflections (peaks in intensity) at certain positions. The height, width and position of these reflections can be used to determine many aspects of the material's structure.

The Rietveld method uses a least squares approach to refine a theoretical line profile until it matches the measured profile²⁸. The introduction of this technique was a significant

step forward in the diffraction analysis of powder samples as, unlike other techniques at that time, it was able to deal reliably with strongly overlapping reflections.

In steel, the peak of Martensite, ferrite and carbides are highly overlapped. Using Rietveld refinement may be able to deal with this problem ²⁹.

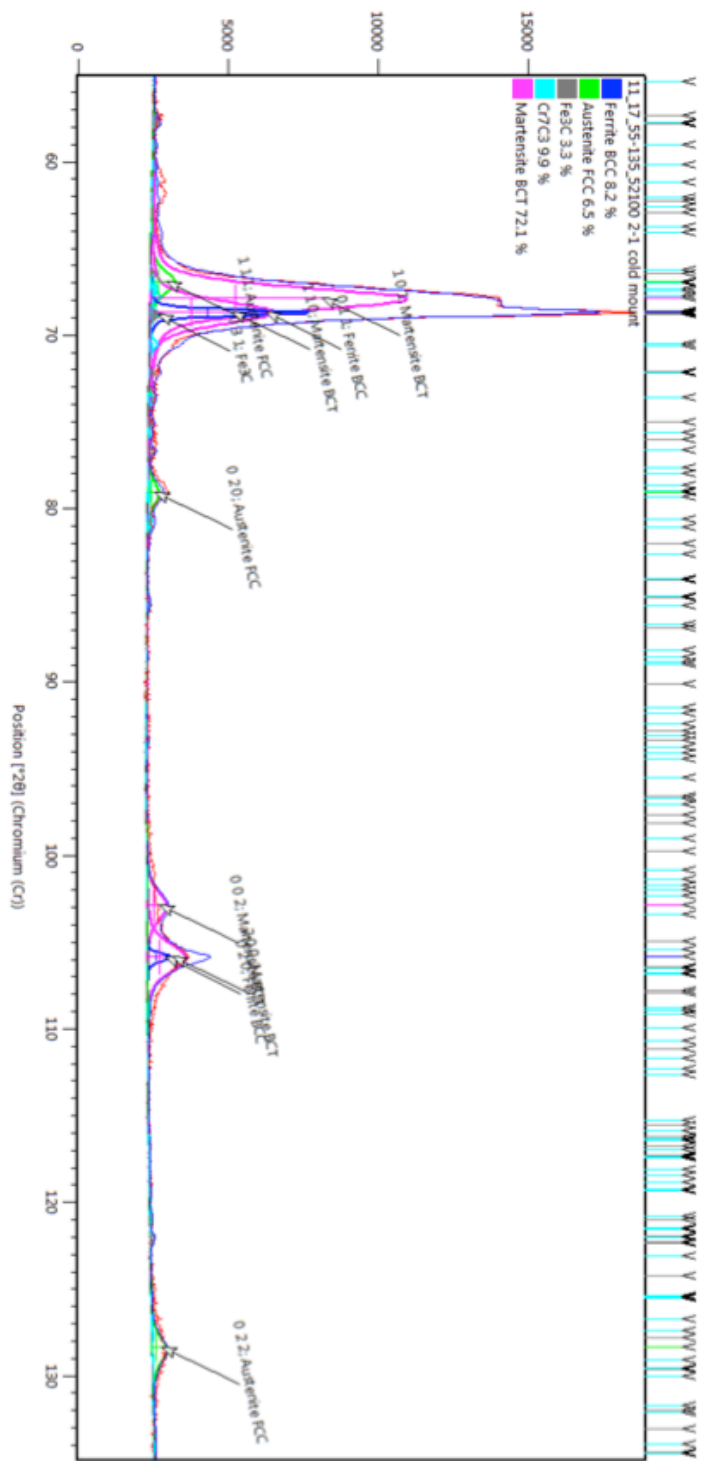


Figure 3.31 The full range XRD pattern of Test6: 52100 steel austenizing 1050C for 40min – water quench – cut - cold mounted– ground and polished – etched with 4% nital

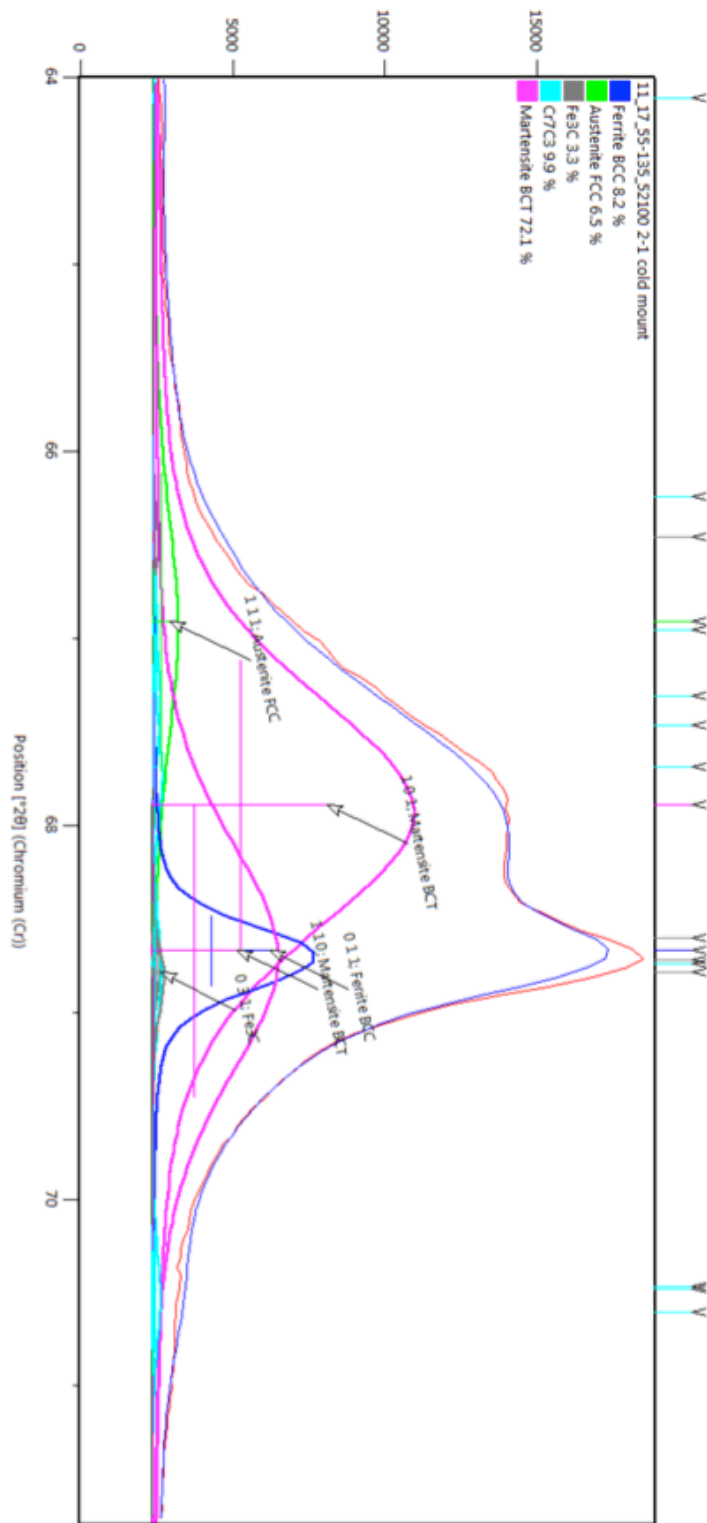


Figure 3.32 64-72 degree XRD pattern of Test6: 52100 steel austenizing 1050C for 40min – water quench – cut - cold mounted– ground and polished – etched with 4% nital

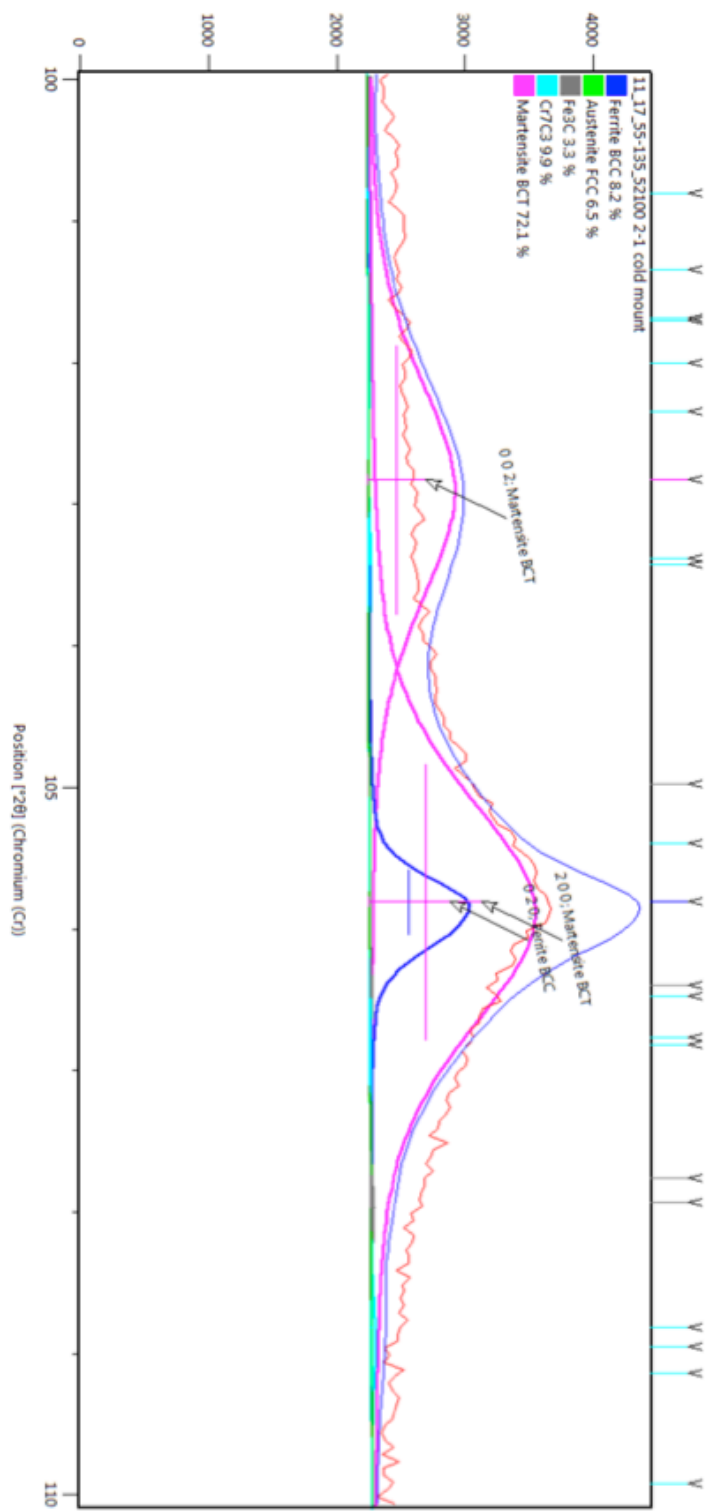


Figure 3.33 100-110 degree XRD pattern of Test6: 52100 steel austenizing 1050C for 40min – water quench – cut - cold mounted– ground and polished – etched with 4% nital

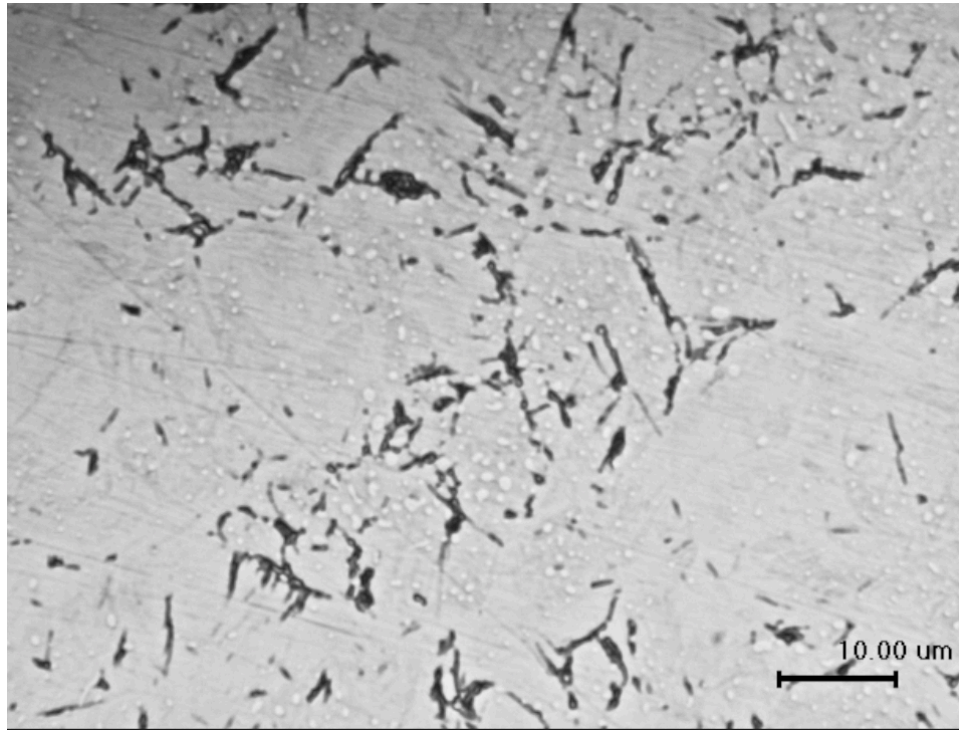


Figure 3.34 Part2-1 microstructure: 52100 steel austenizing 850C for 40min – 810 W/m²C gas quench – cut - cold mounted– ground and polished – etched with 4% nital

Figure 3.31, Figure 3.32 and Figure 3.33 are XRD patterns of 52100 cold mounted and etched sample. From the pattern, Austenite, as quenched Martensite, Ferrite and carbides can be identified. Figure 3.34 is the microstructure of the corresponding samples. The bright area is Martensite. The dark area is ferrite and carbides. The white spot maybe retained austenite. With this XRD pattern, the phase percentage can be accurately measured by profile fit method or Rietveld refinement method²⁶. The Fe₃C and Cr₇C₃ phase percent are not accurate based on current method. More modification will be conducted to improve the quantification accuracy.

The steel is often tempered after quench process, in order to decrease the hardness and increase the ductility. The XRD and Rietveld refinement can also be used to analyze as-quenched Martensite and tempered Martensite.

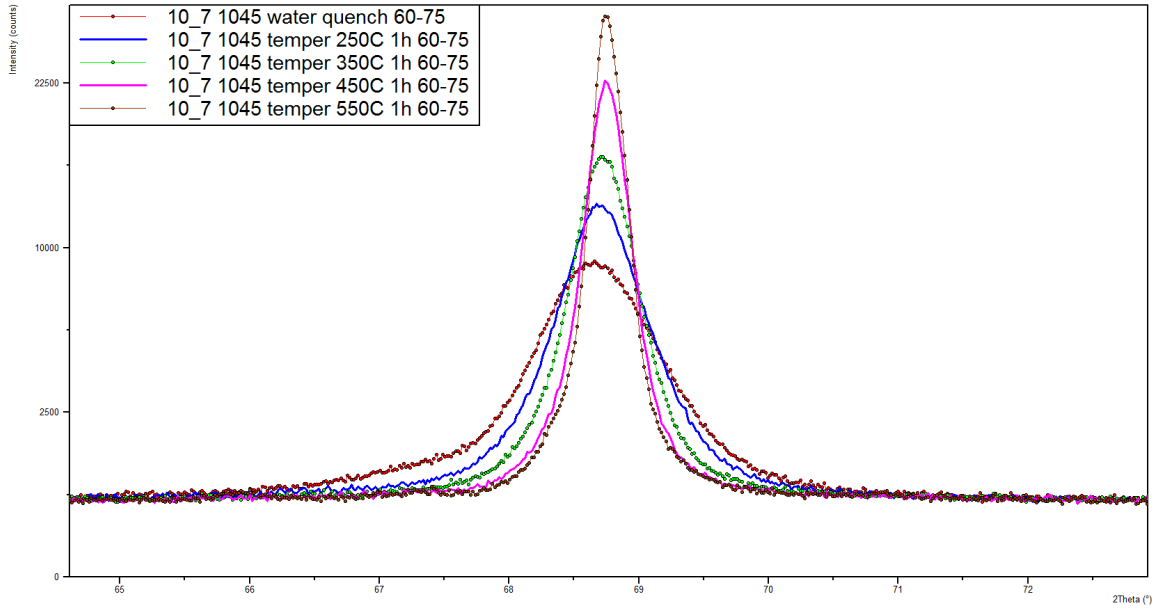


Figure 3.35 1045 XRD pattern when different tempering temperature is applied --peak (011)

Figure 3.35 presents the 1045 XRD pattern for peak (011) when different tempering temperature is applied. The lattice parameter of tempered Martensite decreases as the increase of tempering temperature. The decrease of FWHM indicates that the distortion, defects or twins in as-quenched Martensite tends to be removed with the increase of the tempering temperature. The lattice parameter and line profile data would help to get better understanding of as quenched Martensite, tempered Martensite and ferrite.

Tempering Process	Lattice parameter	Area (counts)	FWHM	Integral Breadth
Water quench	2.8712	7198	0.915	1.234
250C, 1h	2.8694	7162	0.674	0.883
350C, 1h	2.8687	6851	0.485	0.628
450C, 1h	2.8675	6663	0.312	0.41
550C, 1h	2.8675	6848	0.216	0.295

Figure 3.36 Lattice parameter and line profile parameter of 1045 steel tempering

3.5 Summary and Conclusion

In this chapter, the Jominy quench model is proposed and verified based on the Jominy end quench test. Temperature field model, phase transformation model and hardness model are proposed and verified.

The austenizing temperature, heating rates, holding time, grain size and chemical elements effects of steel hardenability are discussed. These information should be recorded when doing steel hardenability test.

The method to get 50% martensite microstructure and hardness based on Grossmann's work is discussed and will provide support on critical HTC, which is proposed in chapter4.

The XRD and Rietveld refinement method is developed to accurately analyze steel microstructure, such as 50% martensite. This method would provide better understanding of steel phase quantification.

4 Critical HTC test for gas quench steel hardenability

Based on previous discussion, the modified Jominy gas quench hardenability test has many limitations. In this chapter, a critical HTC test, based on modified Grossmann test, is proposed. The test and simulation results demonstrate that critical HTC test can be used to determine gas quench steel hardenability.

4.1 Critical HTC test and critical HTC

In the previous discussion, modified Jominy gas quench steel hardenability test is proved to be improper. This leads the author to consider about another familiar and commonly used procedure for steel hardenability test, Grossmann's test. After finding the complexity and limitations of gas quench Jominy test, critical HTC test based on the modified Grossmann test and critical HTC are proposed.

Grossmann's test of measuring hardenability uses a number of cylindrical steel bars of different diameters in a given quench medium. After sectioning each bar at mid-length, the bar that has 50% martensite at its center is selected, and the diameter of this bar is designated as the critical diameter⁴.

In CHTE gas quench steel hardenability test, cylinder samples with same geometry are used (currently cylinder with diameter 25mm and length 100mm is used). The sketch is shown in Figure 4.1. The gas flow is assumed the same at the sample end and the sample side, since the slenderness ratio of sample is relatively large. Gas flow is assumed as laminar flow. In this condition, the gas pressure and velocity are steady during gas quench condition.

In the test, different gas quench HTC conditions are applied to the sample with the same geometry. After sectioning each bar at mid-length, the bar that has 50% martensite at its center is selected, and the applied gas quench HTC of this bar is designated as the critical HTC.

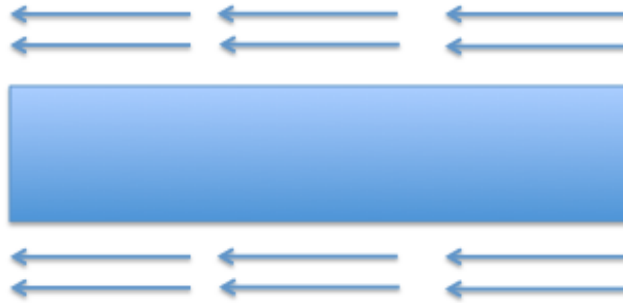


Figure 4.1 The sketch of critical HTC test

4.2 Praxair gas quench system and sample design

With the help of Praxair, Praxair gas quench system was selected as the prototype for CHTE gas quench hardenability test. Figure 4.2 is the sketch of Praxair gas quench system. The steady gas flow is the advantage of the system. Figure 4.3 is the photograph of Praxair gas quench system. In the system, the heating and cooling curve at the center of the sample, gas pressure, gas mass flow rate and gas temperature can be monitored.

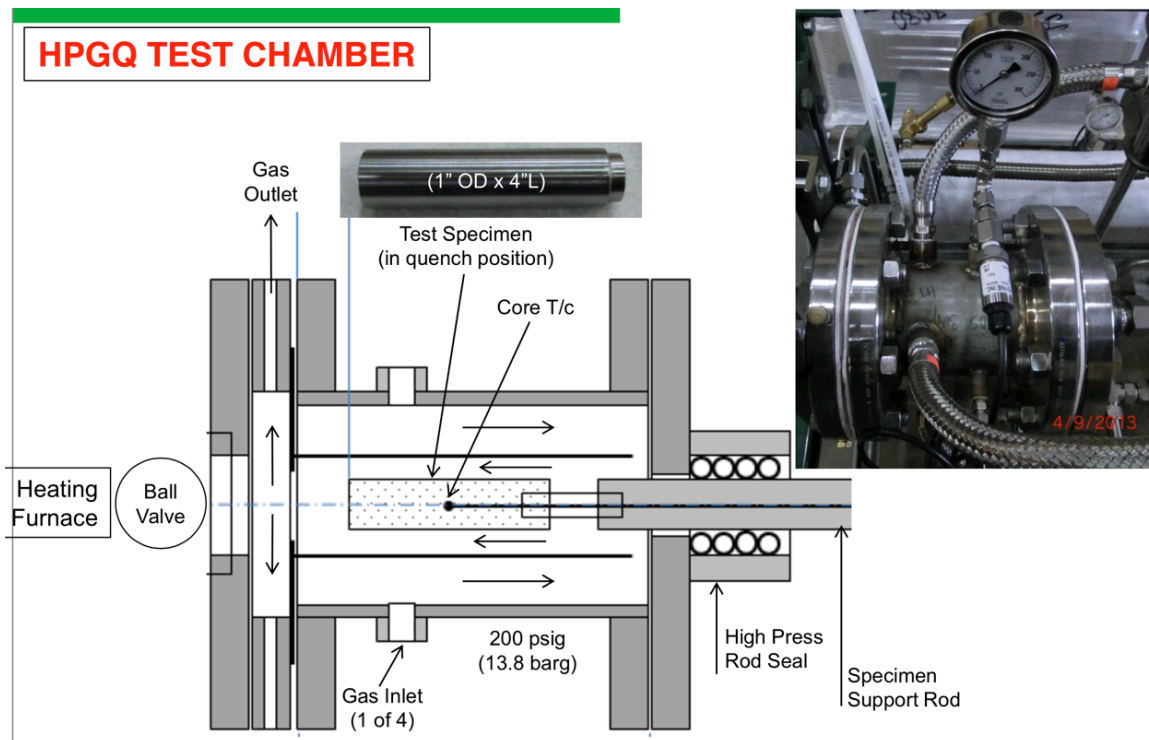


Figure 4.2 Praxair gas quench system sketch³⁰

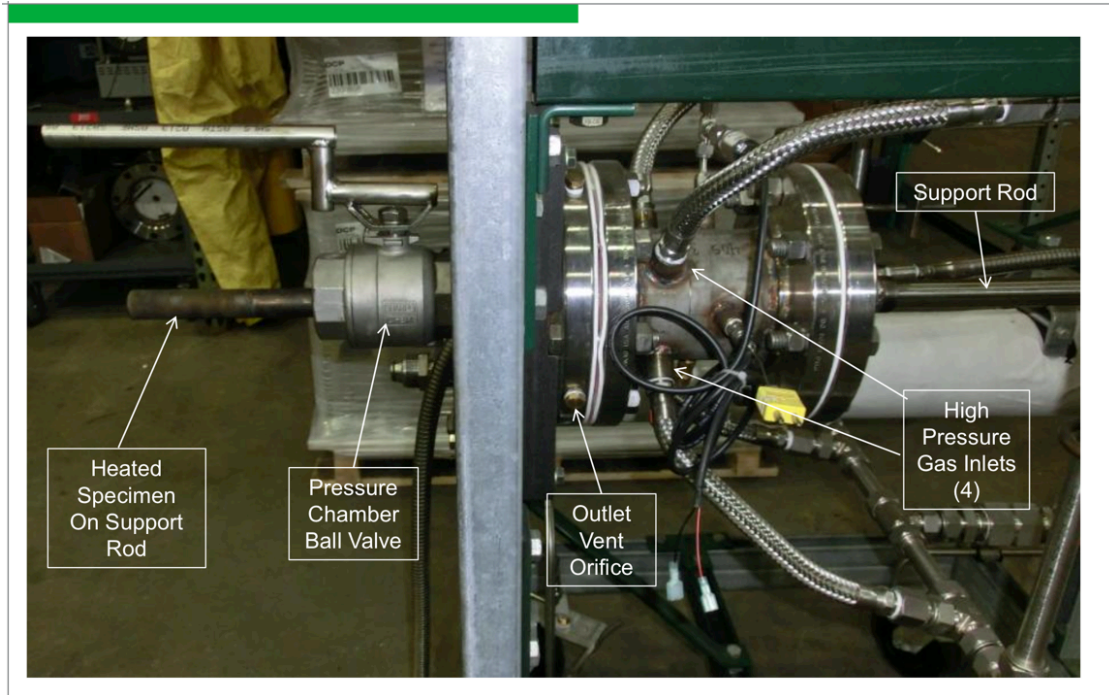


Figure 4.3 Praxair gas quench system³⁰

With the permission of Praxair, the detailed gas quench system assembly is attached as Figure 4.4. The sleeve diameter needs to be carefully determined, since it has direct impact on the gas velocity. In the future, if sample with a larger diameter is applied, the sleeve needs to be changed.

In the original Praxair gas quench system, the cylinder sample is welded with the support rod. Considering the convenience of design for critical HTC test, Praxair redesigned the cylinder sample and the support rod. Figure 4.5 is the sample sketch. The screw thread is machined at one end of the sample. Correspondingly, one end of the support rod is machined as well. The stainless steel support rod thread can be repeatedly used after testing.

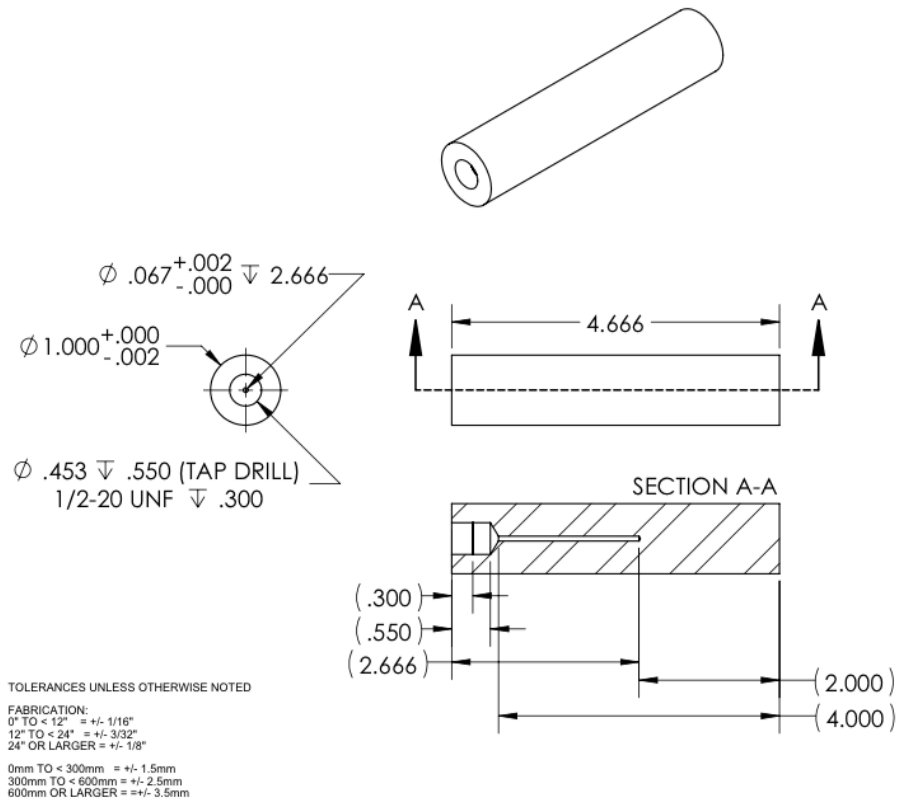


Figure 4.5 Praxair gas quench sample sketch³⁰

4.3 4140 Gas quench hardenability test and analysis

Bars, which have the same geometry (25mm diameter, 100mm length), are quenched in Praxair system under different gas quench HTC condition. After the quench process, the center hardness is measured by Rockwell C tester. The bar that has 50% Martensite at its center is selected, and the applied gas quench HTC of this bar is designated as the critical HTC. With the help of Praxair system, the critical HTC under gas quench condition can be measured.

Based on the simulation by Dante, it is predicted that the critical HTC of 4140 steel under gas quench condition is around 430 W/m²C. A range of gas quench HTC is selected in the experiment as shown in Figure 4.6. The gas is nitrogen and gas temperature is considered as room temperature. The variety of room temperature for all tests in this report is less than 5K.

HTC (W/m ² C)	Gas Pressure (Bar)	Gas Velocity (m/s)
589	12.6	14.81
298	13.7	5.82
206	13.9	3.63
101	14	1.62

Figure 4.6 4140 gas quench HTC

After the gas quench experiments, all the bars were cut to measure the center hardness.

The result is shown as Figure 4.7.

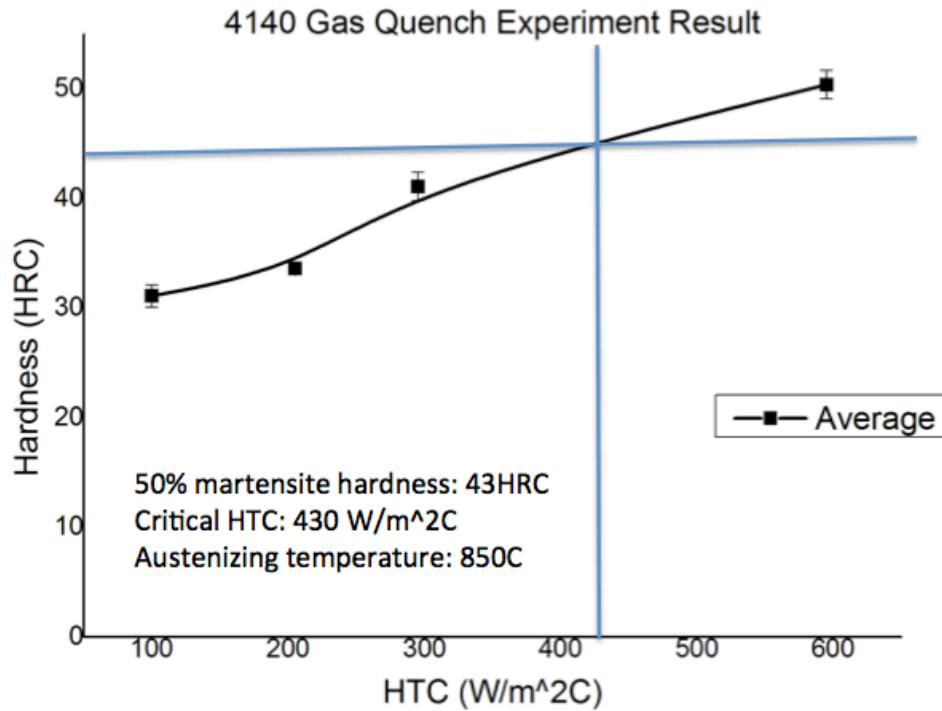


Figure 4.7 4140 gas quench critical HTC test result

From Figure 4.7, with the increase of gas quench HTC, the 4140 center hardness is increasing, since the cooling rate is increasing and more Martensite and lower Bainite form. Based on USS reference³¹, the hardness of 50% Martensite is 43 HRC. After drawing a horizontal line which represents for 43 HRC, the horizontal ordinate of the intersecting point is the critical HTC of 4140, which is 430 W/m^2C . This is the first time that steel gas quench critical HTC is measured by experiment.

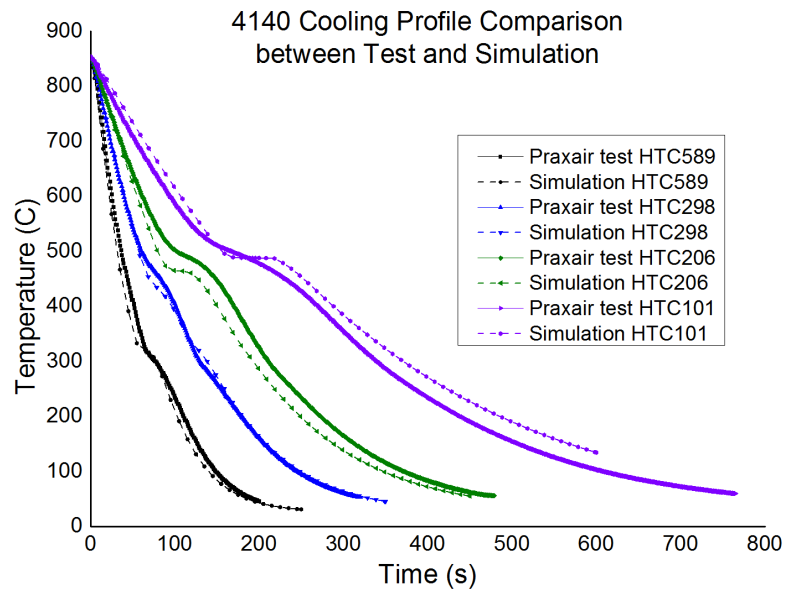


Figure 4.8 4140 cooling profile comparison between test and simulation

Based on chapter 3, the gas quench simulation model has been developed. Figure 4.8 presents the 4140 cooling profile comparison between test and simulation. Considering the test cooling profile, the cooling rate, measured by thermocouple, is increasing with the increase of the gas quench HTC. The inflection point of cooling profile is when the Bainite phase transformation happens. The simulation fits the test result well and demonstrates the accuracy of the gas quench model. Figure 4.9 is the 4140 critical HTC comparison between test and simulation. The simulated critical HTC is the same as the experimental critical HTC.

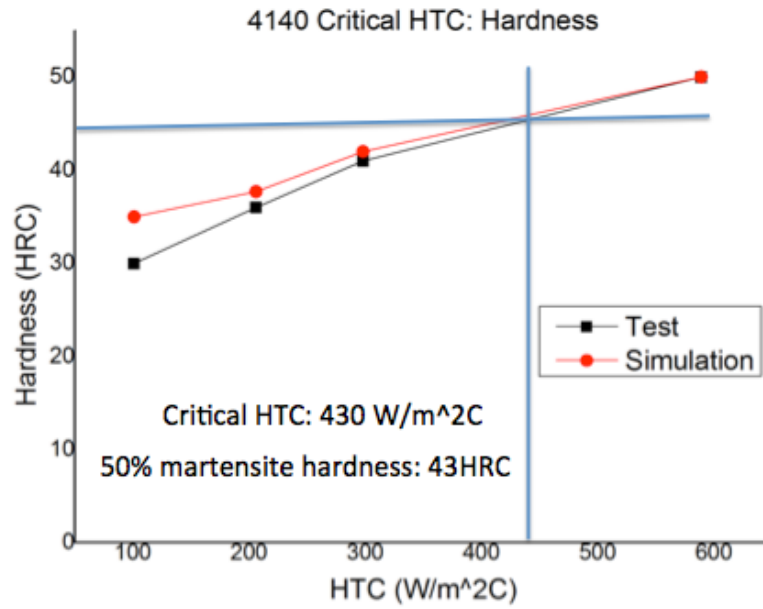


Figure 4.9 4140 critical HTC comparison between test and simulation

In Figure 4.10, the cooling profiles are compared with 4140 CCT diagram generated by JmatPro. With the decrease of gas quench HTC, Martensite decreases and upper Bainite increases.

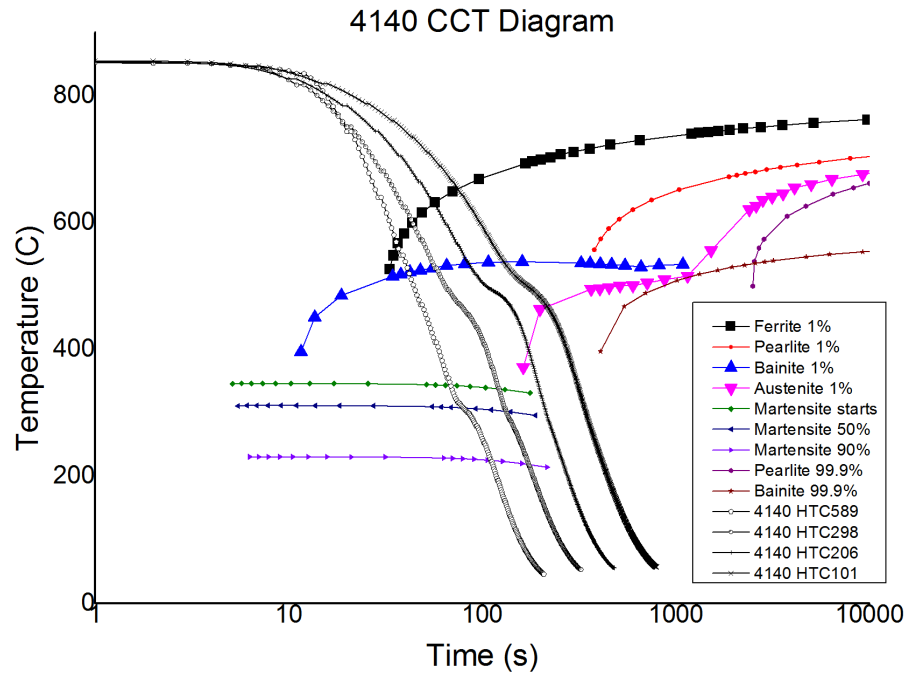


Figure 4.10 4140 CCT diagram

As a conclusion, the 4140 steel gas quench critical HTC is successfully measured at the first time. The simulation matches experiment result, which demonstrates the accuracy of the gas quench model.

4.4 52100 gas quench hardenability test

For 52100 steel, the CHTE gas quench hardenability test follows the same procedures as 4140 steel. Figure 4.11 is the test result. The critical HTC for 52100 steel is 820 W/m²C.

It should be noted that the austenizing temperature has influence on the gas quench hardenability, since the carbides are more easily to dissolve into the Austenite at higher austenizing temperature. For 52100, the carbides will not all dissolve into the Austenite at 850C austenizing temperature until it reaches 1050C. In all gas quench test, the austenizing temperature should be recorded.

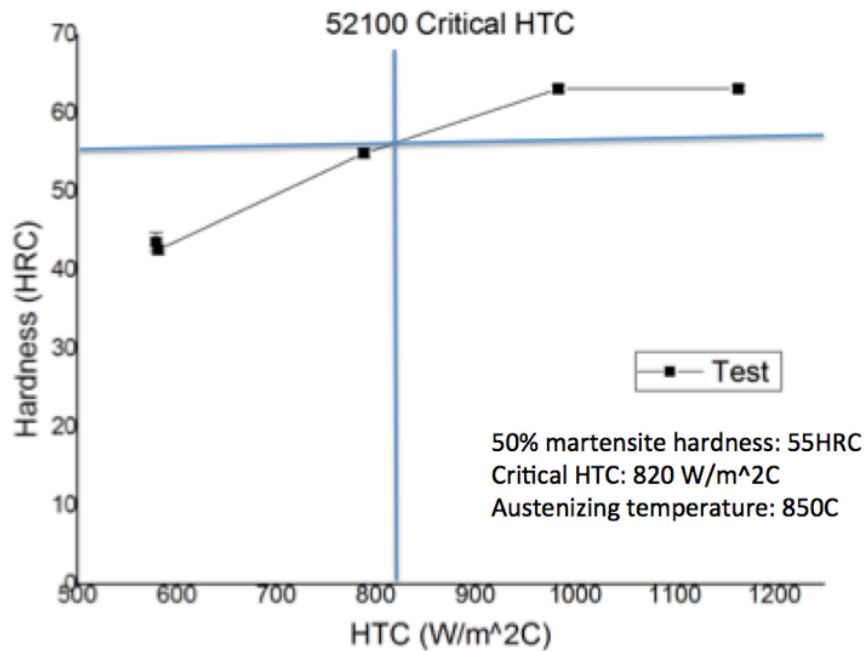


Figure 4.11 52100 gas quench critical HTC test result

Test number	Gas quench HTC (W/m ² C)
T10	579
T11	788
T12	983

Figure 4.12 Gas quench HTC for 52100 tests

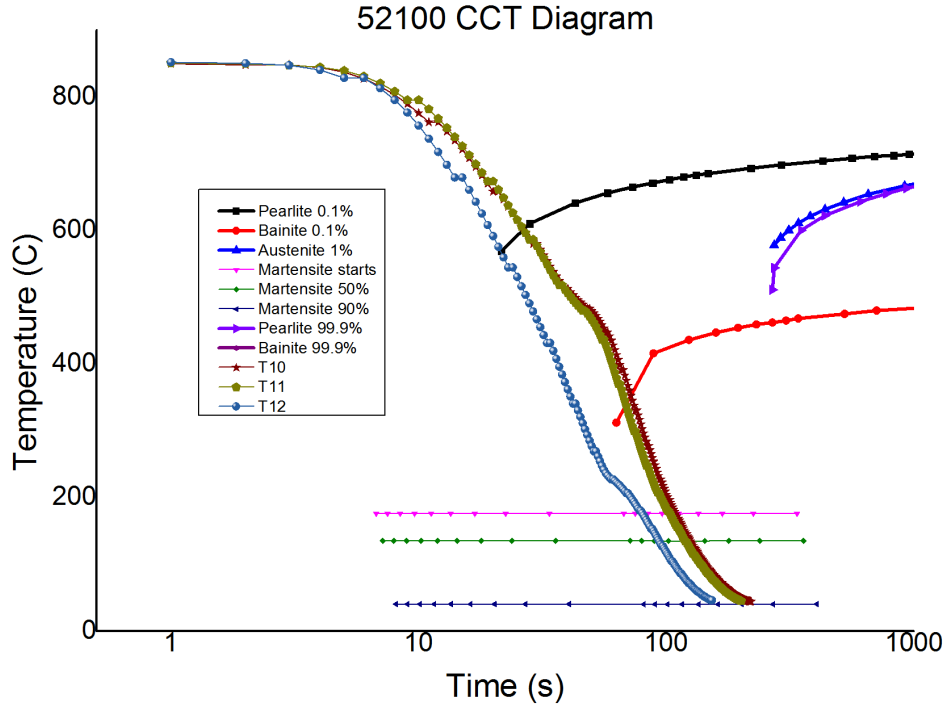


Figure 4.13 52100 CCT diagram

Figure 4.13 is the 52100 CCT diagram. T10, T11 and T12 cooling profiles are drawn in the same figure. For T12, almost 100% Martensite forms. For T11 and T10, the microstructure contain Martensite, Bainite and pearlite. The cooling profiles are measured with thermocouple. The CCT diagram is generated based on JmatPro.

Test number	Hardness (HRC)
T10	43.6
T11	54.9
T12	63.1

Figure 4.14 Hardness result for tests

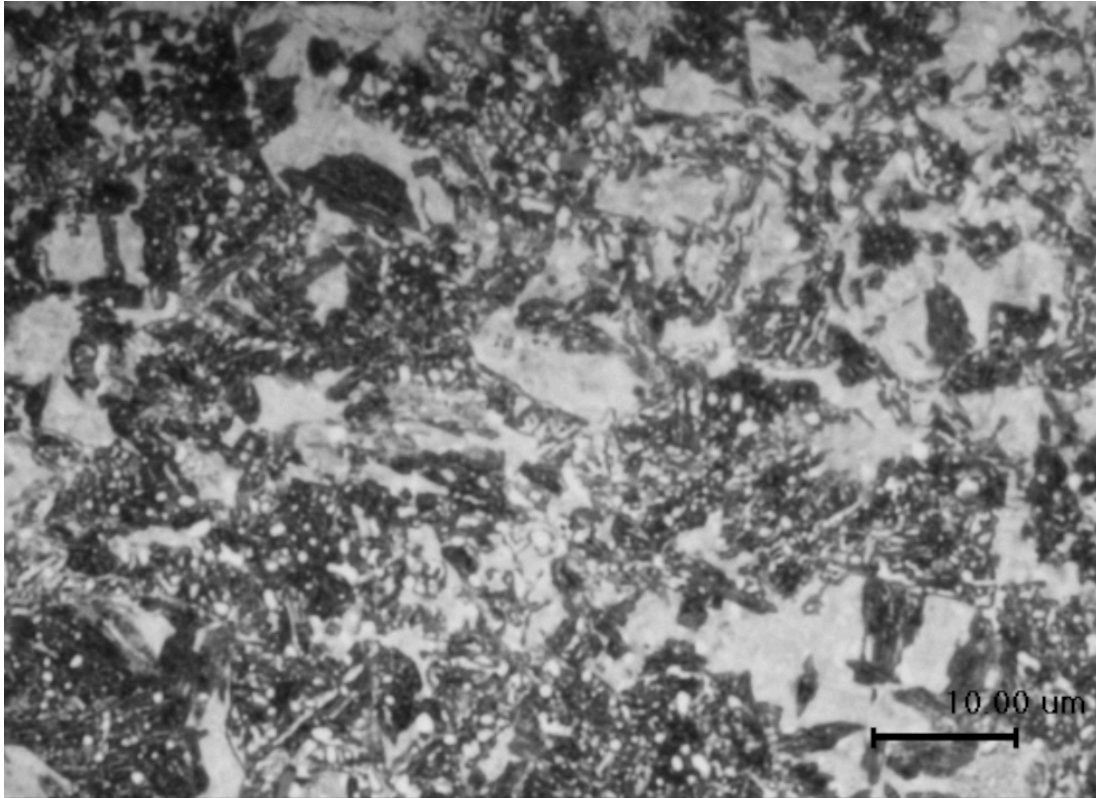


Figure 4.15 T10 Microstructure: 52100 steel austenizing 850C for 40min – 579 W/m²C gas quench – cut - hot mounted – ground and polished – etched with 4% nital

Figure 4.15 presents the microstructure of T10. The grey area is as quenched Martensite. The dark area is Bainite. The bright area may be carbides and retained Austenite. Nano hardness test will be conducted to the dotted white area and bulk white area, in order to distinguish carbides and retained Austenite.

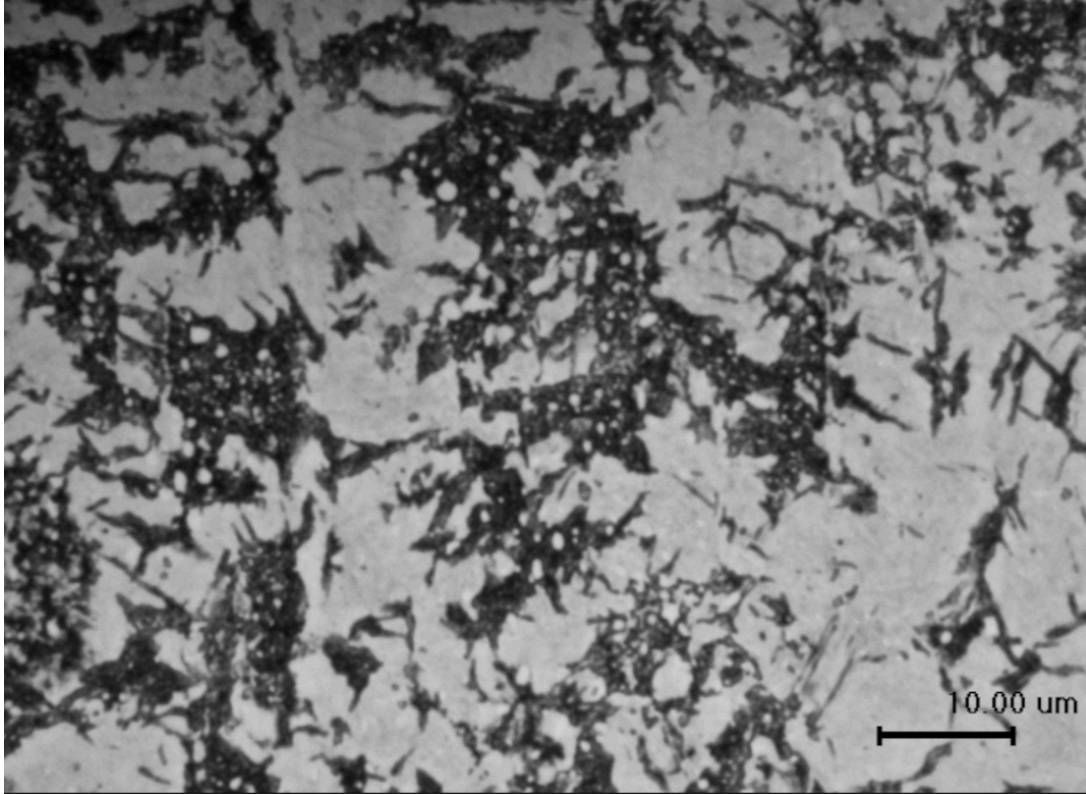


Figure 4.16 T11 microstructure: 52100 steel austenizing 850C for 40min – 788 W/m²C gas quench – cut - hot mounted– ground and polished – etched with 4% nital

Figure 4.16 presents the microstructure of T11. The grey area is as quenched Martensite.

The dark area is Bainite. The bright area may be carbides and retained Austenite.

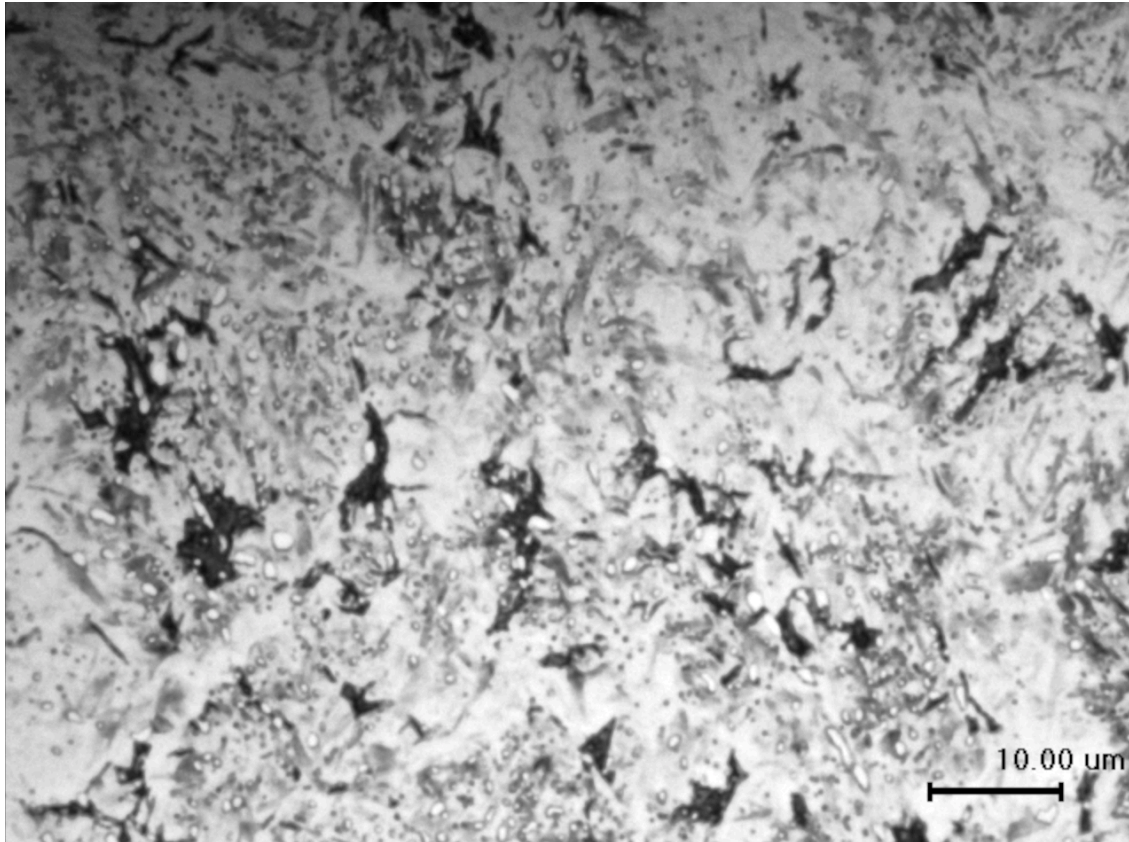


Figure 4.17 T12 microstructure: 52100 steel austenizing 850C for 40min – 983 W/m²C gas quench – cut - hot mounted– ground and polished – etched with 4% nital

Figure 4.17 presents the microstructure of T12. The grey area is as quenched Martensite.

The dark area is Bainite. The bright area may be carbides and retained Austenite.

When comparing the T10, T11 and T12 microstructure, the bright area increases and dark area decreases, which indicates that the percentage of Martensite increases. The microstructure result corresponds to the hardness result and cooling profile result. Higher cooling rate would generate more Martensite. The sample with more Martensite has higher hardness.

4.5 Pyrowear53 gas quench hardenability test and gas quench steel hardenability simulation

For Pyrowear53, very low gas quench $100 \text{ W/m}^2\text{C}$ is selected, since Pyrowear53 is a very high hardenability steel. After the test, the center hardness is measured as 31.5 HRC, which represents nearly 100% Martensite forms ³².

Figure 4.18 is the critical HTC for all steels that have been tested.

Steel	Hardenability	Critical HTC (W/m ² C)
Pyrowear53	High hardenability steel	<100
4140	Medium hardenability steel	430
52100	Medium hardenability steel	820

Figure 4.18 Critical HTC for steels

Steel	Sample geometry: 25mm diameter, 100mm length Critical HTC (50%martensite) W/m ² C
P53	<100
S8680	130
S4150	137
S4340	162
S4140	430
S4047	373
S8650	503
S52100	820
S5140	1102
S4319	1172
S4120	2826
S8620	3098

Figure 4.19 Simulated critical HTC for different steels

Figure 4.19 is the simulated critical HTC result. For low hardenability steels such as 4120 and 8620, the critical HTC is higher than $2000 \text{ W/m}^2\text{C}$, which is the limit of current furnace HTC.

This simulation result would provide a gas quench steel hardenability rank for different steel brand, which helps to find the proper steel for different needs.

4.6 Gas pressure and velocity influence on gas quench hardenability test

Gas pressure and velocity can be adjusted easily based on the requirement during gas quench process. However, the gas pressure and velocity should not be chosen as the parameters to indicate the gas quench condition, since the different combination of gas pressure and velocity may have the same HTC. When discussing about gas quench, the HTC of gas quench condition can be used instead of gas pressure and velocity.

In order to demonstrate the same HTC, which is generated by different combination of gas pressure and velocity, would lead to the same cooling profile, microstructure and properties (hardness), 4140 and 52100 are tested.

Steel	Gas pressure (bar)	Gas velocity (m/s)	HTC (w/m ² C)	Hardness
4140 part2-3	5.2	27.21	502	
4140 part2-4	13.6	10.28	502	
52100 Part2-1	7.1	36.2	810	
52100 Part 2-2R	13.3	19.42	810	

Figure 4.20 HTC and hardness result for gas quench

Figure 4.20 is the HTC and hardness result for gas quench. For 4140, different combination of gas pressure and velocity has the same HTC and the same hardness.

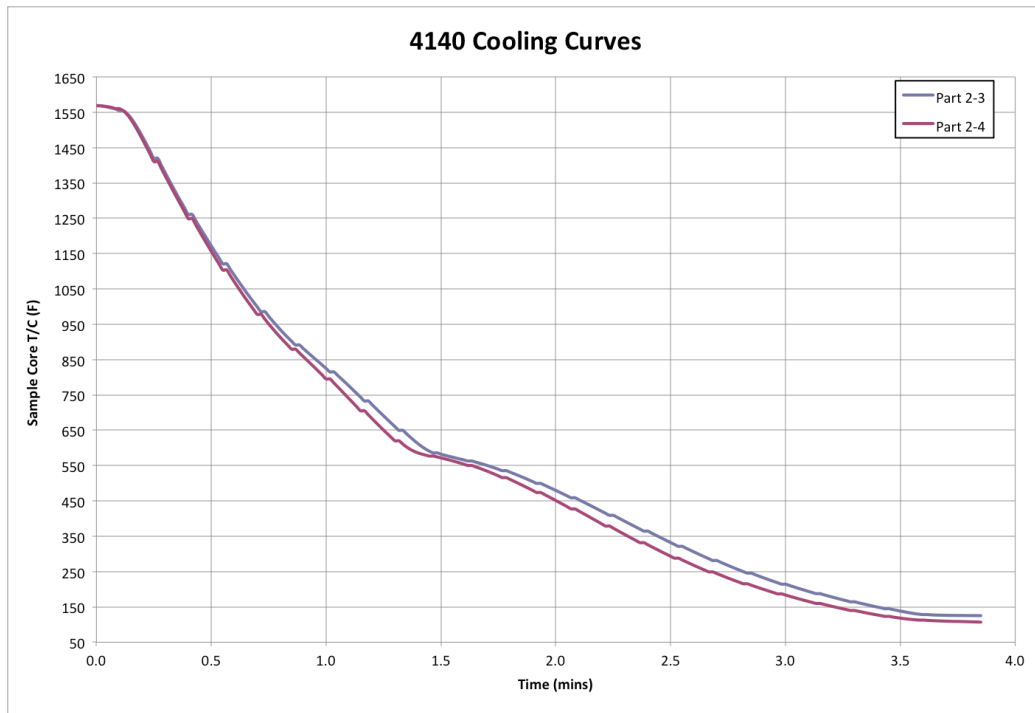


Figure 4.21 4140 cooling curves for gas quench under the same HTC

Figure 4.21 is the cooling curves for 4140 part2-3 and part2-4. Although the gas pressure and velocity are different for part2-3 and part2-4, the cooling curve are very similar, since the HTC is the same.

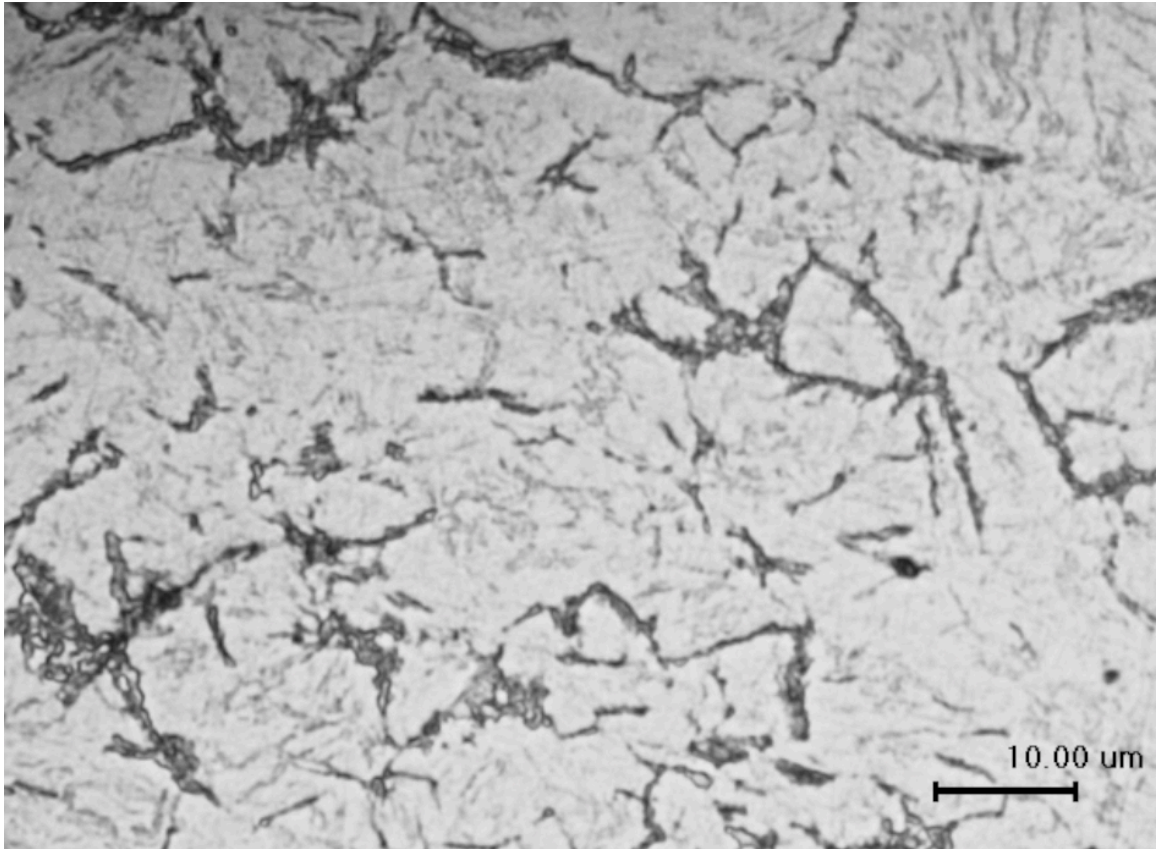


Figure 4.22 4140 Part2-3 microstructure: 4140 steel austenizing 850C for 40min – 502 W/m²C gas quench – cut - cold mounted– ground and polished – etched with 4% nital

Figure 4.22 presents the microstructure for 4140 part2-3. The grey area is as quenched Martensite. The dark area appears to be Bainite that formed at the prior Austenite boundary.

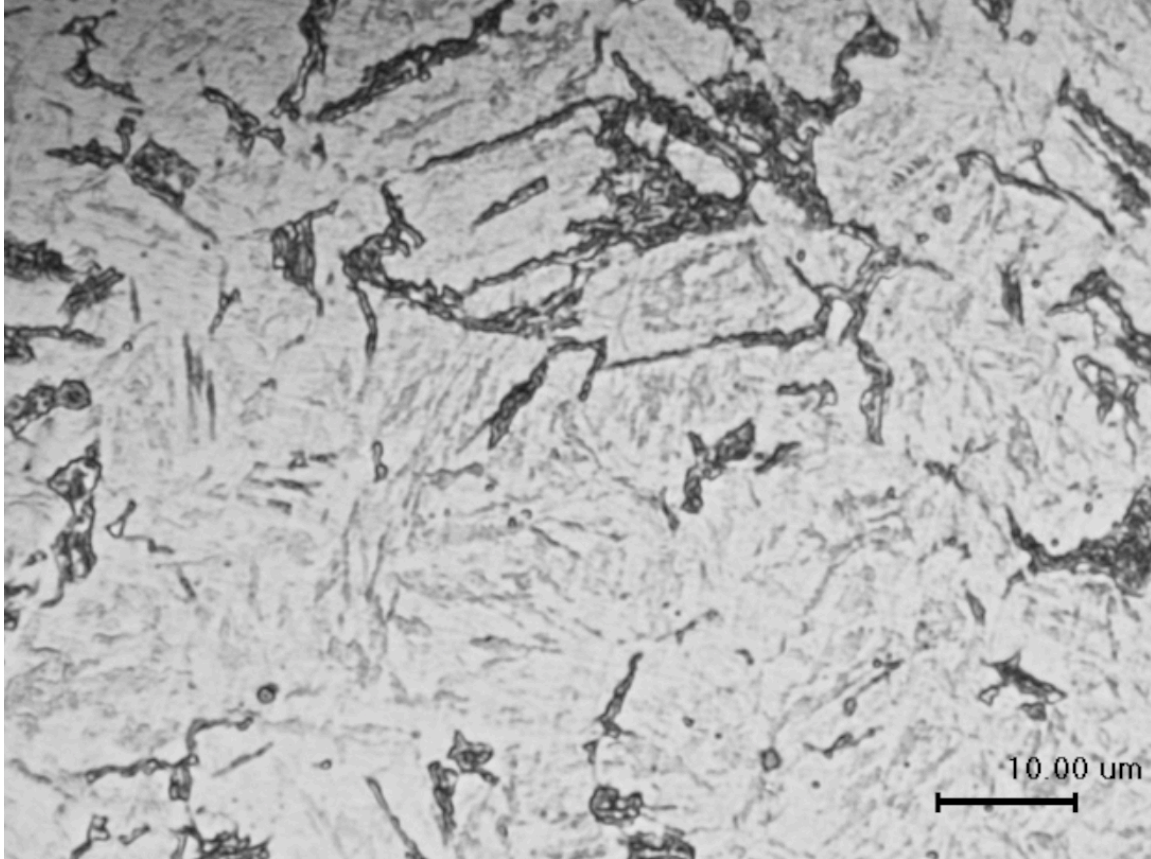


Figure 4.23 4140 part2-4 microstructure: 4140 steel austenizing 850C for 40min – 502 W/m²C gas quench – cut - cold mounted– ground and polished – etched with 4% nital

Figure 4.23 presents the microstructure for 4140 part2-3. The bright and grey area is as quenched Martensite. The dark area appears to be Bainite that formed at the prior Austenite boundary. From the microstructure, the part2-3 sample and part2-4 sample are very similar.

From the analysis above, the cooling curves, microstructure and hardness for 4140 part2-3 sample and part2-4 sample are the same under the same HTC gas quench condition, although the combination of gas pressure and velocity are different.

Based on this experiment, the HTC can be used as the indicator for gas quench, instead of gas pressure and velocity.

4.7 Sample diameter influence on gas quench hardenability test

In the above section, bar geometry is all 25mm diameter and 100mm length. When changing the bar diameter, the cooling rates at the center of the bar will change and that has influence on the hardness.

Based on the model, which has been demonstrated accurate above, bars with different diameters have been gas quenched to find the critical HTC. Figure 4.24 is the simulation result. With the increase of the bar diameter, the critical HTC for steel 4140 increases. The critical HTC is 600 W/m²C when 40mm diameter bar is applied and 270 W/m²C when 20mm diameter bar is applied.

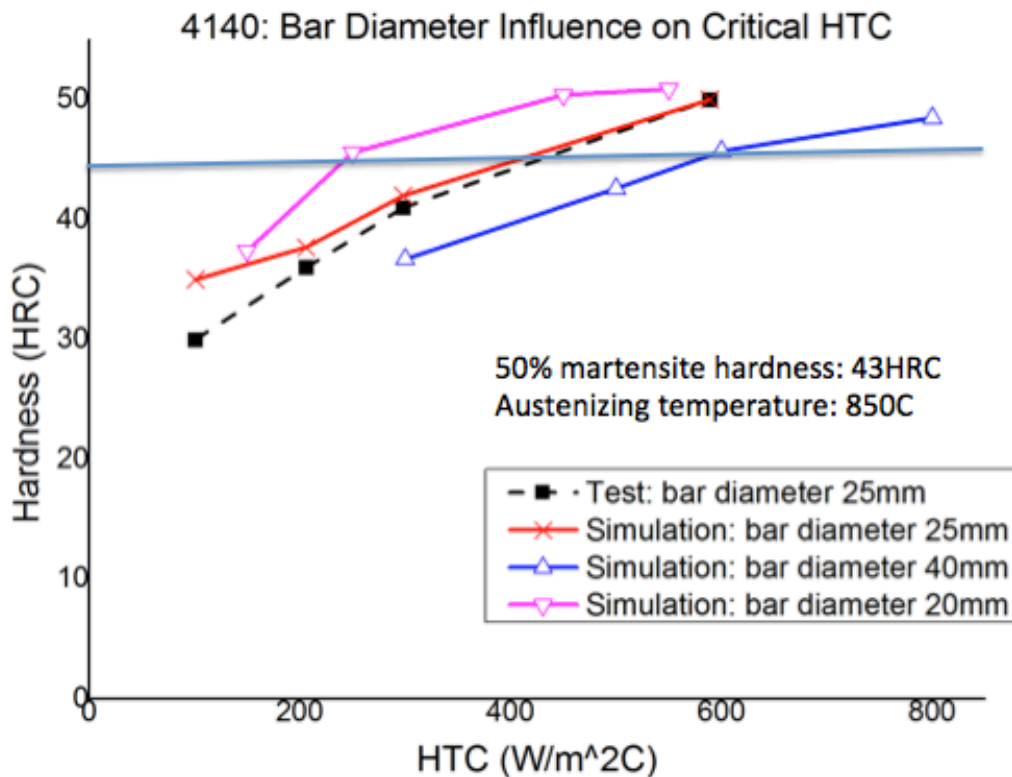


Figure 4.24 4140: Bar diameter influence on critical HTC

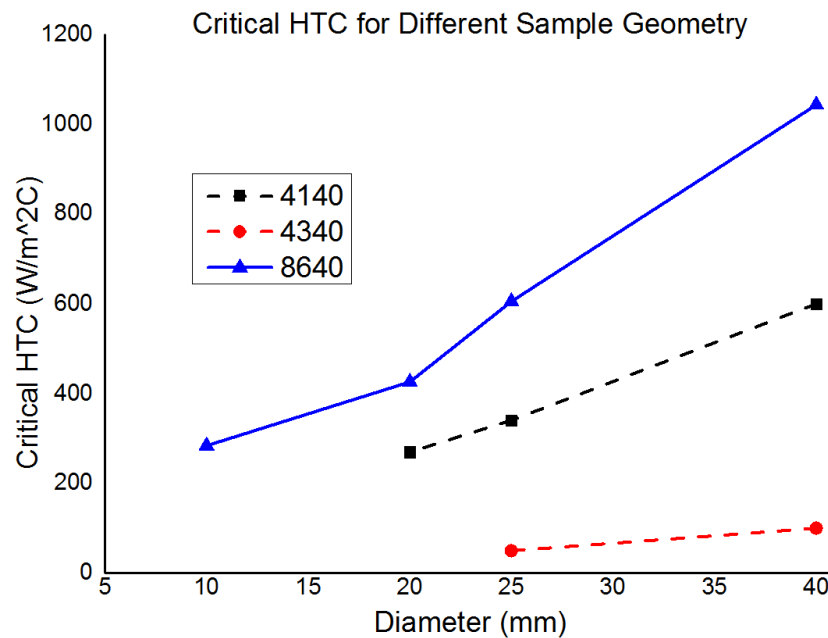


Figure 4.25 Critical HTC for different sample geometry

Figure 4.25 is the critical HTC for different sample geometry when applied to different steels. The bar diameter we are using now is 25mm. The result indicates that too large or too small sample diameter is not proper for the critical HTC test.

If the sample diameter is too small, the difference of critical HTC for steels is not significant, which is difficult to tell the difference from medium and high hardenability steels. If the sample diameter (say 100mm) is too large, the critical HTC will be higher than the maximum HTC we can achieve.

Compared the diameter among 25mm (1 inch), 1.5 inch and 2 inch, 2 inch diameter sample may be better, since the critical HTC difference among high, medium and low hardenability steels are more significant than 1 inch diameter sample, which is used as the current test.

4.8 Summary and Conclusion

CHTE gas quench hardenability test is proposed using cylinder samples with same geometry under different gas quench conditions. After sectioning each bar at mid-length, the bar that has 50% martensite at its center is selected, and the applied gas quench HTC of this bar is designated as the critical HTC.

Critical HTC test has many advantages:

- (1) It is closer to real gas quench condition compared to Jominy test.
- (2) No insulation is needed in CHTE method.
- (3) The gas flow is steady and can be well controlled.
- (4) High, medium and low hardenability steels can be tested in the same system.
- (5) The sample geometry is simple and not changed.

Since HTC is used to replace the gas type, gas pressure and gas velocity, the test result is more repeatable. Even the same gas with same pressure and velocity, the cooling performance can be different due to various gas flow patterns.

Although the critical HTC concept and critical HTC test have many advantages, it still needs industry to understand and generate the relationship between critical HTC and original Jominy hardenability.

5 Controllable gas quench process

Fundamentally, the objective of the quenching process is to cool steel from the austenizing temperature sufficiently quickly to form the desired microstructural phases, sometimes lower bainite but more often martensite ¹. In order to obtain martensite, the cooling rates should be larger than the critical cooling rate. However, the steels may crack while martensite forms if the cooling rate is too rapid. Martempering can overcome this difficulty.

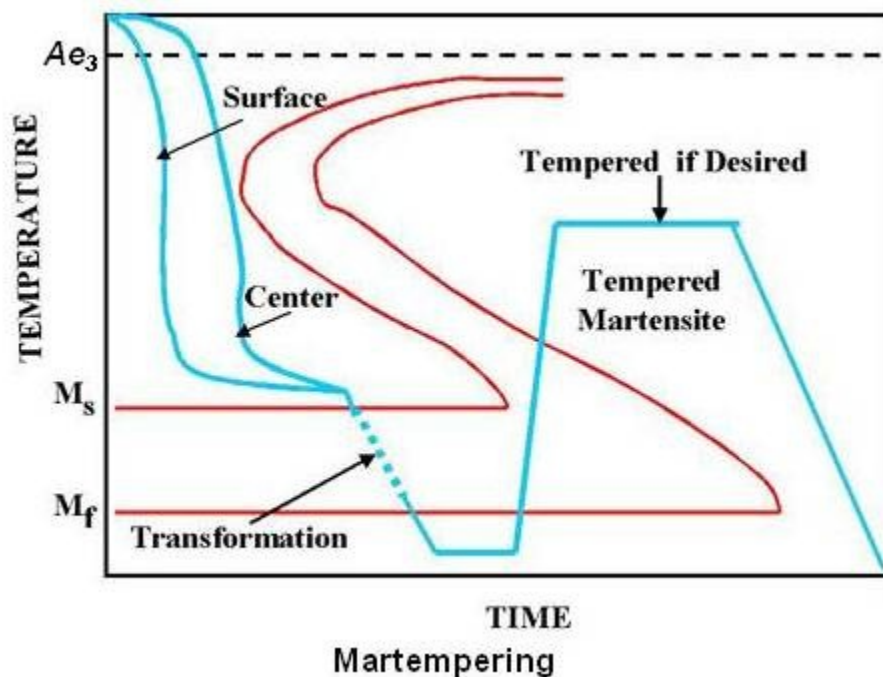


Figure 5.1 Martempering technology ²

At the beginning of the cooling, the cooling rate should be large enough to avoid crossing the nose of the CCT diagram. The percentage of austenite is still 100% when the sample temperature is a little higher than M_s temperature. Then the cooling rate should be reduced in case of sample crack or large distortion.

Marquenching is not easy to use when liquid quench media are applied. In order to obtain two different cooling rates, the quench media should be different. Water quench is often used to obtain high cooling rates at the first stage of quench process. Then the sample is taken out the water quench tank and transfer to oil quench tank or keeps air cooling to obtain lower cooling rate. With this cooling rate limitation, few steels can be used for marquenching.

As discussed above, one of the advantages of gas quench is greater process flexibility to vary cooling rates. The sample could be in the same furnace during the whole marquenching process. The cooling rates are easy to be adjusted by control the gas pressure and velocity. Moreover, nearly all medium and high hardenability steels can be used for marquenching, since the cooling rates for two different stages can be obtained easily.

In this chapter, Jominy bar is used to simulate marquenching process.

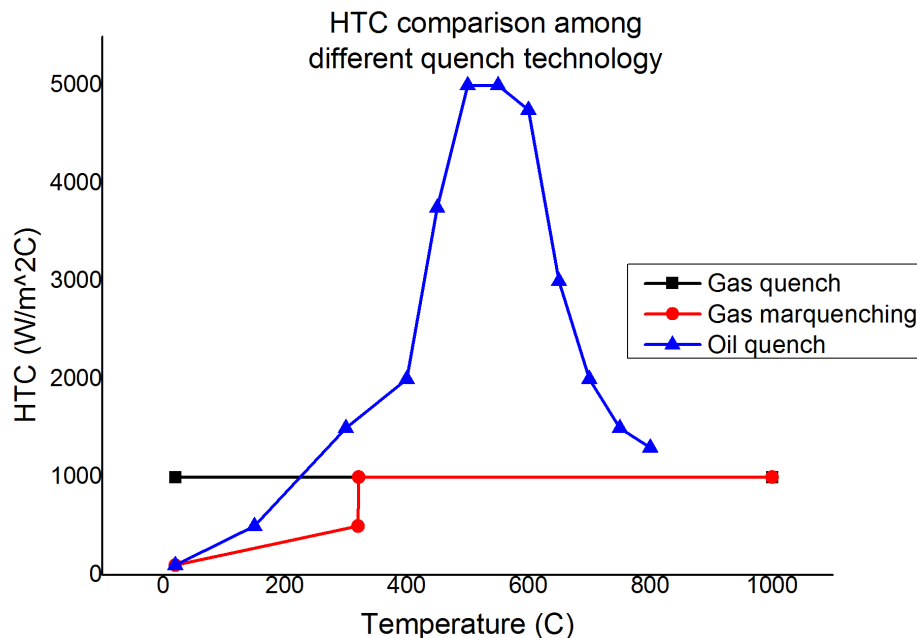


Figure 5.2 HTC comparison among different quench technology

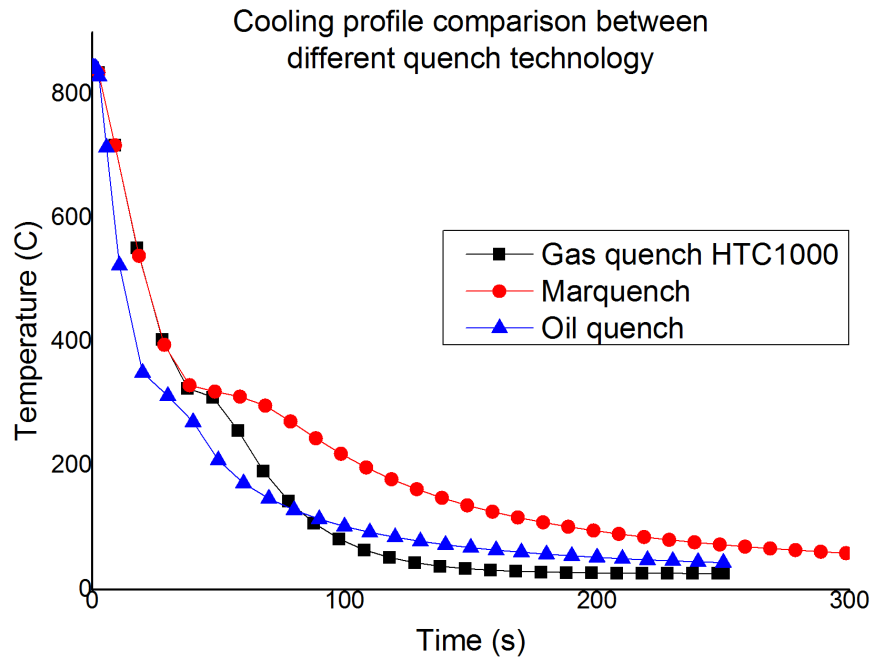


Figure 5.3 Cooling profile comparison between different quench technology

Figure 5.2 is the HTC of different quench technology and Figure 5.3 is the cooling profile comparison (at the center of Jominy bar). These three quench technology obtain the same martensite percentage 92% with different cooling profile. When compared the gas marquenching with the oil quench, the cooling rate for gas marquenching is lower than oil quench during the whole quench process. That gives the gas marquenching sample less distortion and stress.

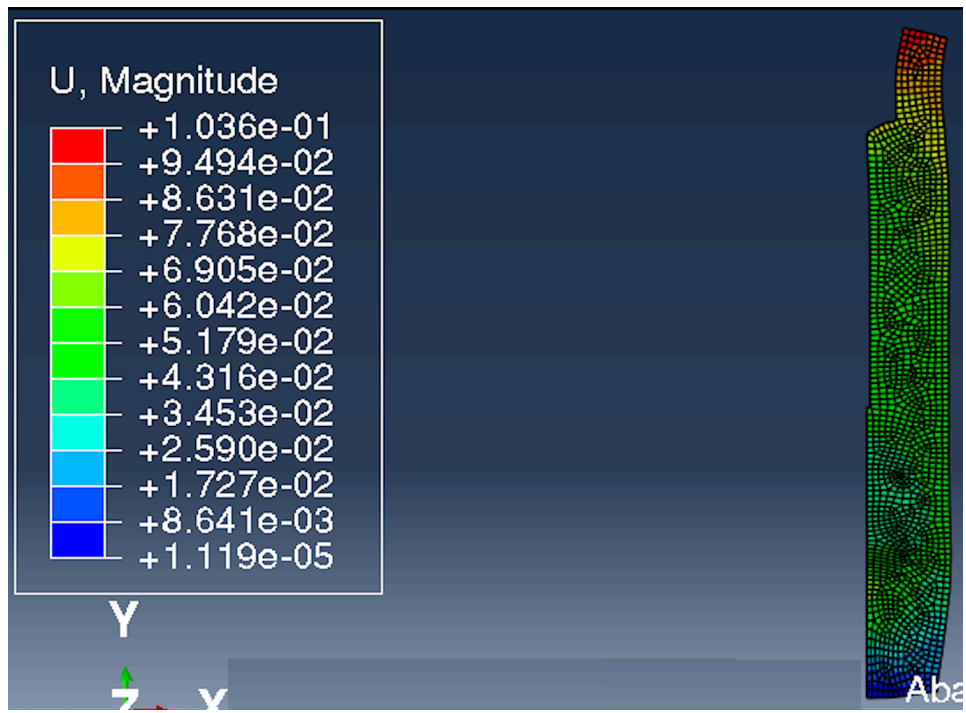


Figure 5.4 Gas marquenching distortion

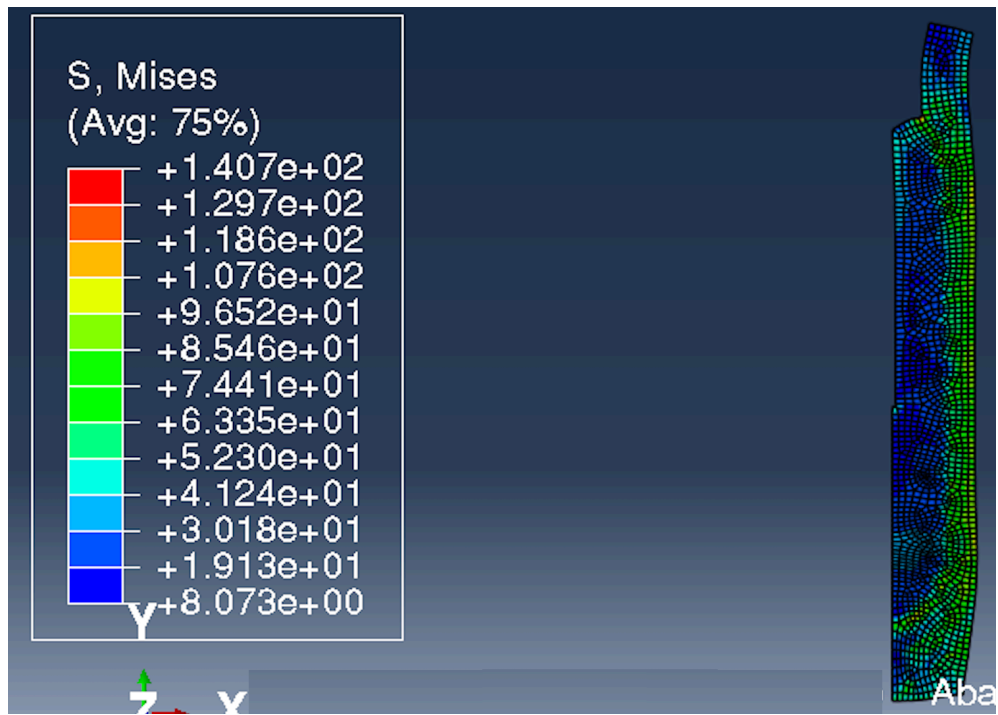


Figure 5.5 Gas marquenching stress

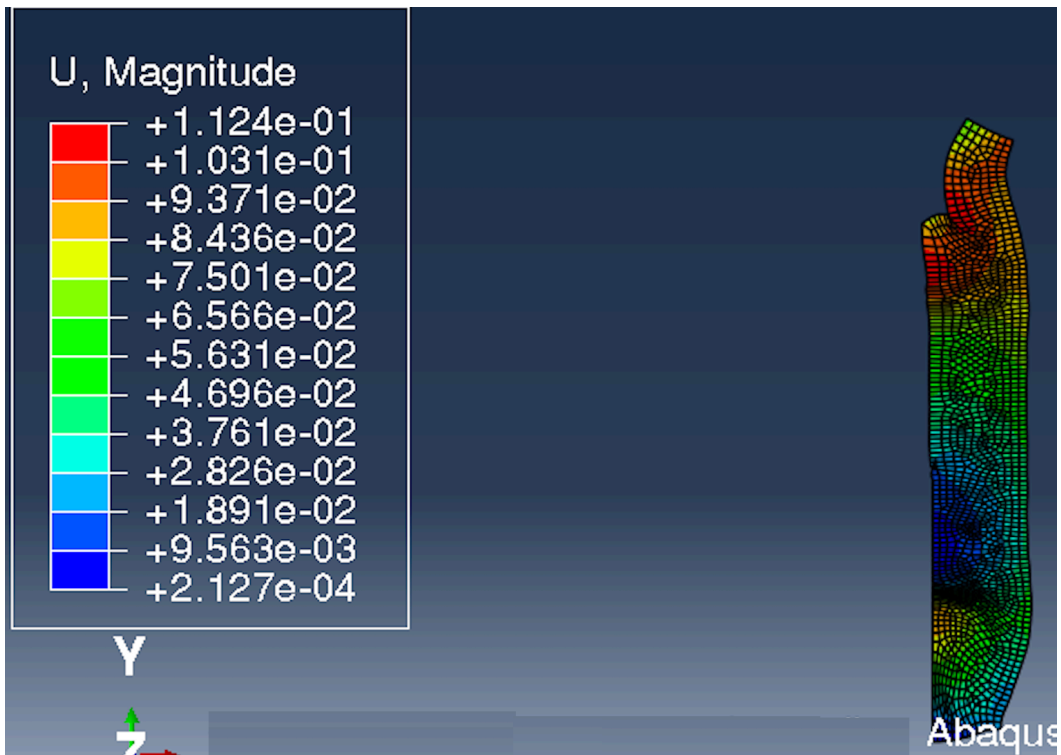


Figure 5.6 Oil quench distortion

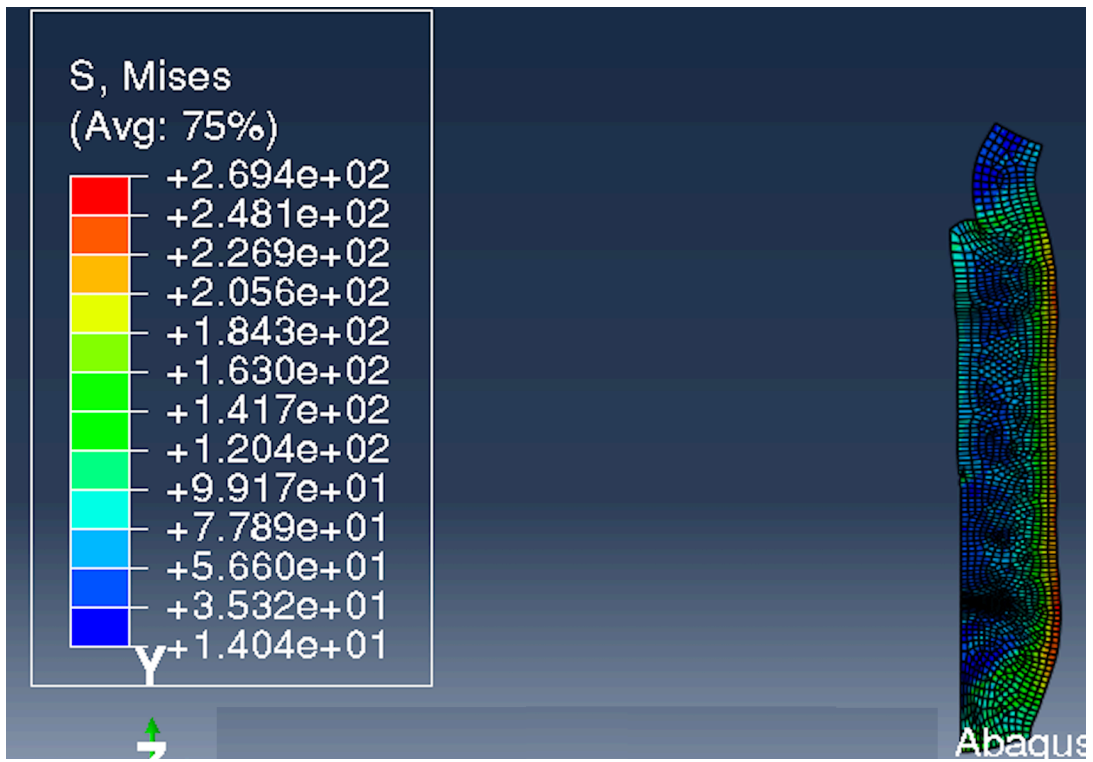


Figure 5.7 Oil quench stress

6 Summary and Conclusion

In the thesis, the comparison between liquid quench and gas quench are discussed. The equivalent gas quench HTC is determined to have the same cooling curve, microstructures and hardness when compared with liquid quench. However, the workpiece with the same hardness after liquid and gas quench process may have different microstructures due to different cooling curves. That leads the workpiece has other properties difference, such as strength, toughness and ductility.

After analysis of water quench hardenability test (Jominy and Grossmann test), several influencing factors on steel hardenability should be noted in steel hardenability test, such as austenizing temperature, heating rate, holding time, composition variation and grain size difference. The XRD and Rietveld refinement methods are used to quantify microstructure weight percent. This technic is more accurate compared to traditional metallographic method to determine 50% martensite phase.

The modified Jominy gas quench tests are discussed. Several limitations are found such as side flow effect and unsteady gas flow. Related improvements are proposed such as adding insulation and changing the gas inclination angle. The fundamental limitation of Jominy gas quench test is that one gas quench condition cannot be used for both low hardenability steel and high hardenability steel at the same time. The same steel grade would have different hardenability curves under different gas quench conditions.

The critical HTC test based on Grossmann test is proposed to overcome the limitations. In the test, different gas quench HTC conditions are applied to the sample with the same geometry. After sectioning each bar at mid-length, the bar that has 50% martensite at its

center is selected, and the applied gas quench HTC of this bar is designated as the critical HTC. This test has many advantages to take the place of modified Jominy gas quench test.

Since one of the advantages of gas quench is greater process flexibility to vary cooling rates, gas marquenching technology is proposed to obtain martensite with less severe cooling rates and reduce the distortion and stress. The simulation result shows that the gas marquenching technology is potential to reduce distortion and stress.

References

- [1] ASM handbook volume 4 Heating Treating
- [2] Jon L. Dossett, Practical heat treating second edition, ISBN:0-87170-829-9
- [3] Robert Honeycombe, Steels microstructure and properties second edition, ISBN 0 340 58946 9
- [4] Bozidar Liscic, Hans M.Tensi, Lauralice C.F.Canale, George E.Totten, Quenching theory and technology, 2010, ISBN 978-0-8493-9279-5
- [5] Herring. D. H., A review of gas quenching from the perspective of the heat transfer coefficient, Industrial Heating, February 2006.
- [6] Wang, J., Gu, J., Shan, X., Hao, X., Chen, N., & Zhang, W. (2008), Numerical simulation of high pressure gas quenching of H13 steel. Journal of Materials Processing Technology, 202(1-3), 188–194.
- [7] Elkatatny, I., Morsi, Y., Blicblau, A.S., Das, S., Doyle, E.D., 2003, Numerical analysis and experimental validation of high pressure gas quenching. Int. J. Therm. Sci. 42, 417–423.
- [8] Xiao, B., Wang, G., Wang, Q., Maniruzzaman, M., Sisson, R. D., Jr, & Rong, Y. (2011), An Experimental study of heat transfer during forced air convection. Journal of Materials Engineering and Performance, 20(7), 1264–1270
- [9] Cosentino, F., Warnken, N., Gebelin, J.-C., & Reed, R. C. (2013), Numerical and experimental study of post-heat treatment gas quenching and its impact on microstructure and creep in CMSX-10 superalloy. Journal of Materials Processing Technology, 213(12), 2350–2360.

- [10] Herring, D.H. A review of gas quenching from the perspective of the heat transfer coefficient, *Industrial Heating* 2006, February, 67–72
- [11] ISO 642 Steel – hardenability test by end quenching (Jominy test)
- [12] Robert Hill, Gas vs. liquid quenching: a direct comparison in hardenability to reduce distortion, *Thermalprocessing2013spring*
- [13] Landek, D., Liščić, B., Filetin, T., Lübben, T. & Lisjak, D., 2009, Hardenability Testing and Simulation of Gas-Quenched Steel, *Materials and Manufacturing Processes*, 24(7-8), pp. 868-72
- [14] B. Liscic: Hardenability. In *Steel Heat Treatment Metallurgy and Technologies*; Totten, G.E., Ed.; CRC Press, Taylor & Francis Group: Boca Raton, 2007; 213-275.
- [15] Jeffrey Mocsari, High pressure gas quenching: heat transfer analysis report, Praxair, 7/9/2014
- [16] Gensamer, M., Pearsall, E. B., Pellini, W. S., & Low, J. R., Jr. (2012), The Tensile Properties of Pearlite, Bainite, and Spheroidite. *Metallography, Microstructure, and Analysis*, 1(3-4), 171–189.
- [17] Erik Khzouz, Grain Growth Kinetics in Steels, A major qualifying project report submitted to the faculty of the Worcester Polytechnic Institute in partial fulfillment of the requirements for the degree of bachelor of science in mechanical engineering, 4/28/2011
- [18] Timken practical data for metallurgists seventeenth edition
- [19] Atlas of isothermal transformation and cooling transformation diagrams, American society for metals, 1977

- [20] M.A. Grossmann and E.C. Bain, Principles of heat treatment, American society for metals
- [21] B.D.Cullity, Elements of X-ray diffraction second edition, ISBN 0-201-01174-3
- [22] Oleg D Sherby and etc., Revisiting the Structure of Martensite in Iron-Carbon Steels, MATERIALS TRANSACTIONS, 2008 vol. 49 (9) pp. 2016-2027.
- [23] Littmann, Walter Edward, The influence of the grinding process on the structure of hardened steel, Thesis (Sc.D.) Massachusetts Institute of Technology. Dept. of Metallurgy, 1954.Vita.Bibliography: leaves 70-72.
- [24] Speer, J., Matlock, D. K., De Cooman, B. C., & Schroth, J. G. (2003). Carbon partitioning into austenite after martensite transformation. Acta Materialia, 51(9), 2611–2622. doi:10.1016/S1359-6454(03)00059-4
- [25] Krauss, G. (1999). Martensite in steel: strength and structure. Materials Science and Engineering: A, 273-275, 40–57. doi:10.1016/S0921-5093(99)00288-9
- [26] Stone, H. J., Peet, M. J., Bhadeshia, H. K. D. H., Withers, P. J., Babu, S. S., & Specht, E. D. (2008). Synchrotron X-ray studies of austenite and bainitic ferrite. Proceedings of the Royal Society a: Mathematical, Physical and Engineering Sciences, 464(2092), 1009–1027. doi:10.1098/rspa.2007.0201
- [27] H.M.Rietveld, A profile refinement method for nuclear and magnetic structures, J.Appl.Cryst. (1969).2,65-71.
- [28] H.M. Rietveld, Line profiles of neutron powder-diffraction peaks for structure refinement, Acta Cryst. (1967).22,151-152

- [29] S.S.Babu and etc., In-situ observations of lattice parameter fluctuations in Austenite and transformation to Bainite, Metallurgical and materials transactions A, Volume 36A, December 2005-3289
- [30] Praxair report by Jeffrey Mocsari
- [31] United States Steel, Isothermal transformation diagrams
- [32] Worldwide guide to equivalent irons and steels, 4th edition, 2000